OUTLINE

I. Radar imaging - Spatial resolution

II. Polarization - Polarimetry

III. Radar response sensitivity

IV. Relief effects

V. Speckle and Filtering

Université Gustave Eiffel

pierre-louis.frison@univ-eiffel.fr

The radar equation

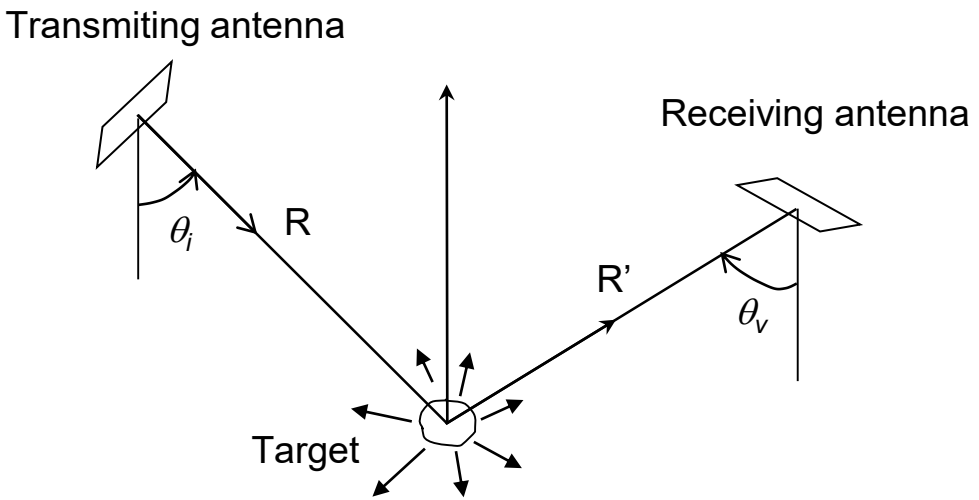

Transmited power:

$$P_i = \frac{P_e G_e}{4\pi} d\Omega \qquad (W)$$

Receiving irradiance at distance R:

$$E_i = \frac{P_e G_e}{4\pi R^2} \qquad (W/m^2)$$

Intercepted power from the target *(W)*:

$$P_s = \frac{P_e G_e}{4\pi R^2} RCS$$

Radar Cross Section (m²)

Intensity emited from the target (isotrope):

$$I = \frac{P_S}{4\pi} = \frac{P_e G_e}{4\pi R^2} \frac{RCS}{4\pi} \qquad (W/sr)$$

Power received by surface dS at distance R':

$$P_r = I\, d\Omega = I \frac{dS}{R'^2} = \frac{P_e G_e}{4\pi R^2} \frac{RCS}{4\pi R'^2} dS \qquad (W)$$

The radar equation

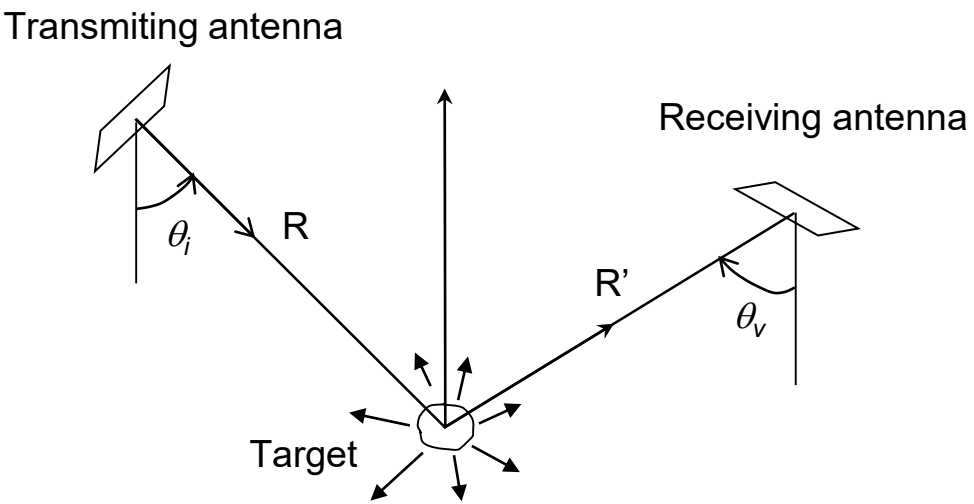

Power received by dS at distance R'

$$P_r = \frac{P_e G_e}{4\pi R^2} \frac{RCS}{4\pi R'^2} dS \qquad (W)$$

Recived irradiance at distance R'

$$E_r = \frac{P_e G_e}{4\pi R^2} \frac{RCS}{4\pi R'^2} \qquad (W/m^2)$$

Power received by the antenna: $P_r = E_r \, dA = E_r \frac{G_r \lambda^2}{4\pi} = \frac{P_e G_e}{4\pi R^2} \frac{RCS}{4\pi R'^2} \frac{G_r \lambda^2}{4\pi}$

(W)

The radar equation

Radar Cross Section (m²)

Power received by the antenna: $$dP_r = \frac{P_e G_e}{4\pi R^2} \frac{RCS}{4\pi} \frac{G_r \lambda^2}{4\pi R^2} \quad (W)$$

Case of expanse surfaces:

Radar Backscattering Coefficient: $$\sigma^0 = \frac{RCS}{d\Sigma} \quad (m^2/m^2)$$

➔ *Analogous to the reflectance in Optical domain*

$$dP_r = \frac{P_e G_e}{4\pi R^2} \frac{\sigma^0 d\Sigma}{4\pi} \frac{G_r \lambda^2}{4\pi R^2}$$

$$\sigma^0 = \frac{(4\pi)^3}{\lambda^2} \frac{\langle P_r \rangle}{P_e} \frac{R^4}{\iint_{Surf.obs.} G_e G_r \, d\Sigma}$$

σ^0 high dynamic

==> dB units (log. scale)

$$\sigma^0_{dB} = 10 \cdot \log_{10} \left(\sigma^0_{Nat} \right)$$

Radar images interpretation rules

2 cases of figure:

Surface scattering (interaction occurs at the interface between beth media)

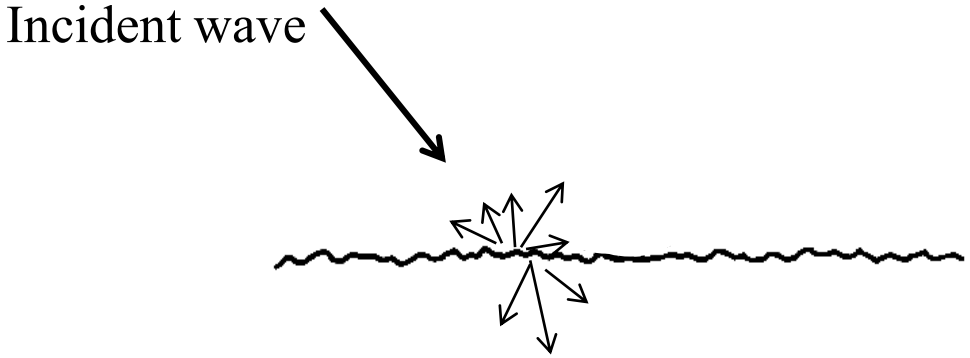

Volume scattering (interaction with multiple elements = scatterers)

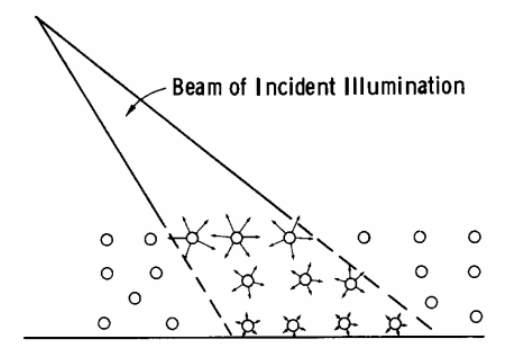

Radar response sensitivity

bare soils or water surfaces

Surface Scattering

Radar images interpretation rules

Surface scattering

Soil: homogeneous medium ==> scattering at the interface

Influence of roughness

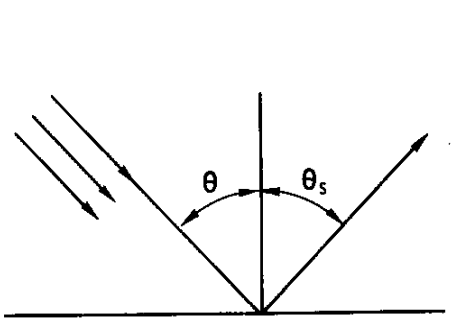

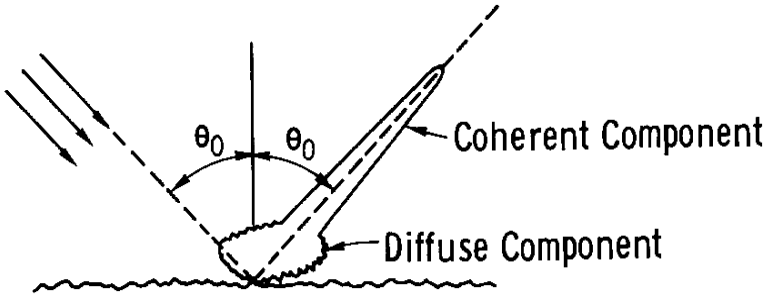

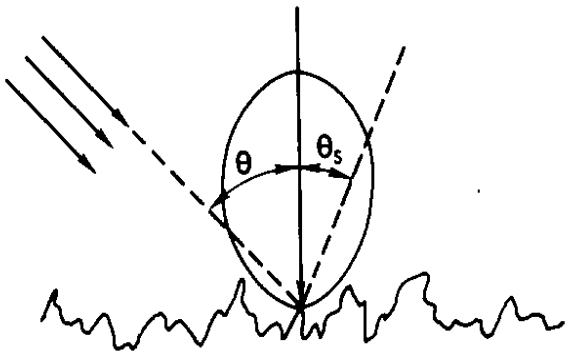

Surface roughness is refered to the radar wavelength

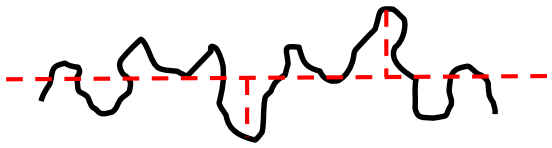

σ: rms height

$$\sigma < \frac{\lambda}{8 \cos \theta}$$ ==> smooth surface

ERS (λ = 5 cm, θ = 23°): s > 2.10^{-2}: every soil is rough!

Radar images interpretation rules

Surface scattering

Smooth surface

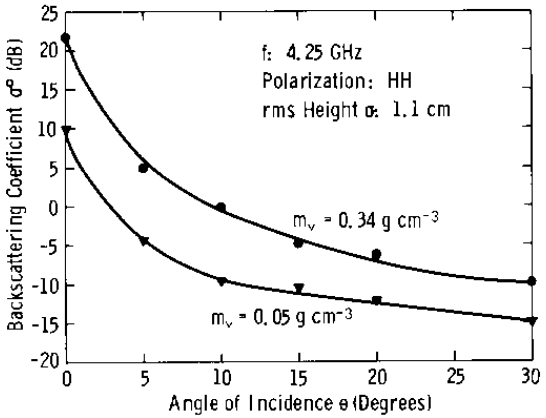

Rough surface

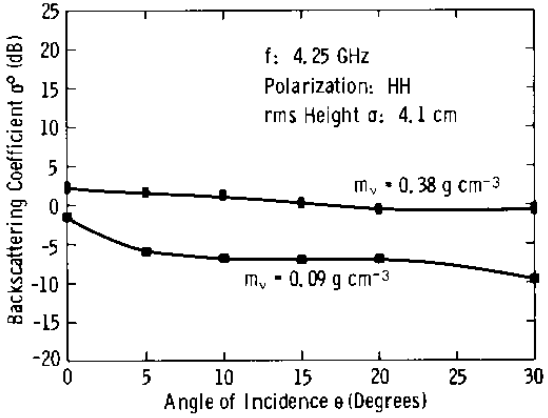

(b)

Soil *roughness*: ***angular*** effect

Soil *moisture*: ***shift level*** effect

Radar response sensitivity

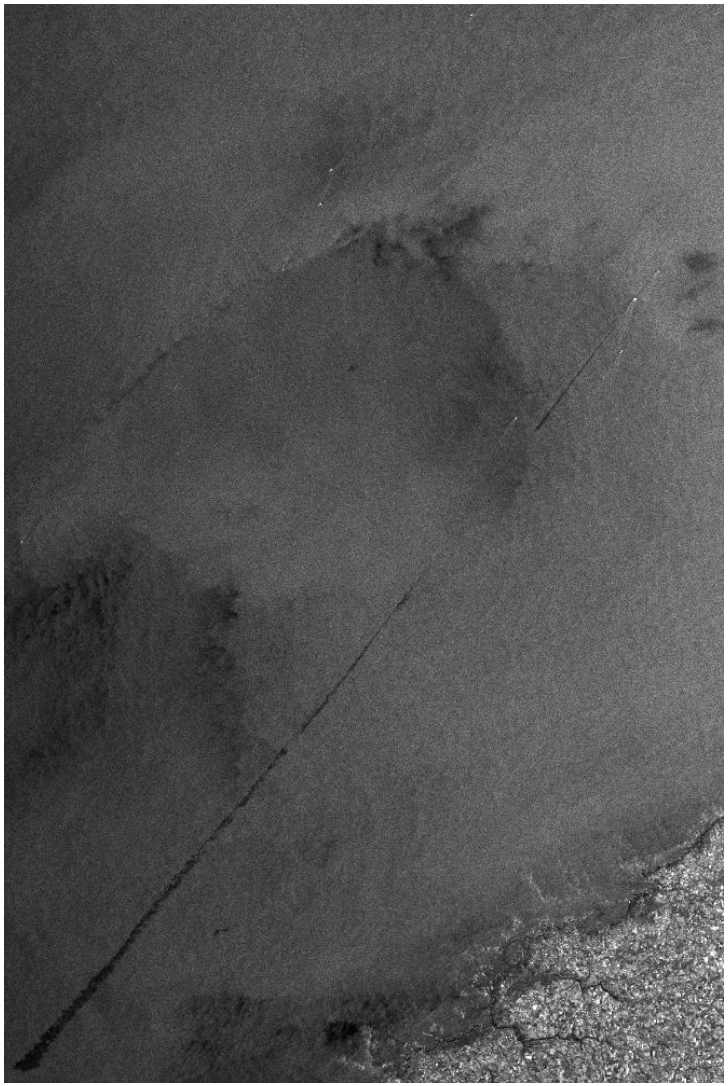

ERS (bande C, 23°, VV): 9 mars 1999

Radar response sensitivity

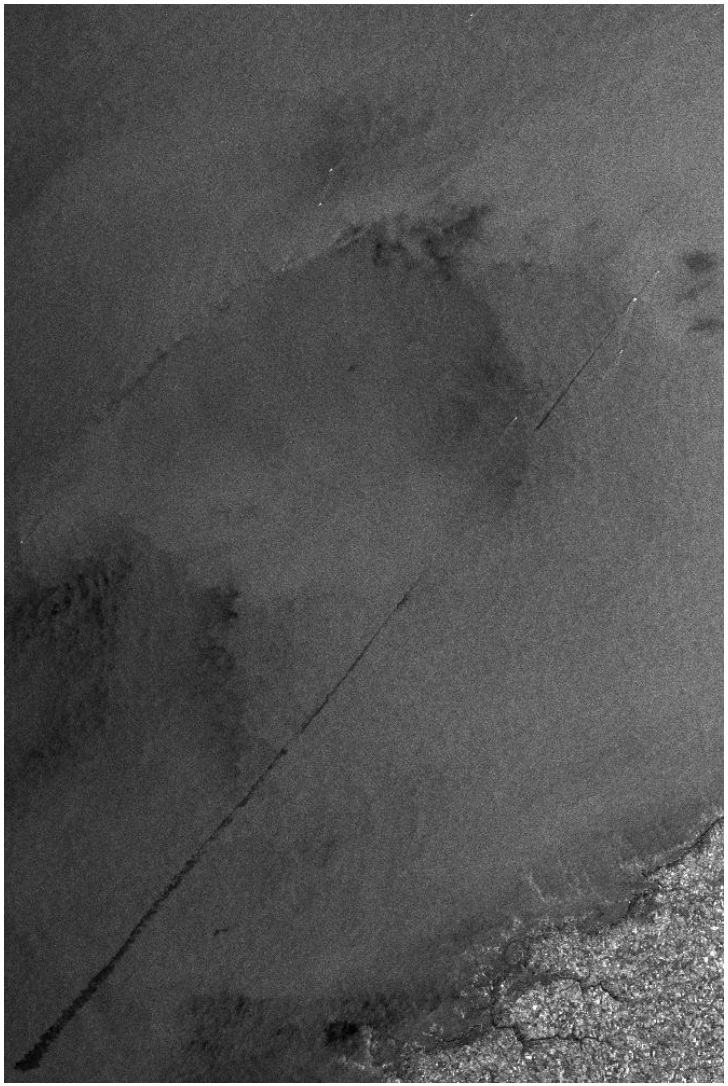

ERS (bande C, 23°, VV): 9 mars 1999

Over surface water:

surface roughness too

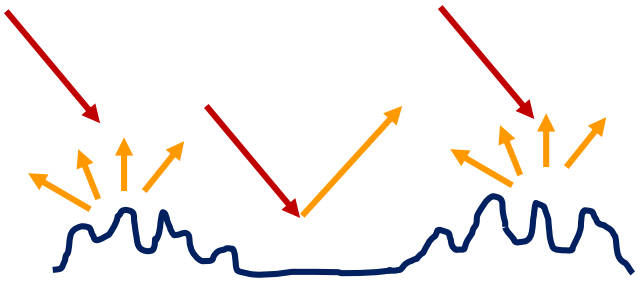

Typhon Isidore
Mexico - 21.09.2002

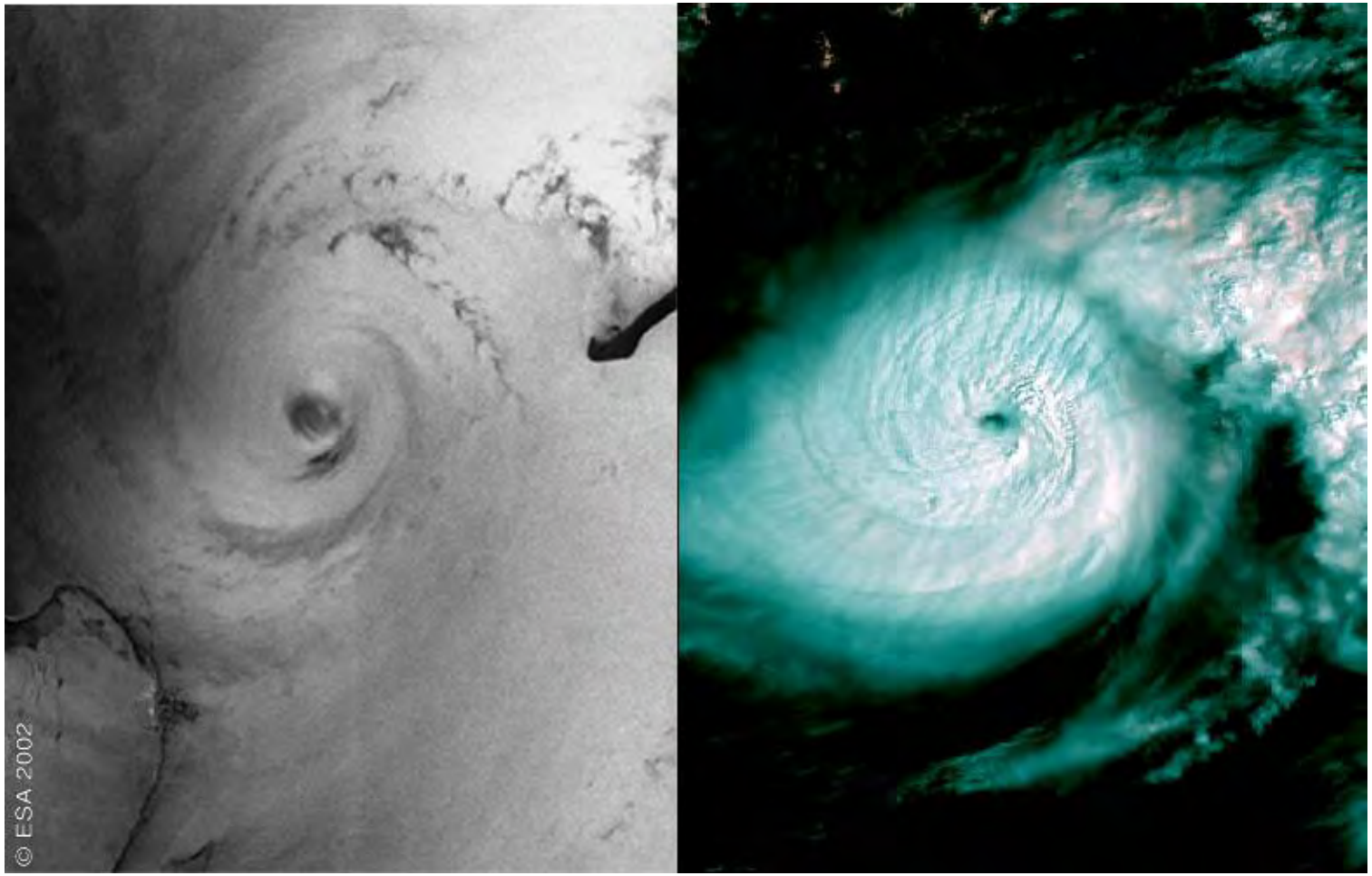

ASAR

MERIS (600 m)

Frequency - wavelength

Exercice: why is it required to know the wavelength λ?

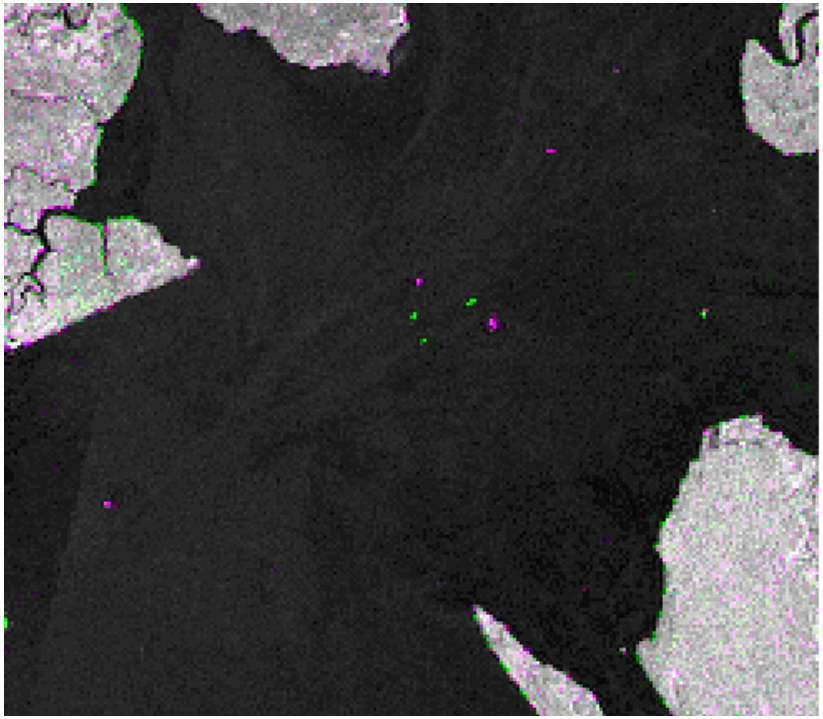

JERS sensor

(Bande L, λ = 25 cm)

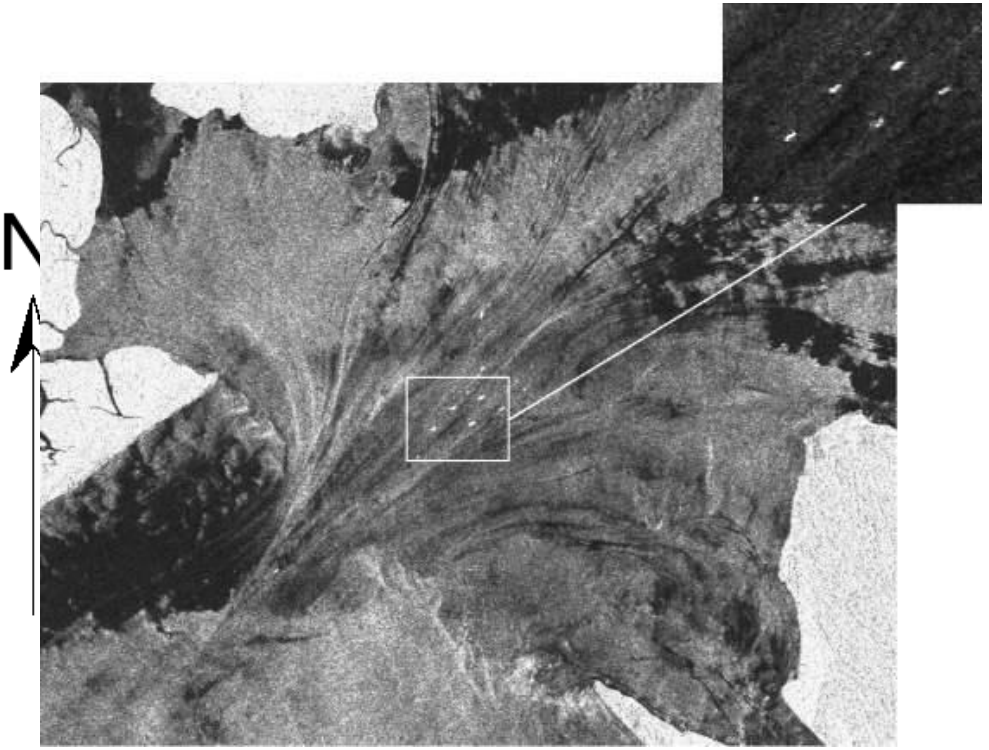

ERS sensor

(Bande C, λ = 6 cm)

ERS radar image in Sahel

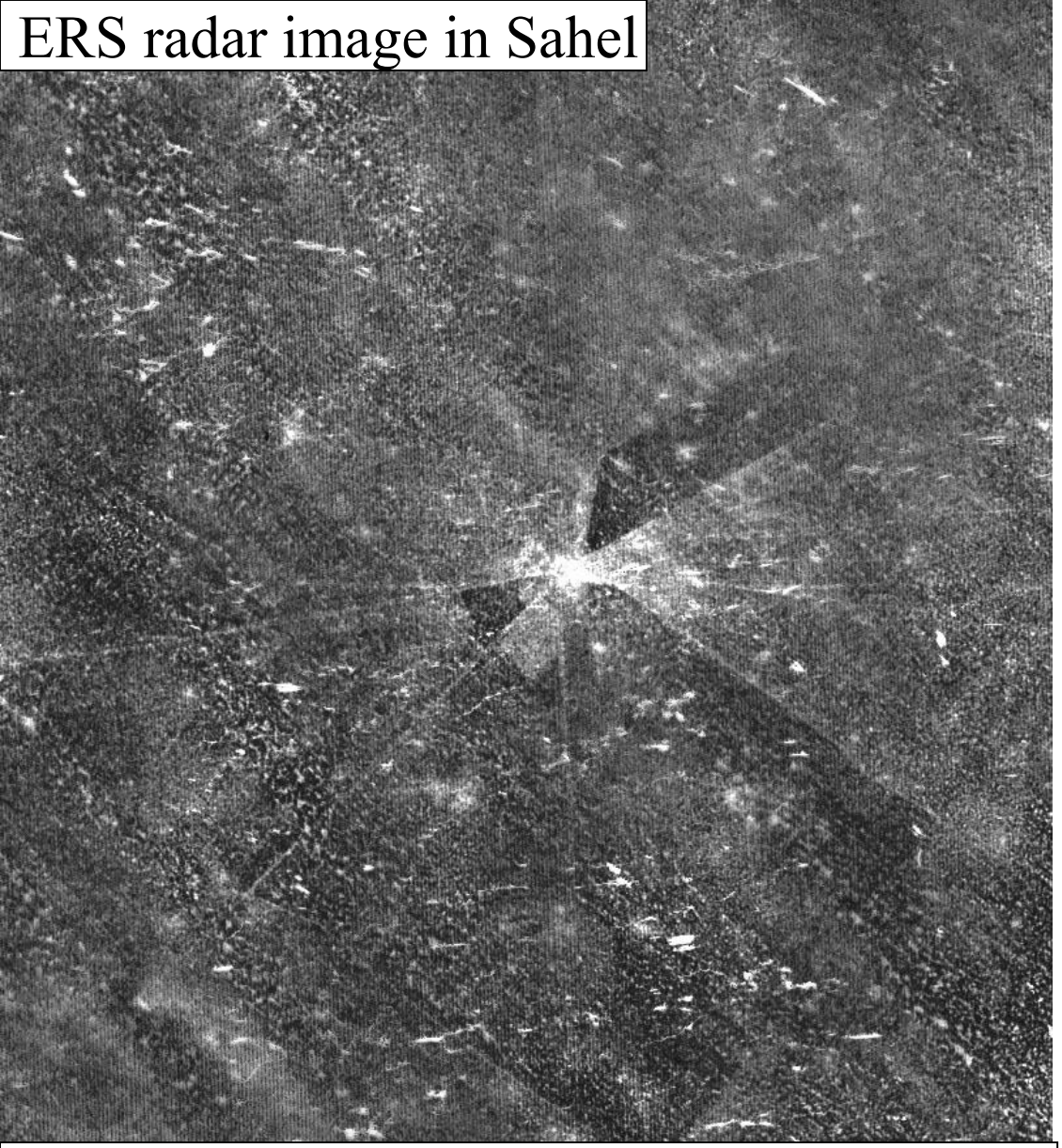

Over bare soil: depends on

Roughness

Soil moisture

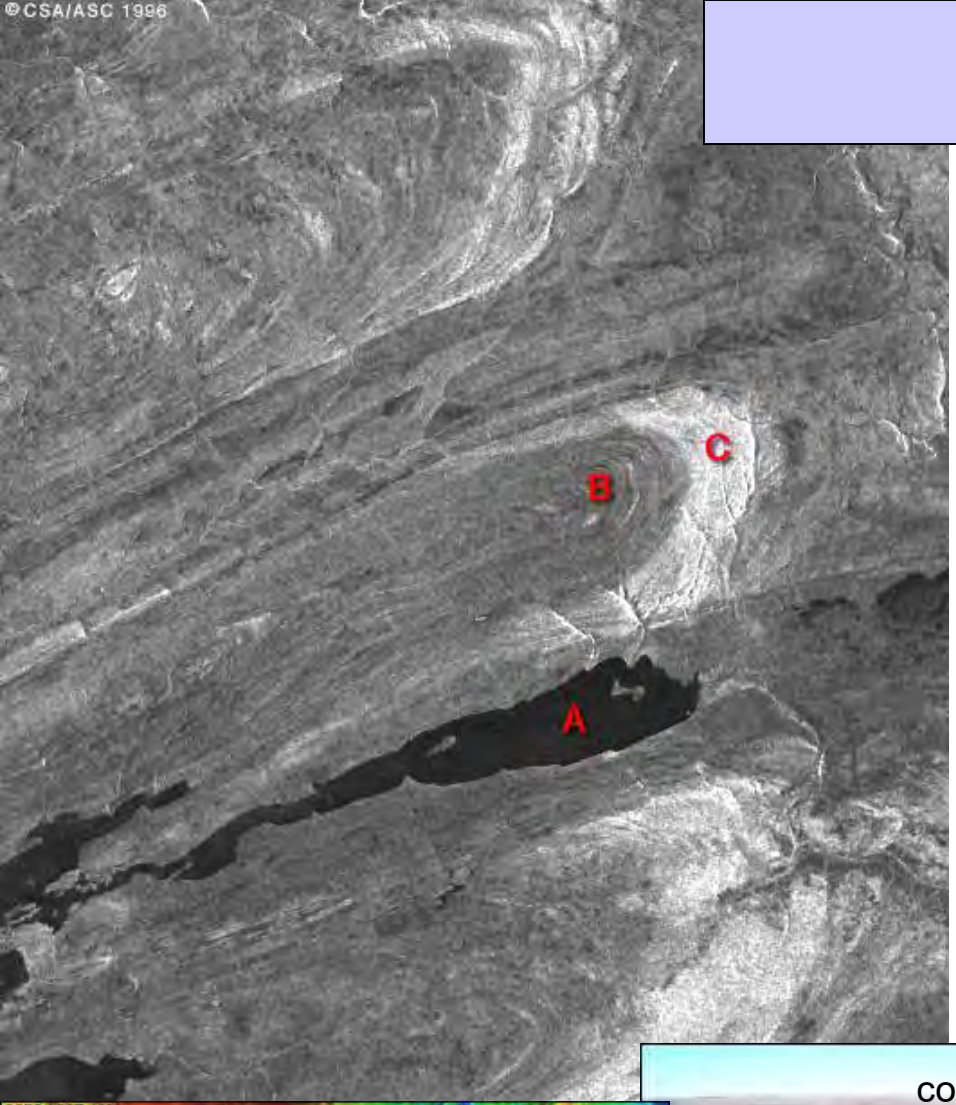

Canada

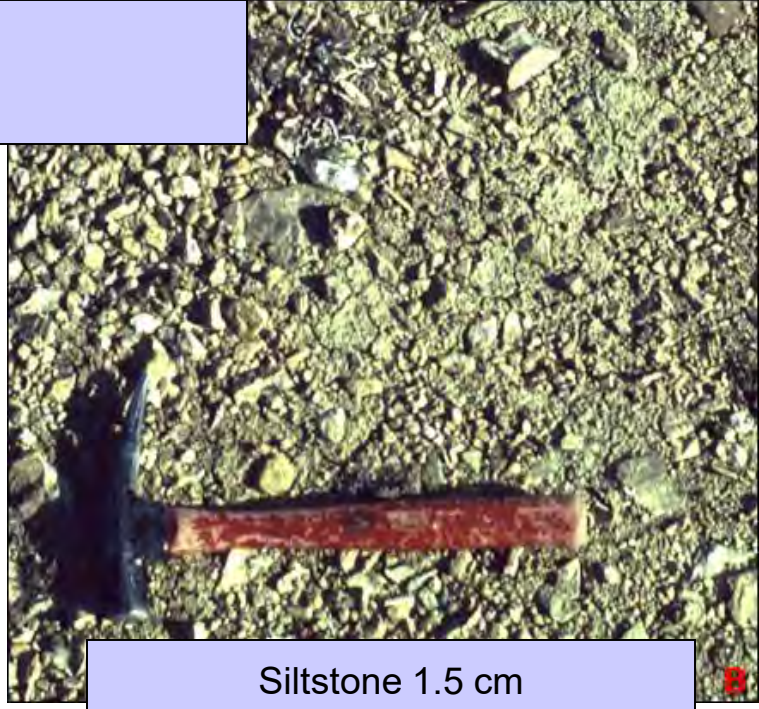

Siltstone 1.5 cm

limestone 4.5cm

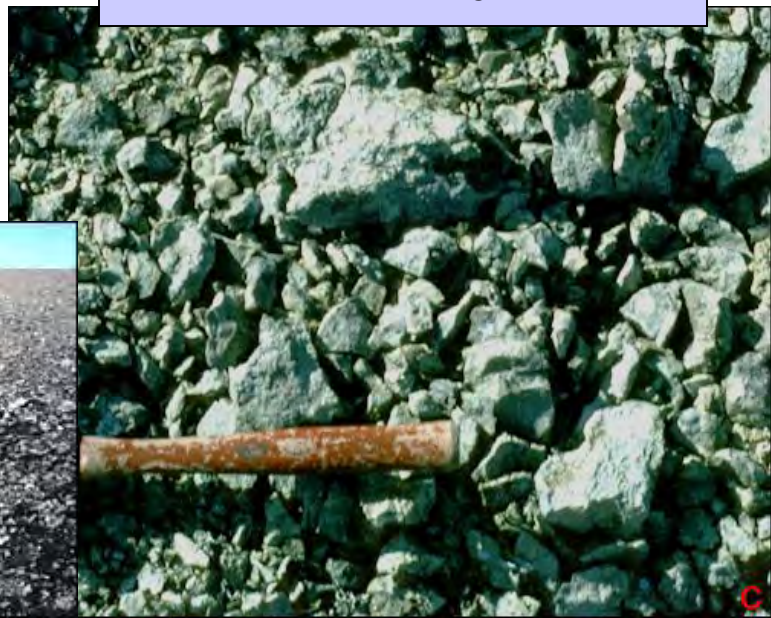

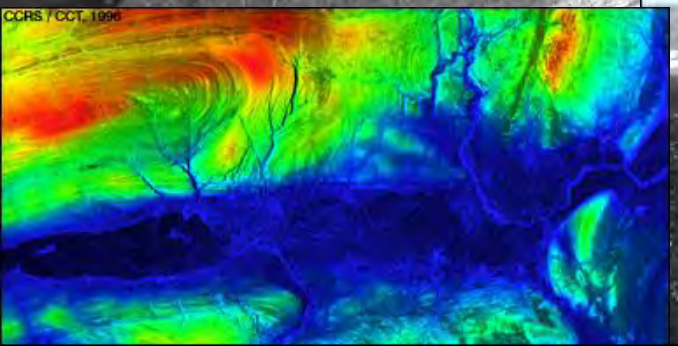

contact

Flooded areas monitoring

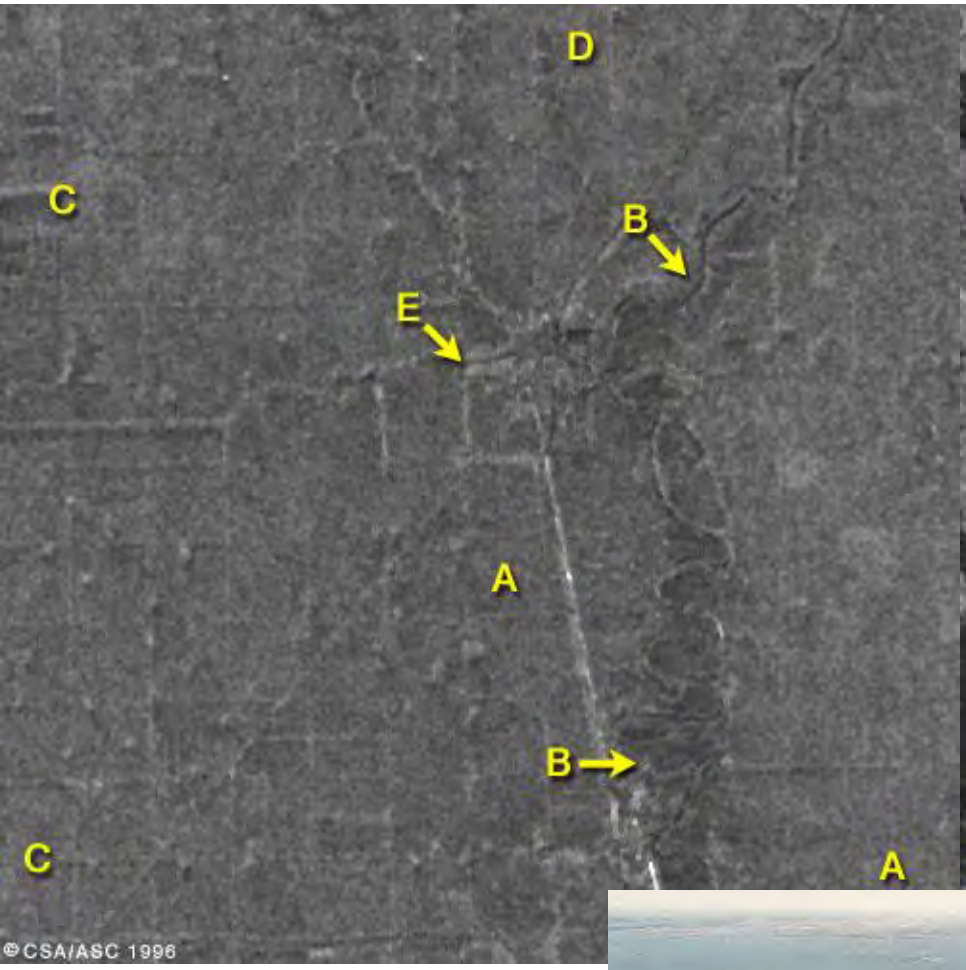

March 23 1996

The Red River, China

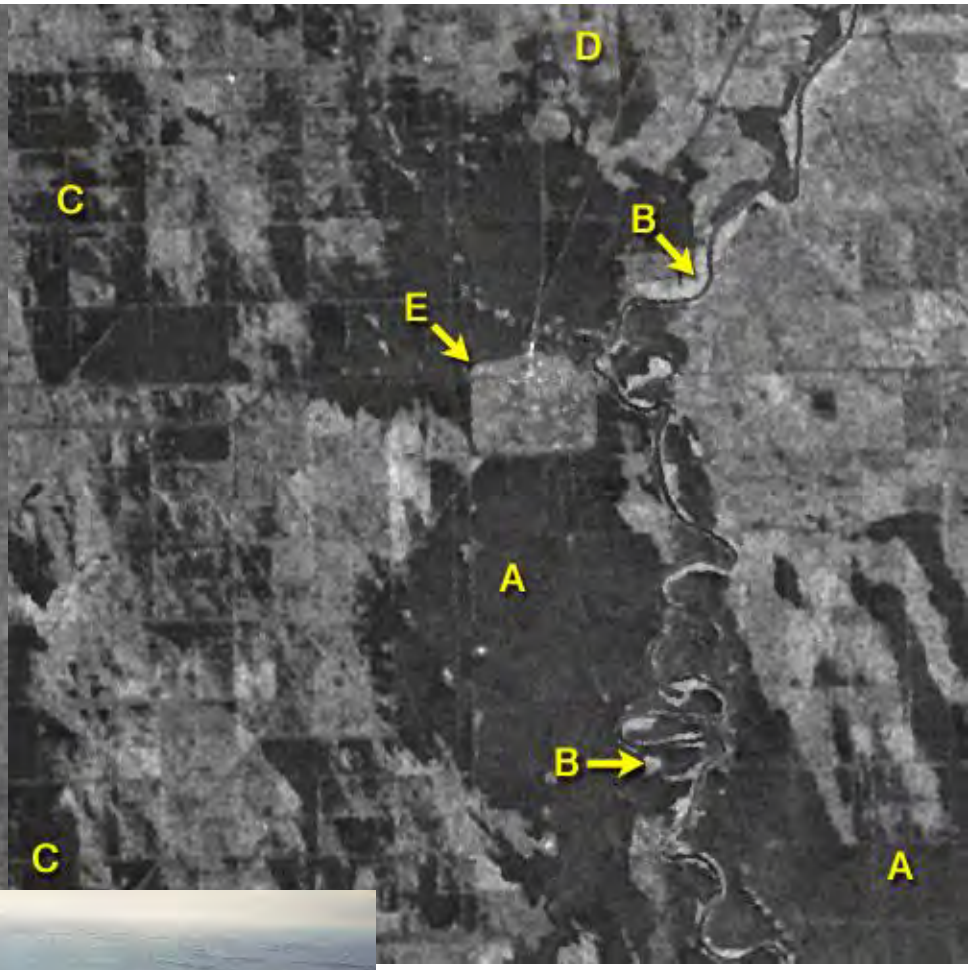

April 25 1996

Penetration effect

Radar ERS optical

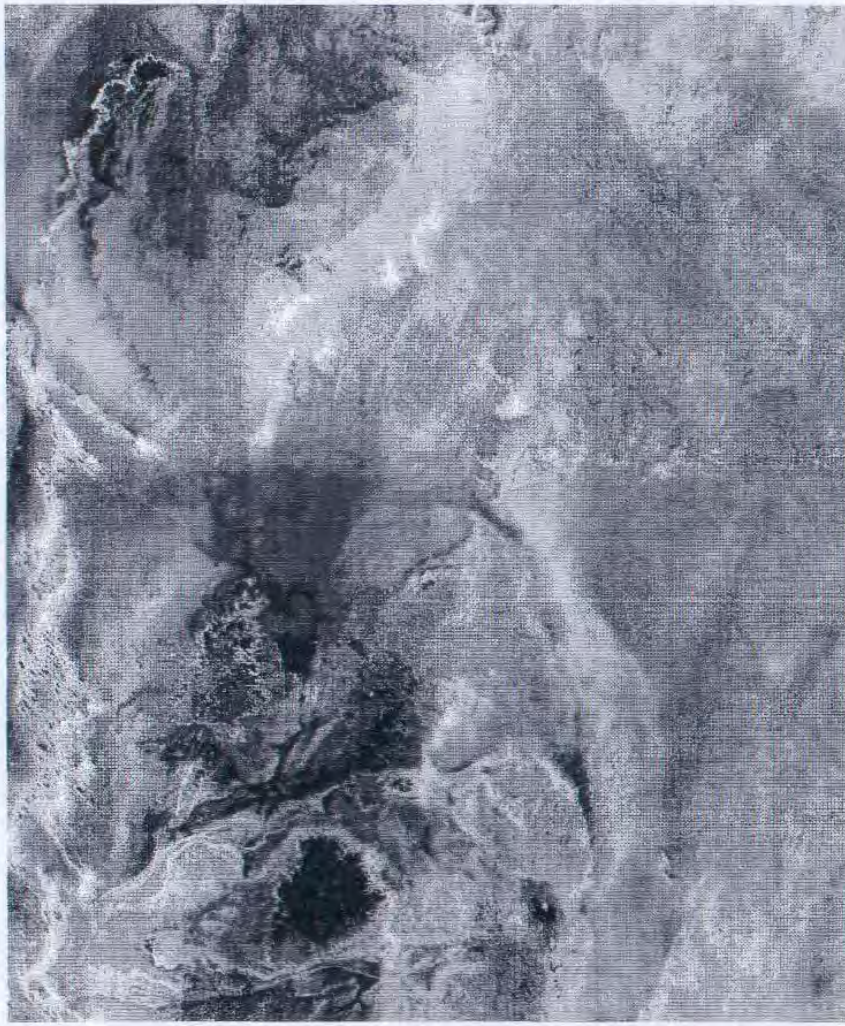

"Tin Erkri" Ain Cheikr Oued Tamanrasset

Desert Algeria

Effect of penetration

SIR A
band L

The Chott El Jerid, Tunisia

A vast evaporitic (80 x 120 km) area

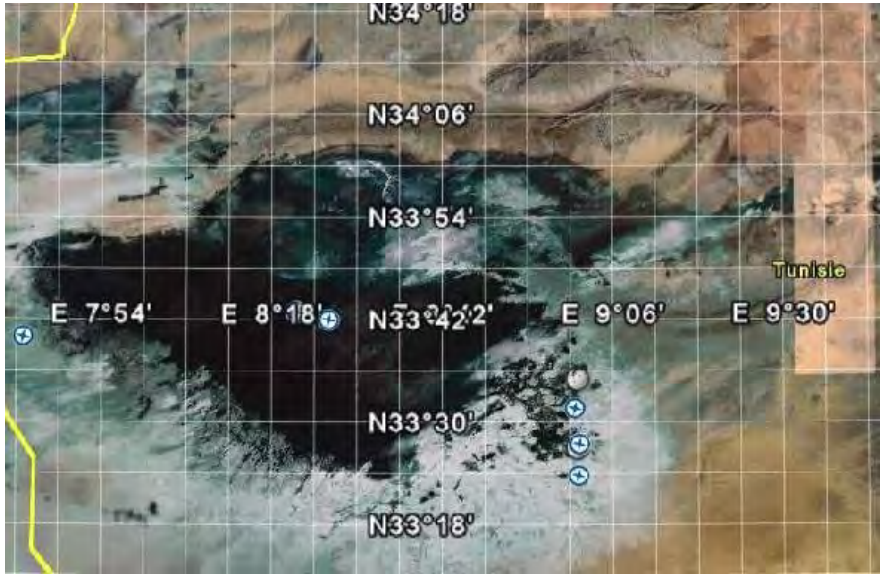

Discharge playa from a major aquifere
(upward percolation)

+

occasional runoff from neighbouring playa (Fedjadj).

➔ ***Temporary flooding***

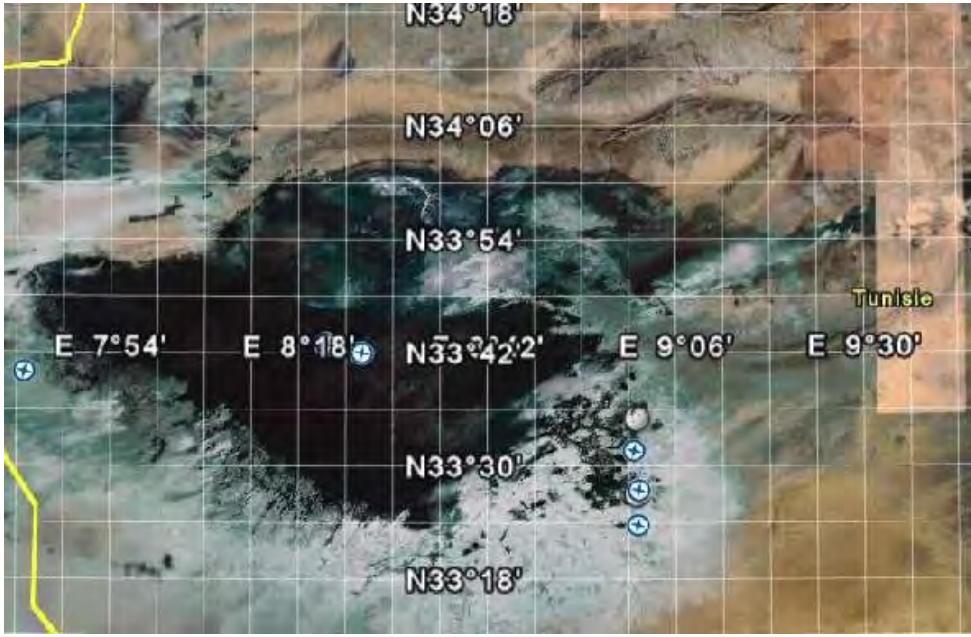

Playas: Evaporites (saline deposits)

Flooded / dry surface

Wettest months

sudden smoothing due to dissolution of saline crust

+ dramatic change of diel. const. (saline solution)

Summer months:

evaporation ➔ halite crystal growth ➔ increase of roughness

Lab and ground measurements, Death Valley
(roughness, dielectric constant)

ASCAT temporal signature over the **Chott el Jerid**

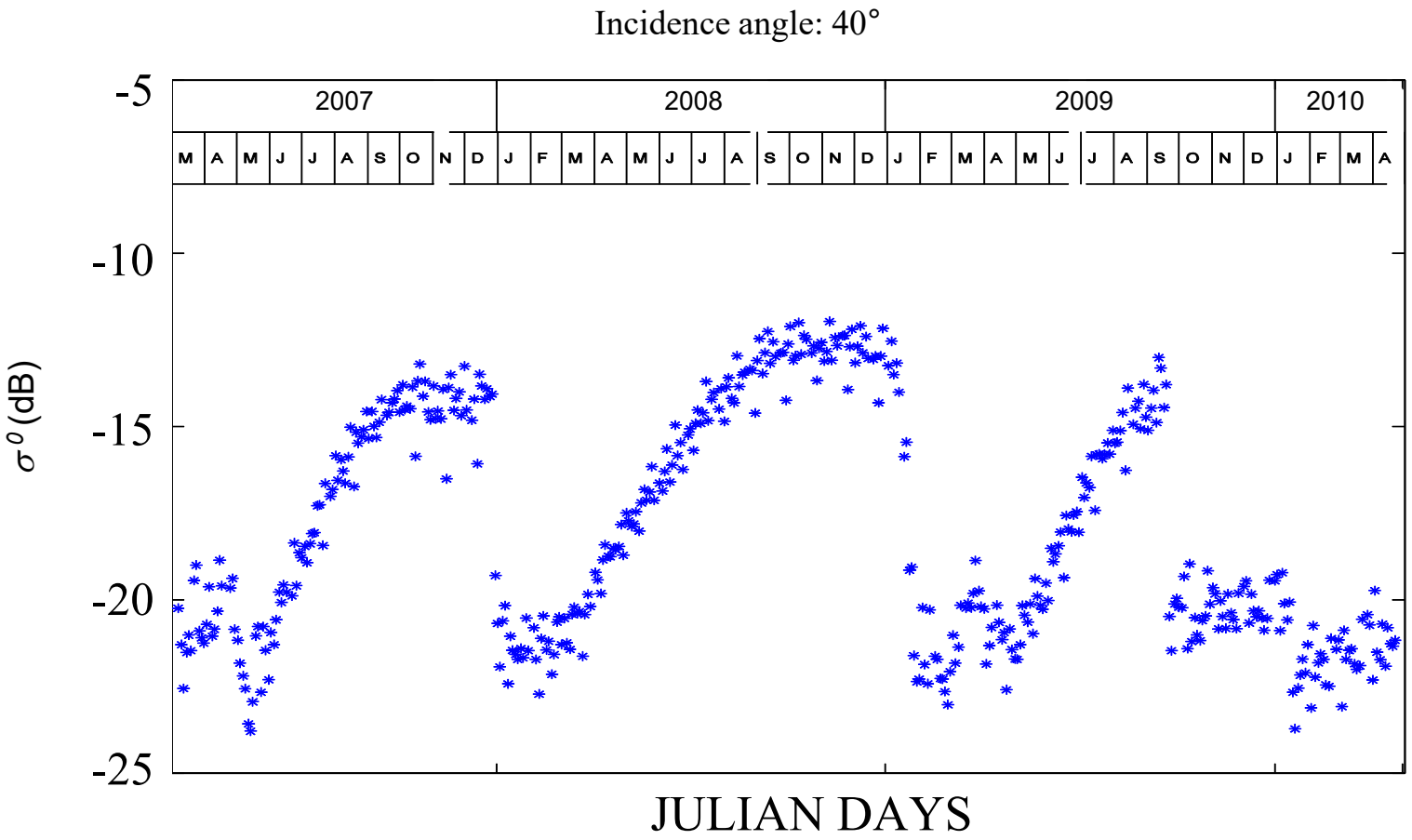

High temporal dynamic (> 10 dB)

Linked to environment seasonal variations

ASCAT temporal signature over the **Chott el Jerid**

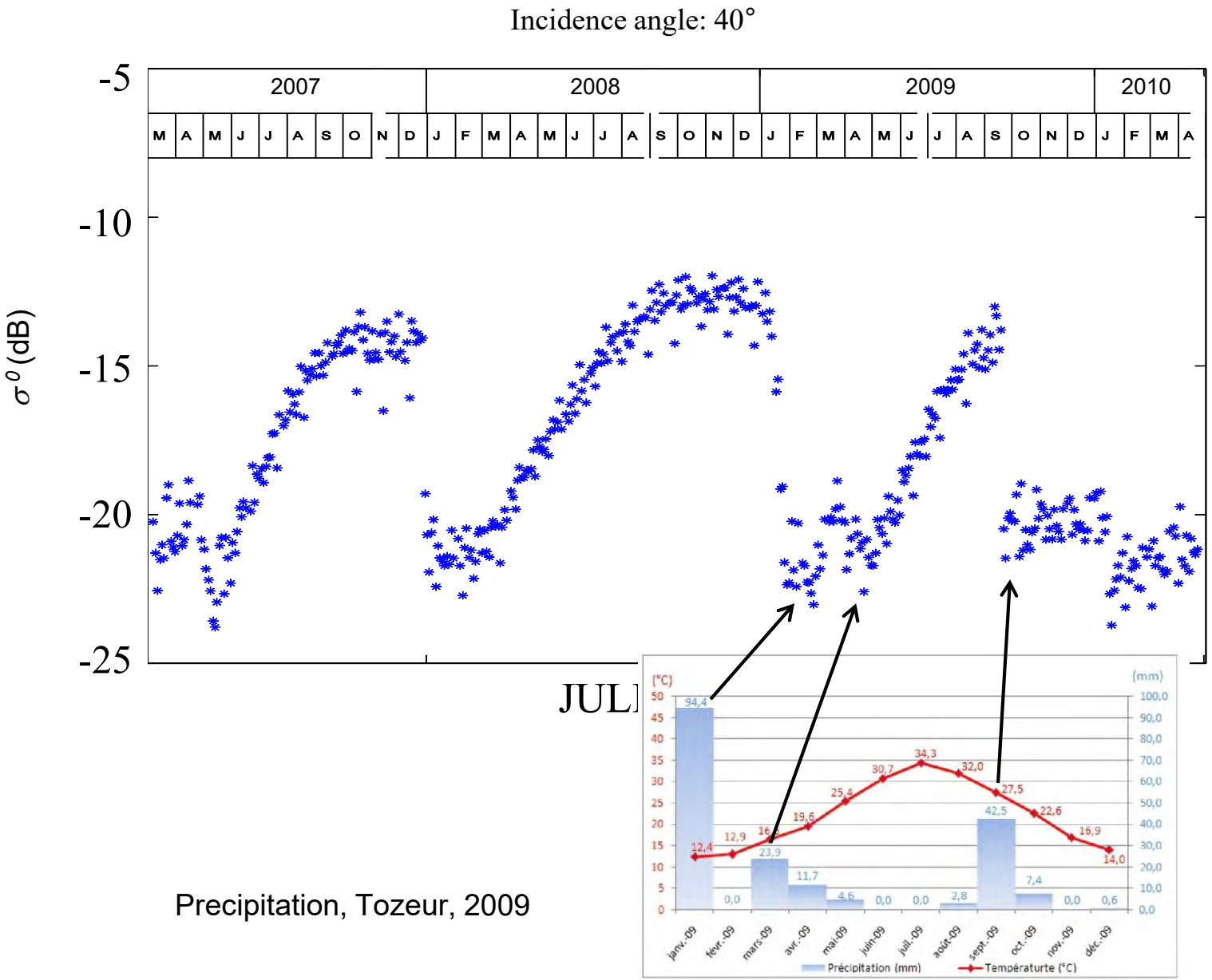

Precipitation, Tozeur, 2009

ASCAT/ASAR temporal signature over the **Chott el Jerid**

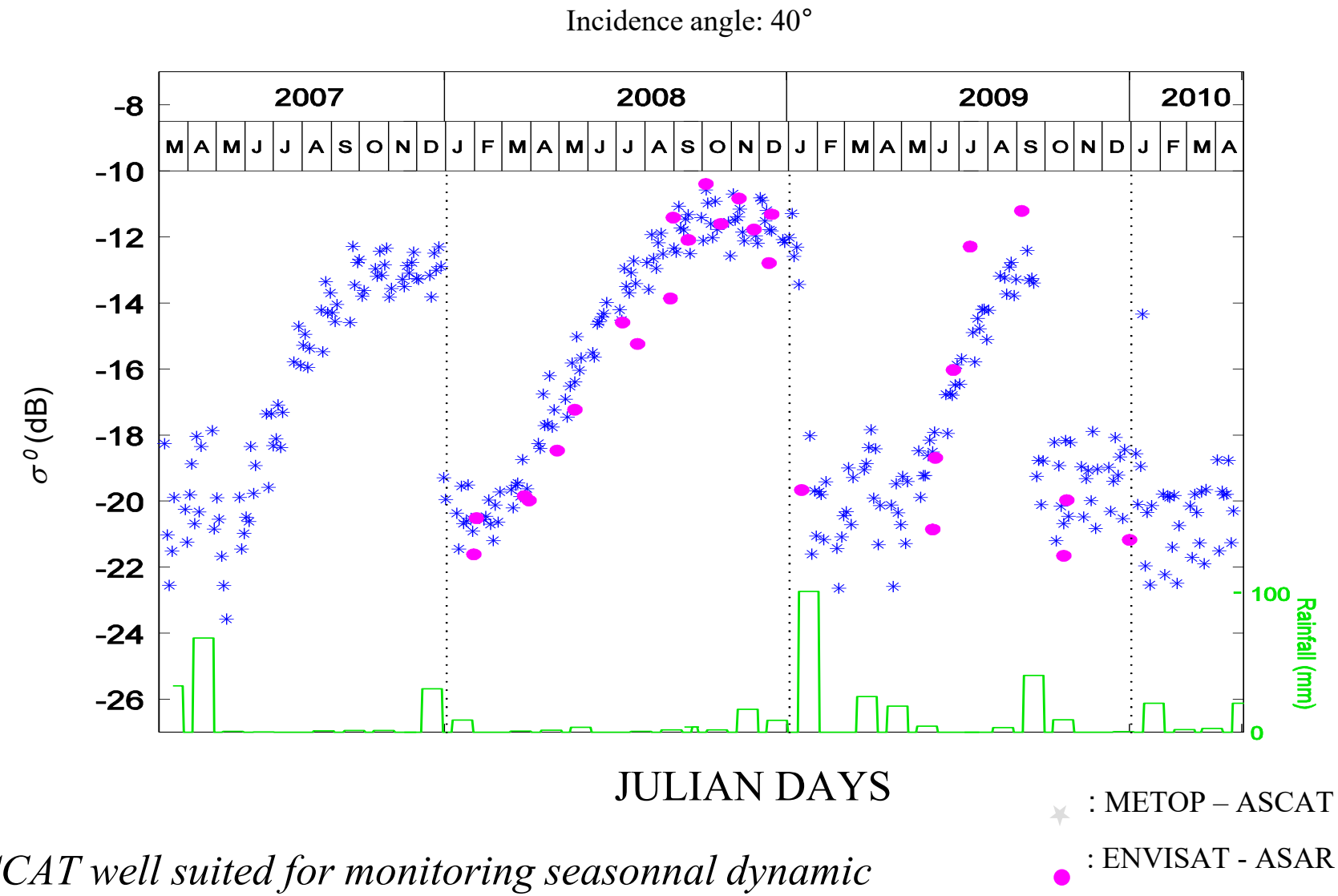

ASCAT well suited for monitoring seasonnal dynamic

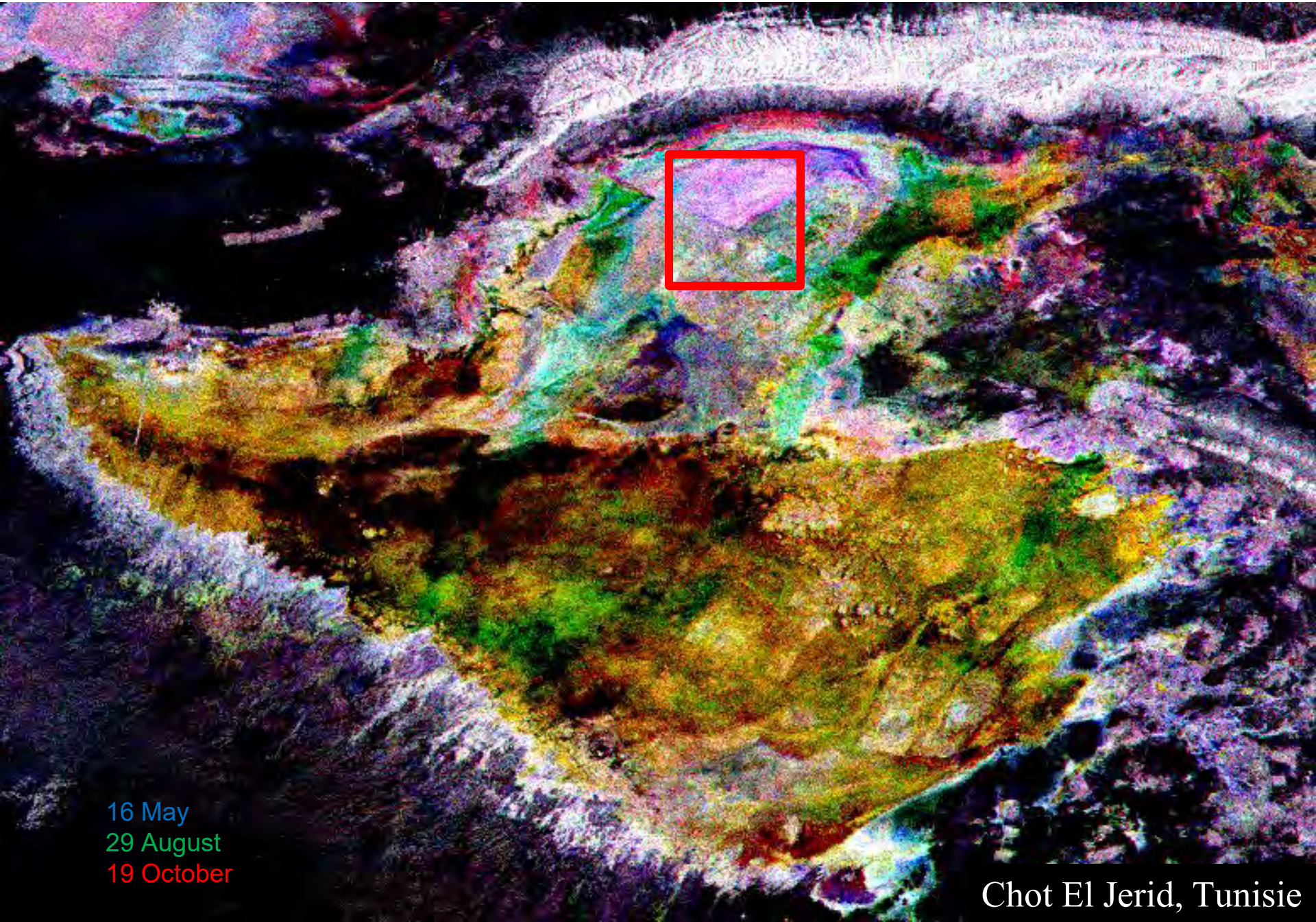
16 May
29 August
19 October
Chot El Jerid, Tunisie

Polarimetric data classification

Chott El Djerid

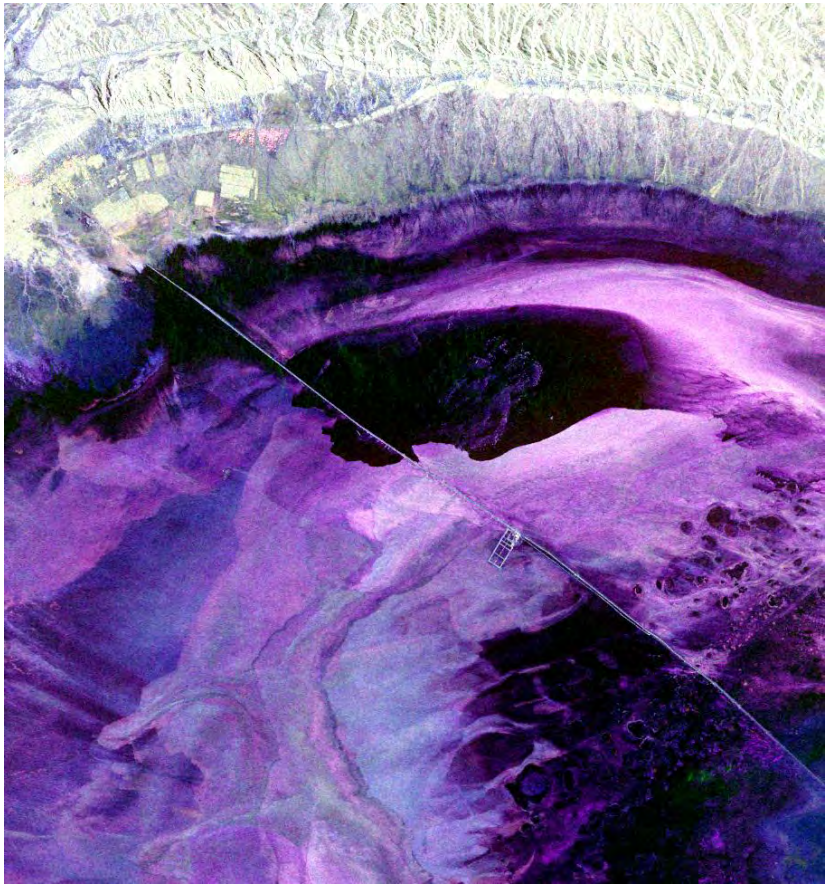

Decomposition de Pauli

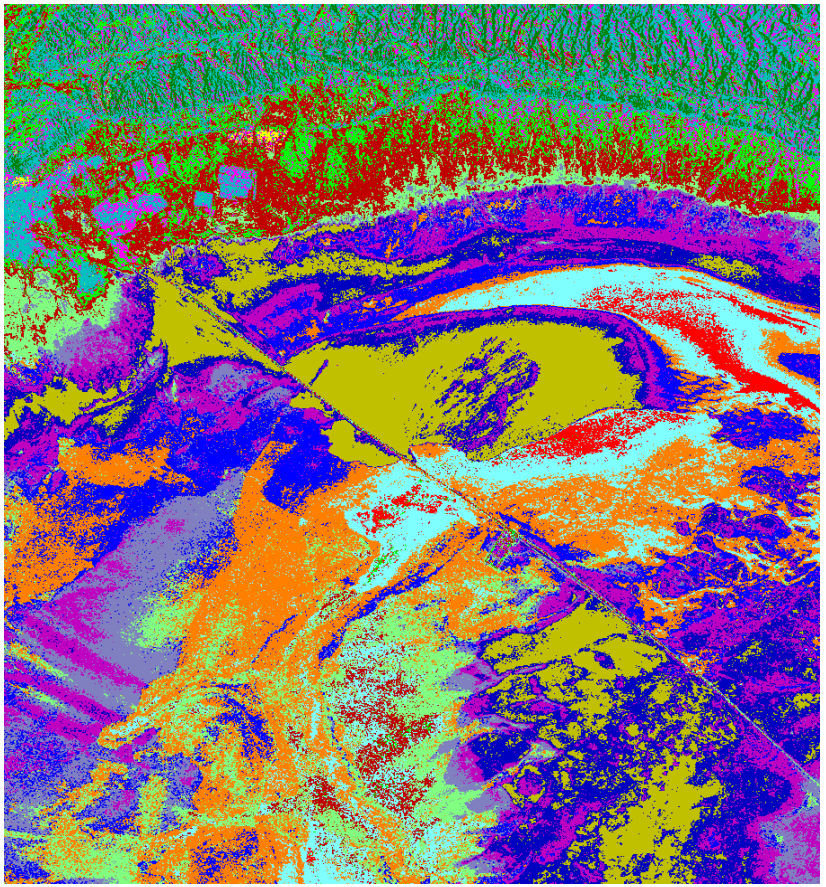

Classification H/A/alpha

Radarsat-2 - 17 avril 2009

Radar response sensitivity

Over vegetation

Volume scattering

Radar images interpretation rules

Volume scattering

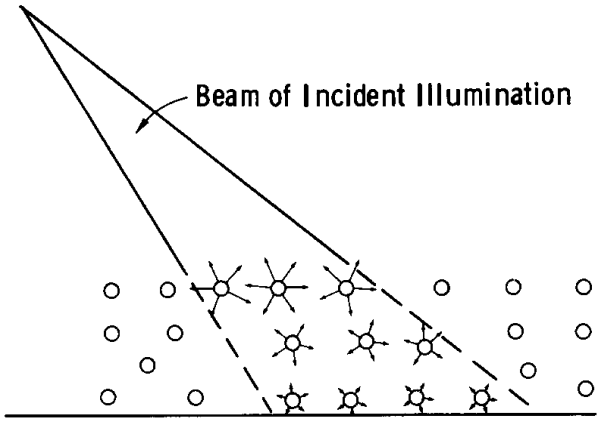

Inhomogeneous medium (vegetation cover)

each inhomogeneity (leaves, branches….)
scatters incident wave in all directio

Multiple scattering
+
Absorption
} ==> wave attenuation within the layer

Radar images interpretation rules

Volume scattering

Penetration Depth:

$$\delta = \frac{\lambda}{4\pi \ \mathrm{Im}(\sqrt{\varepsilon})}$$

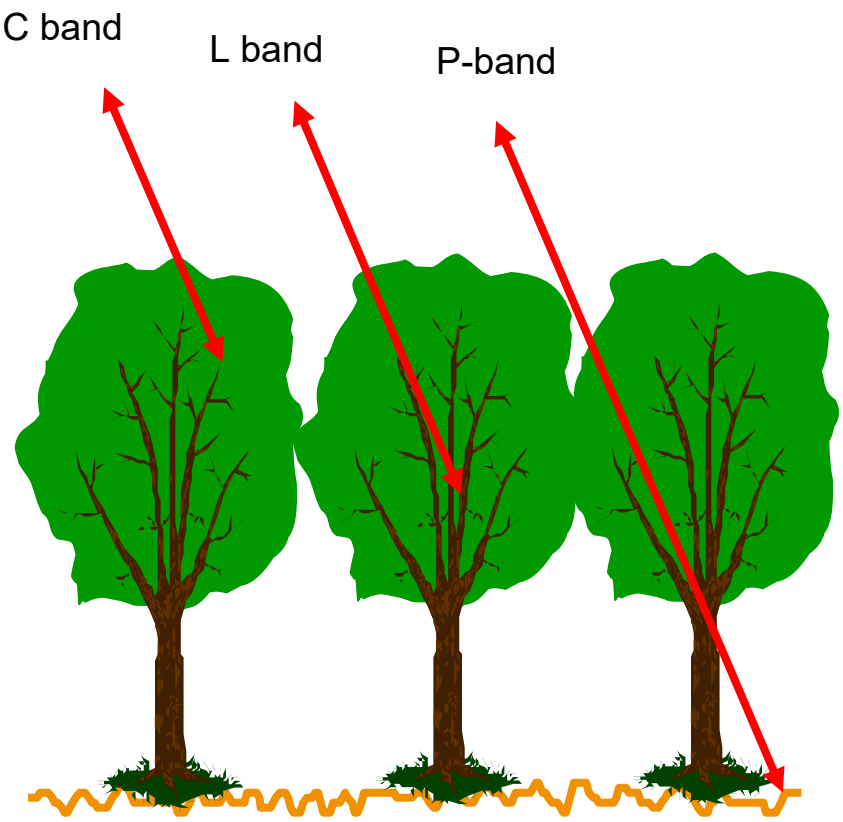

Penetration ↗ { Biomass ↘ ; wavelength ↗ }

Bande C

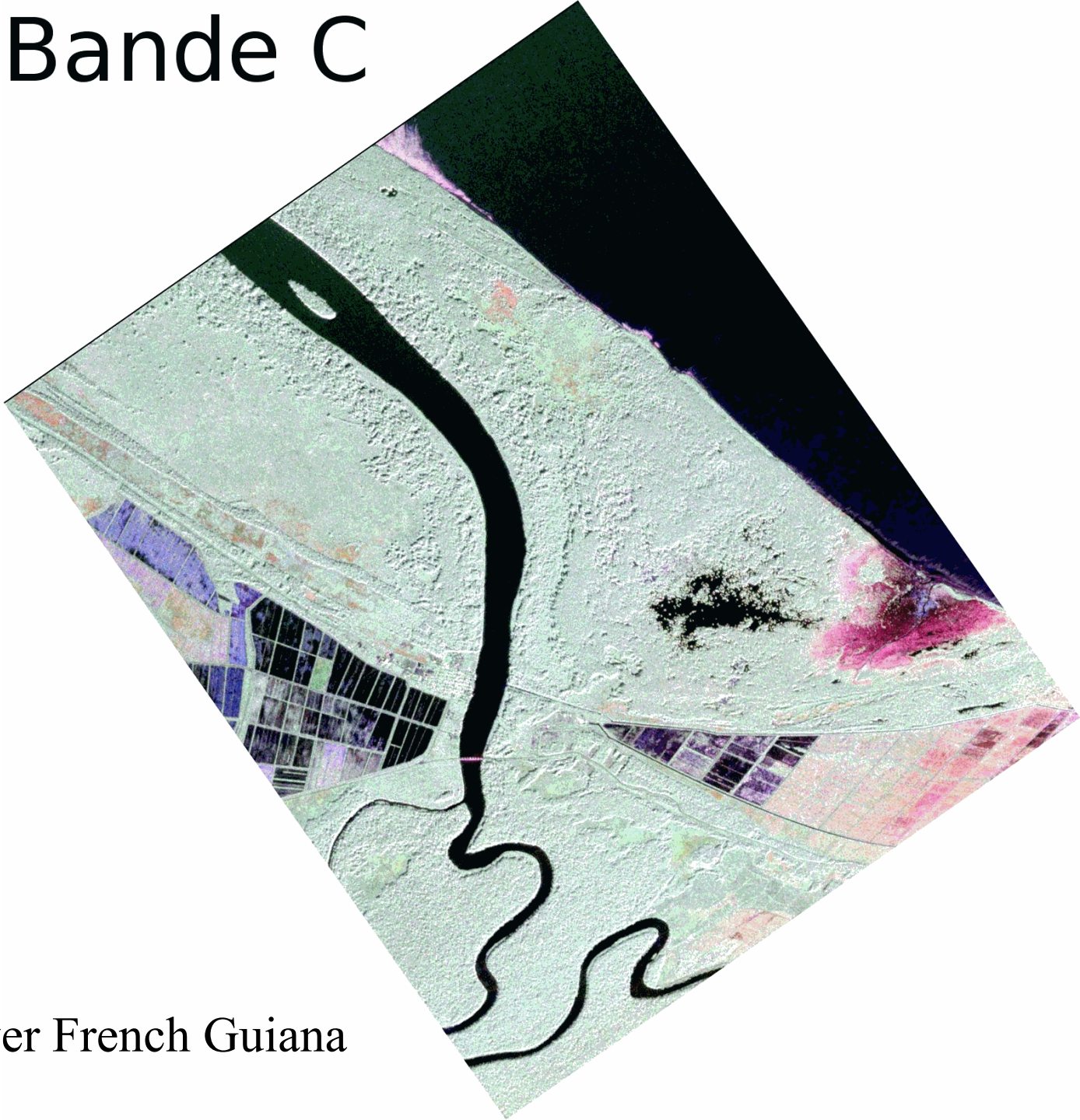

Radar response over French Guiana

Frequency - wavelength

Tubuai Island, Vegetation discrimination

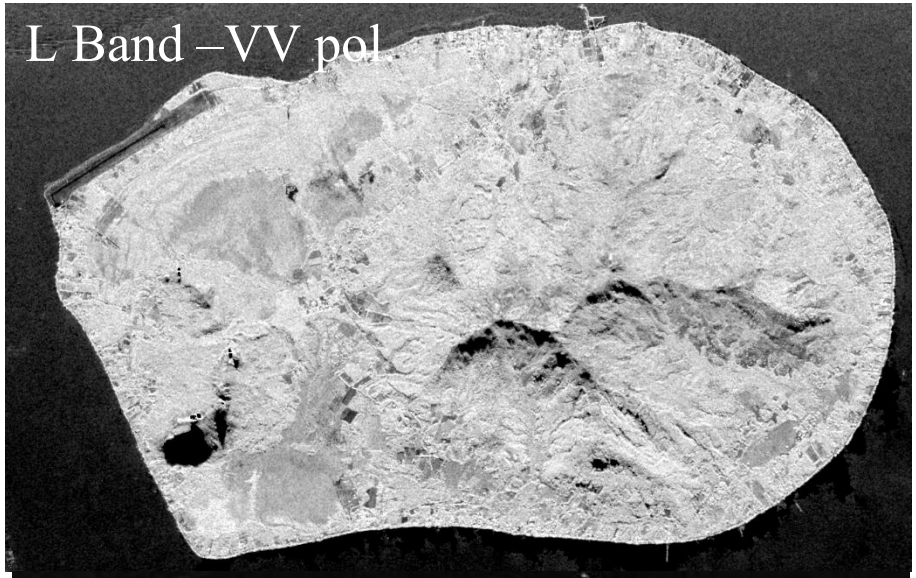

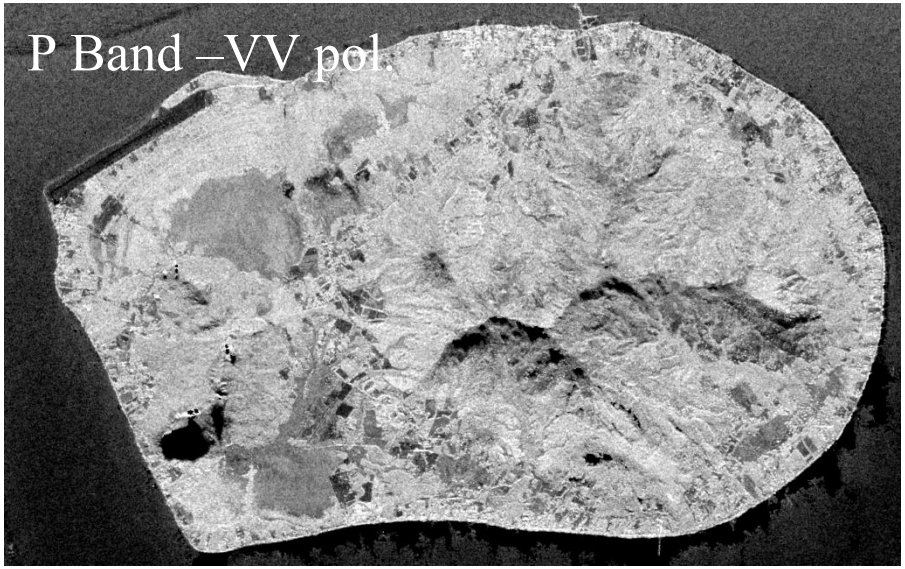

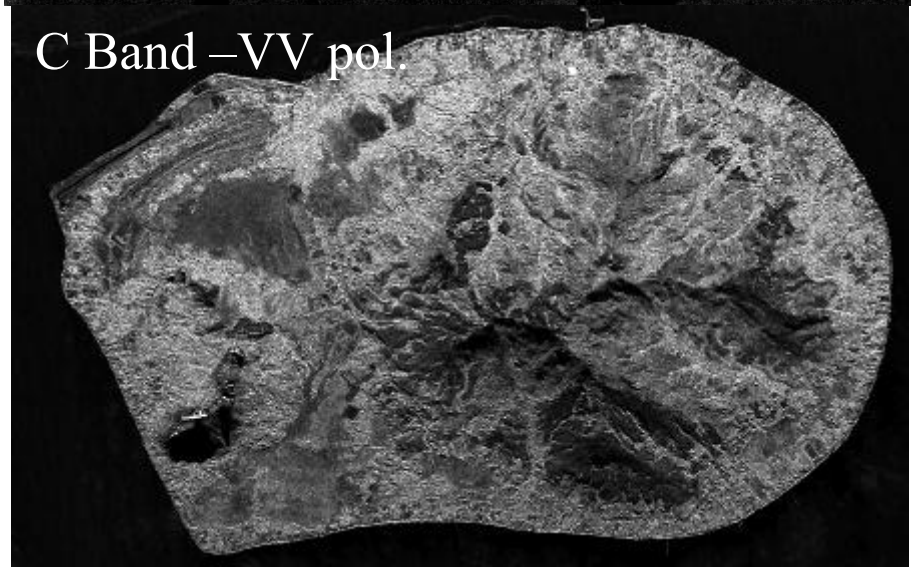

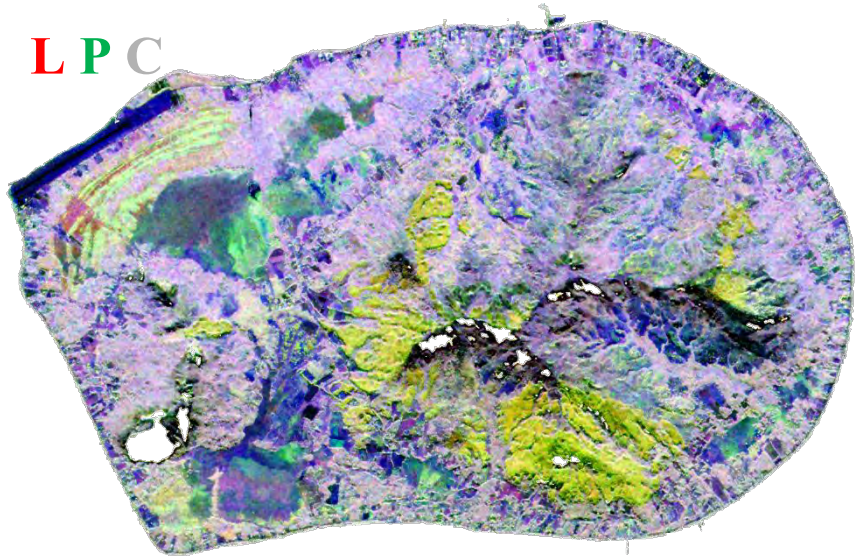

Radar response sensitivity

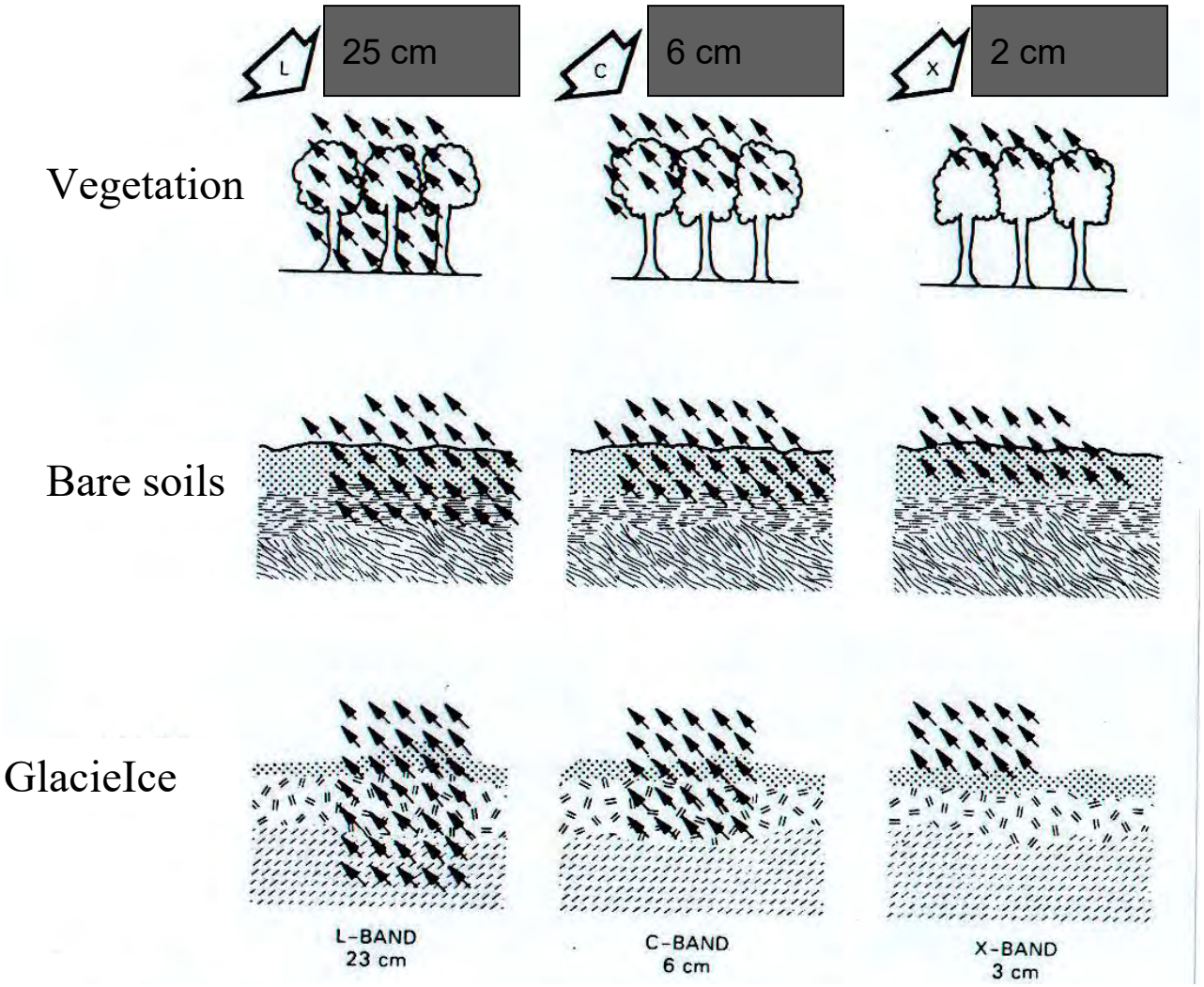

Penetration depth is proportional to λ

Radar images interpretation rules

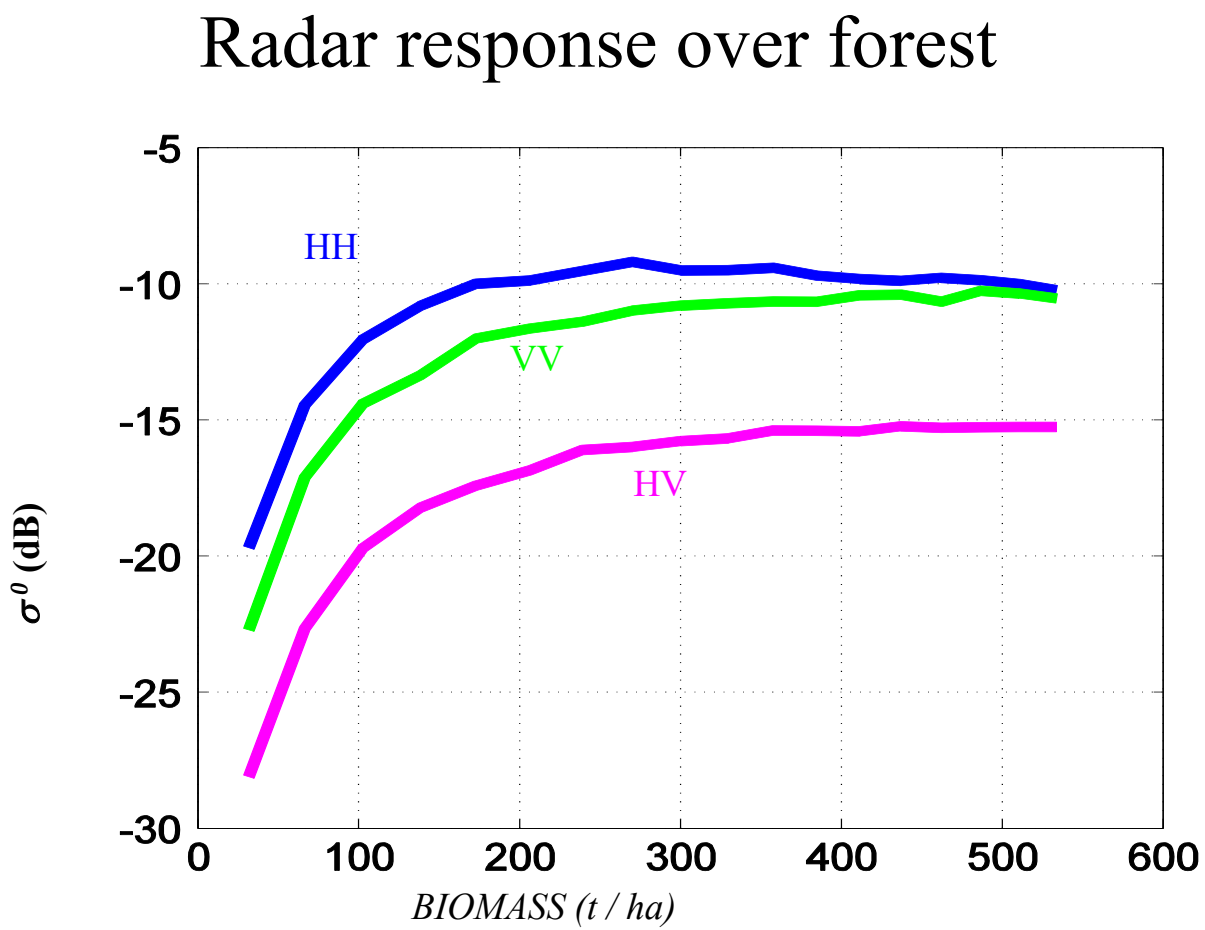

Volume Scattering

Radar saturation level with vegetation density

C band

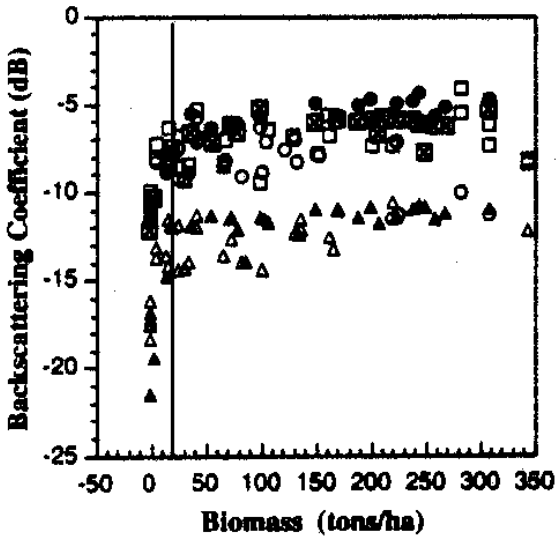

20 tons/ha

L band

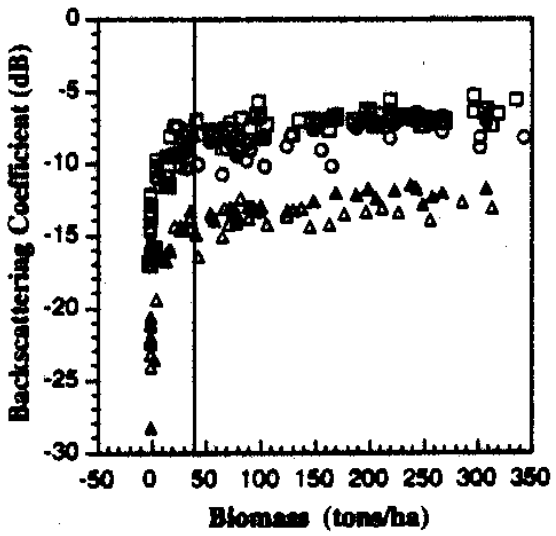

40 tons/ha

P band

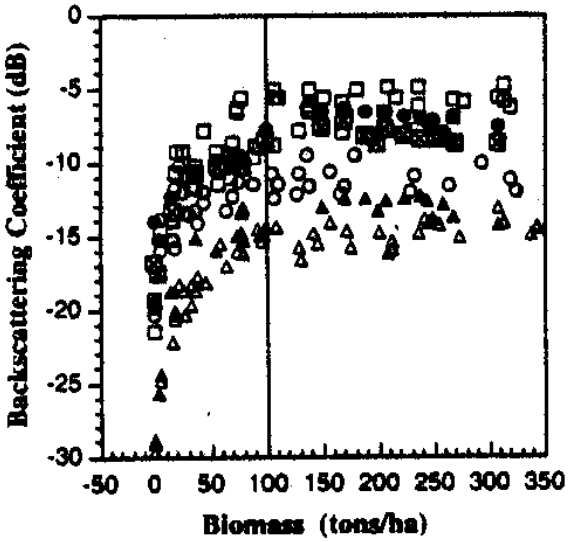

100 tons/ha

from Imhoff et al. 19?

Radar response sensitivity

Backscattering mechanism on vegetation

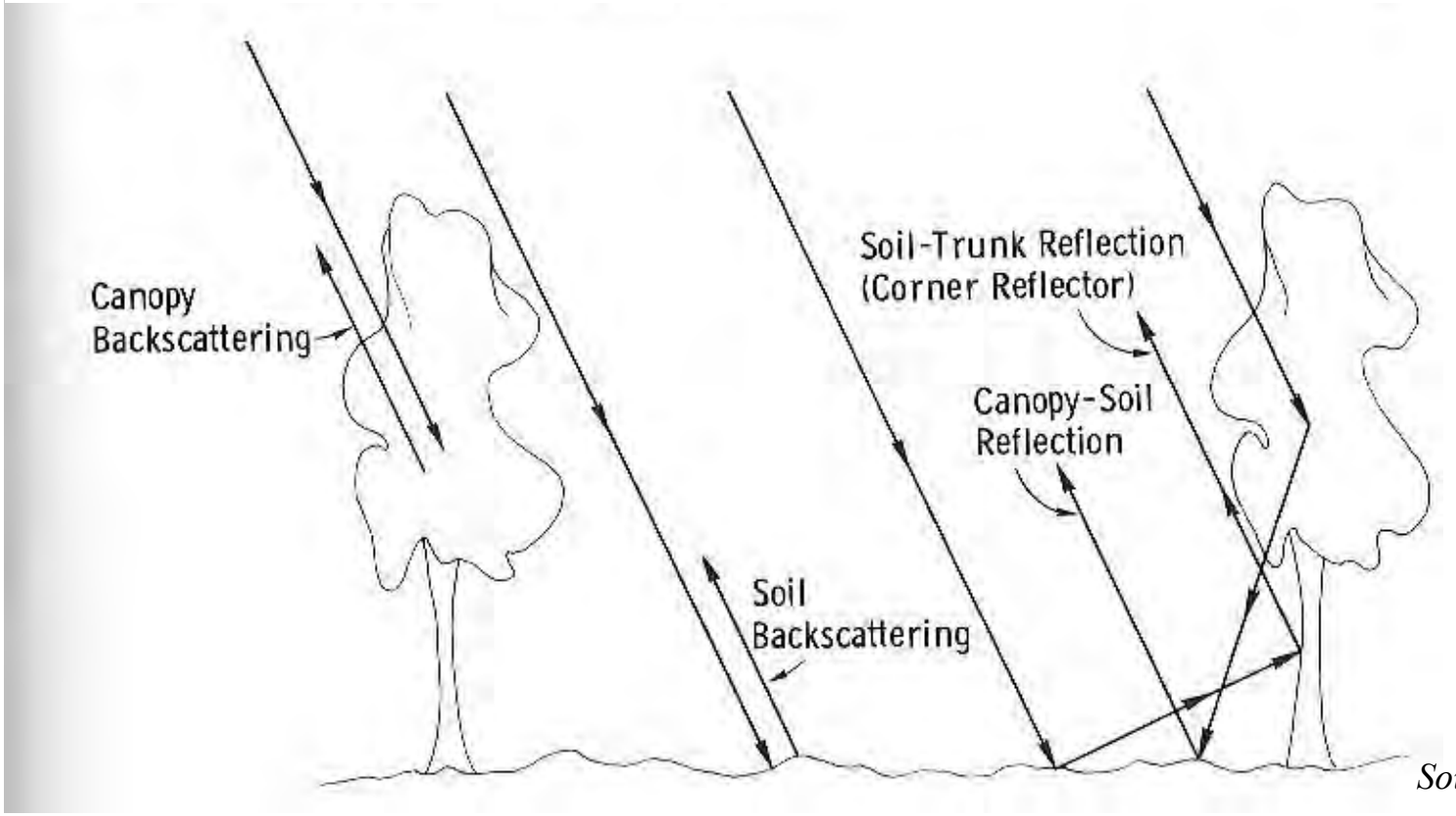

Source: Ulaby et al.

Land surfaces monitoring with radar data

Radar observations sensibility

- Biomass
- Structure and moisture of vegetation
- Roughness and moisture of soils

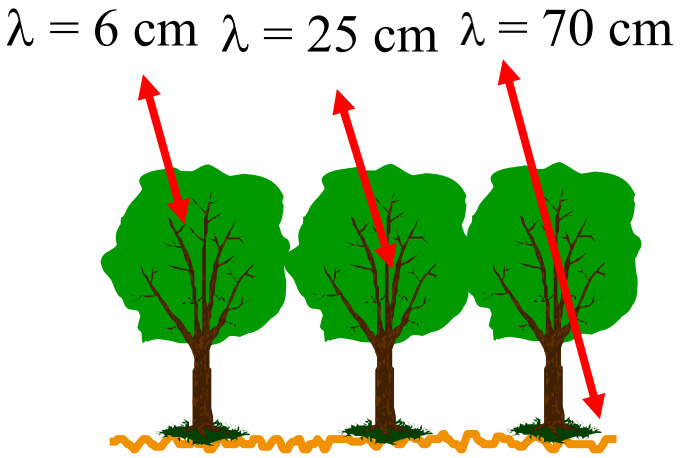

Access to key variables of ecosystem functionning

- Vegetation discrimination (type, espèces, état,….)
- Biomass (Net Primary Productivity)
- Vegetation phenology (periods of activity)
- Hydrological states of plant covers (stress, ….)
- Soil moisture

Radar response sensitivity

Local Agricultural Deforestation along road

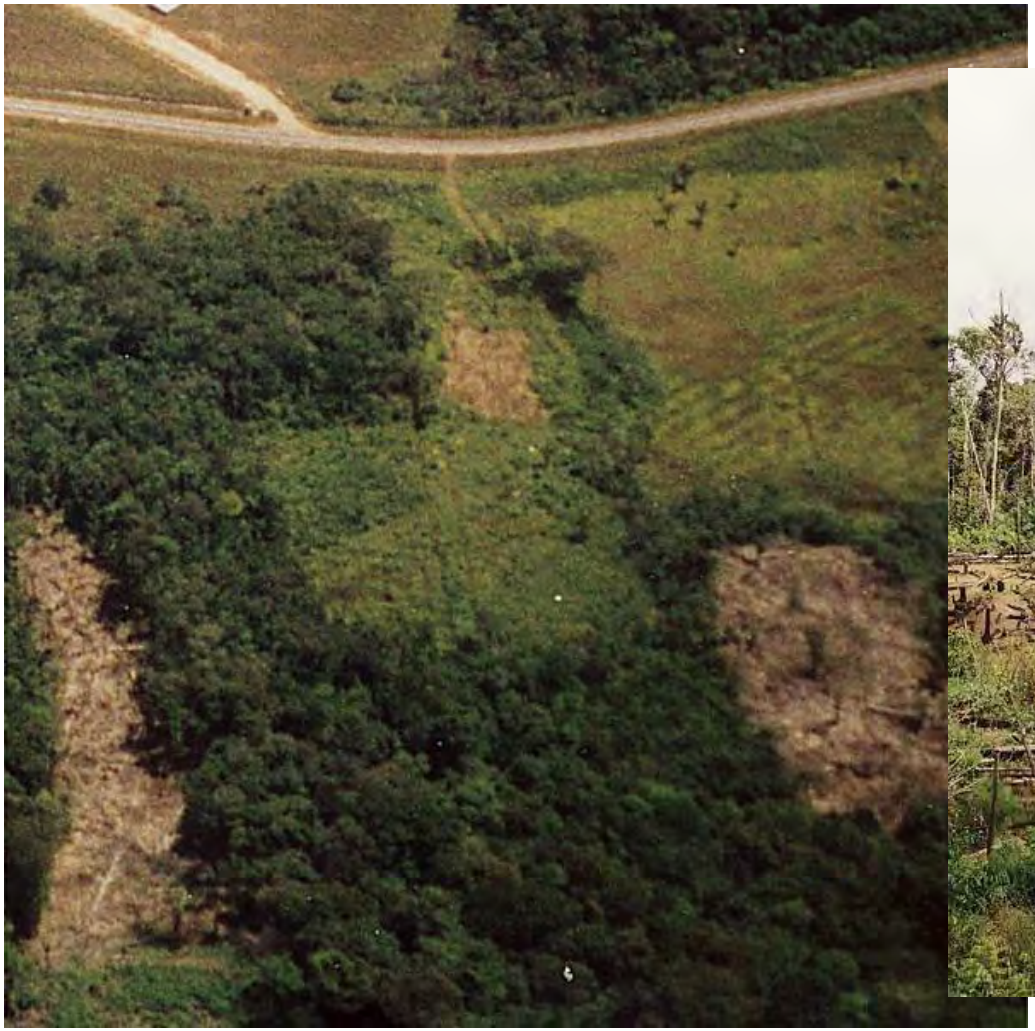

Radar response sensitivity

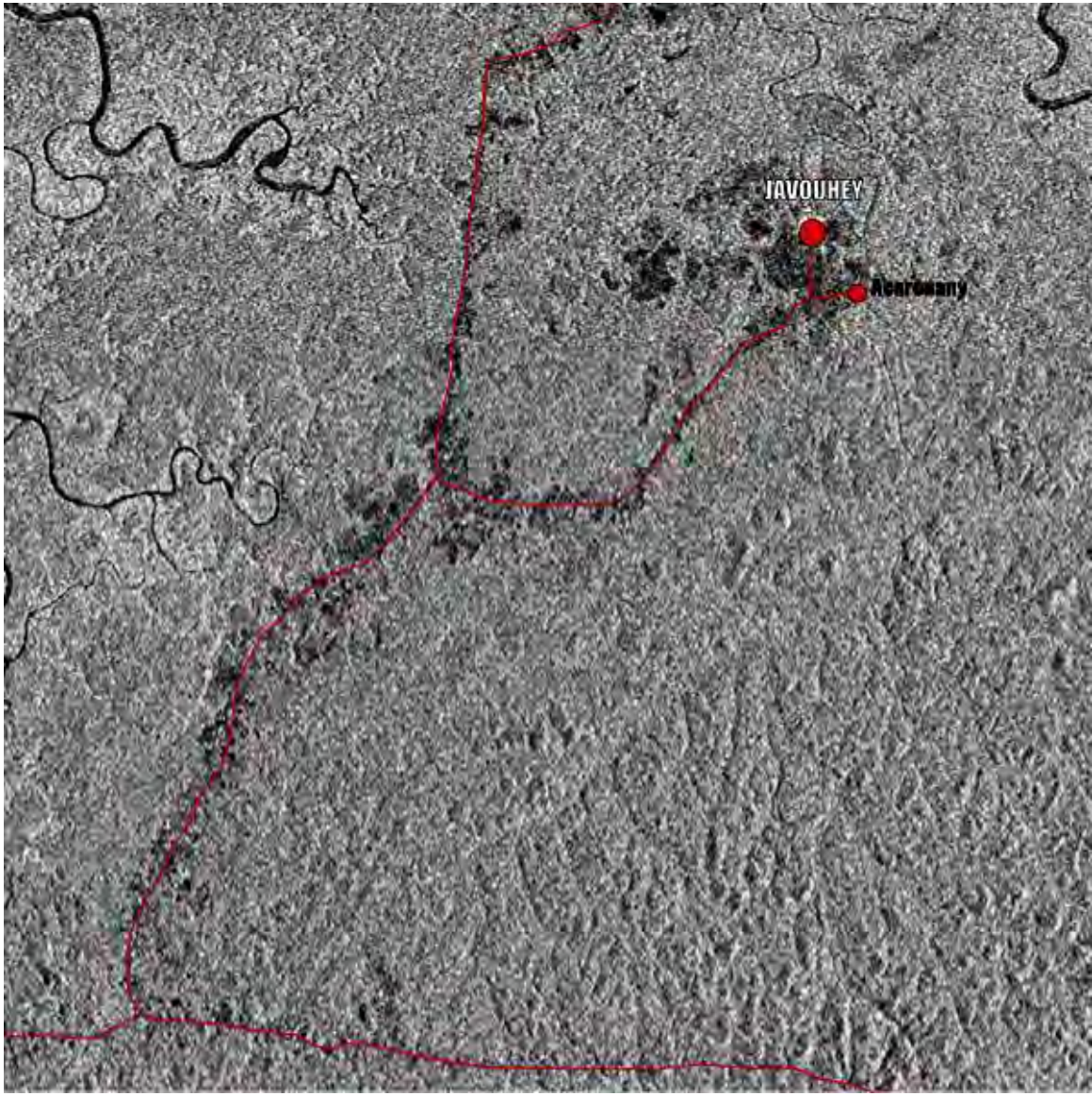

Radar response sensitivity

Cameroun (Ngaoundéré région : Cultural practice, burned area

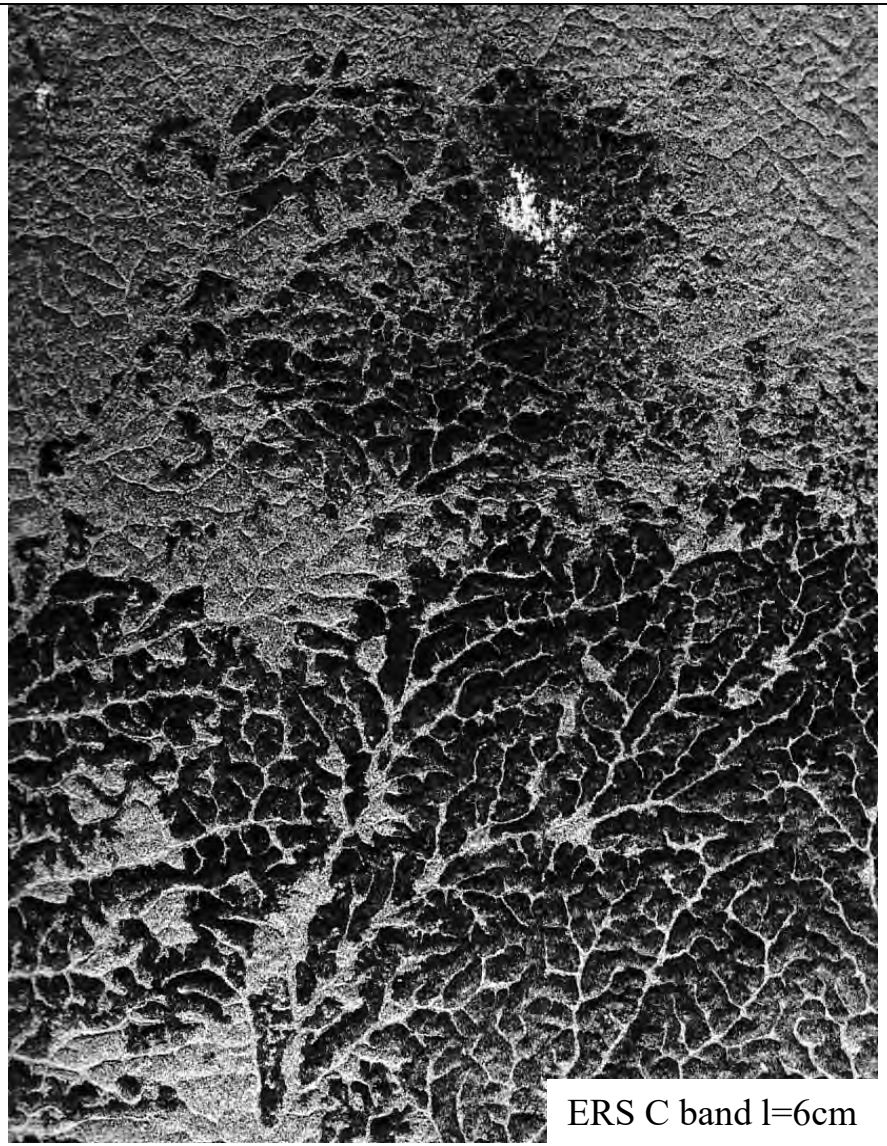

ERS C band l=6cm

JERS

λ = 25cm

Dry season

Wet season

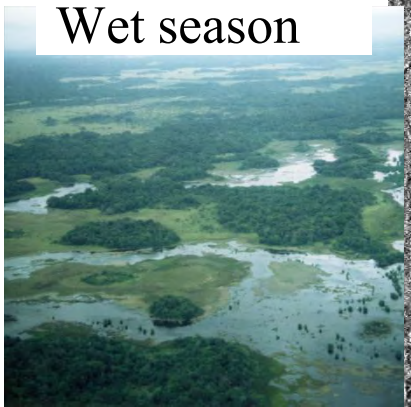

ERS

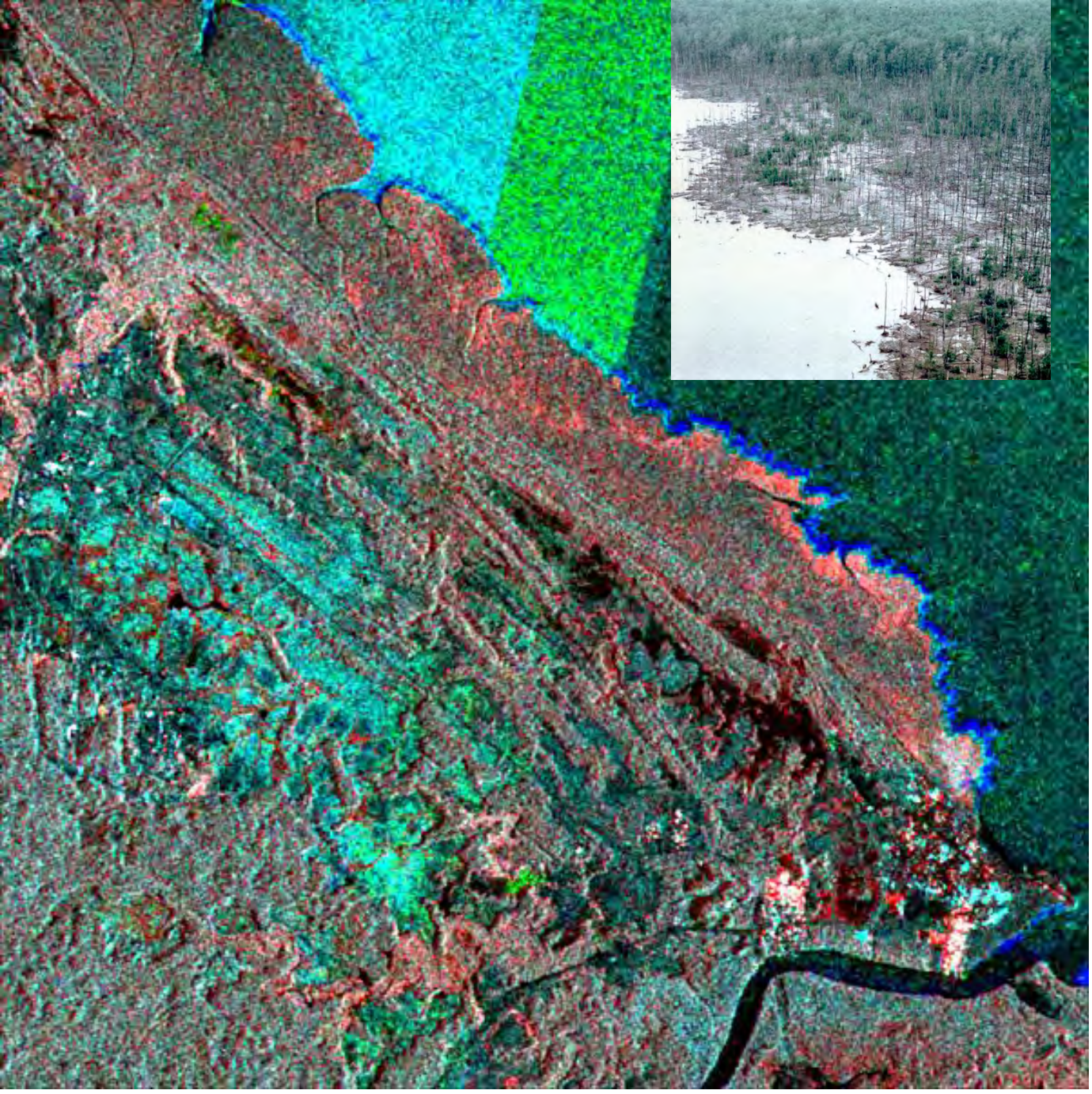

Color Composite

ERS and **JERS**

Radar response sensitivity

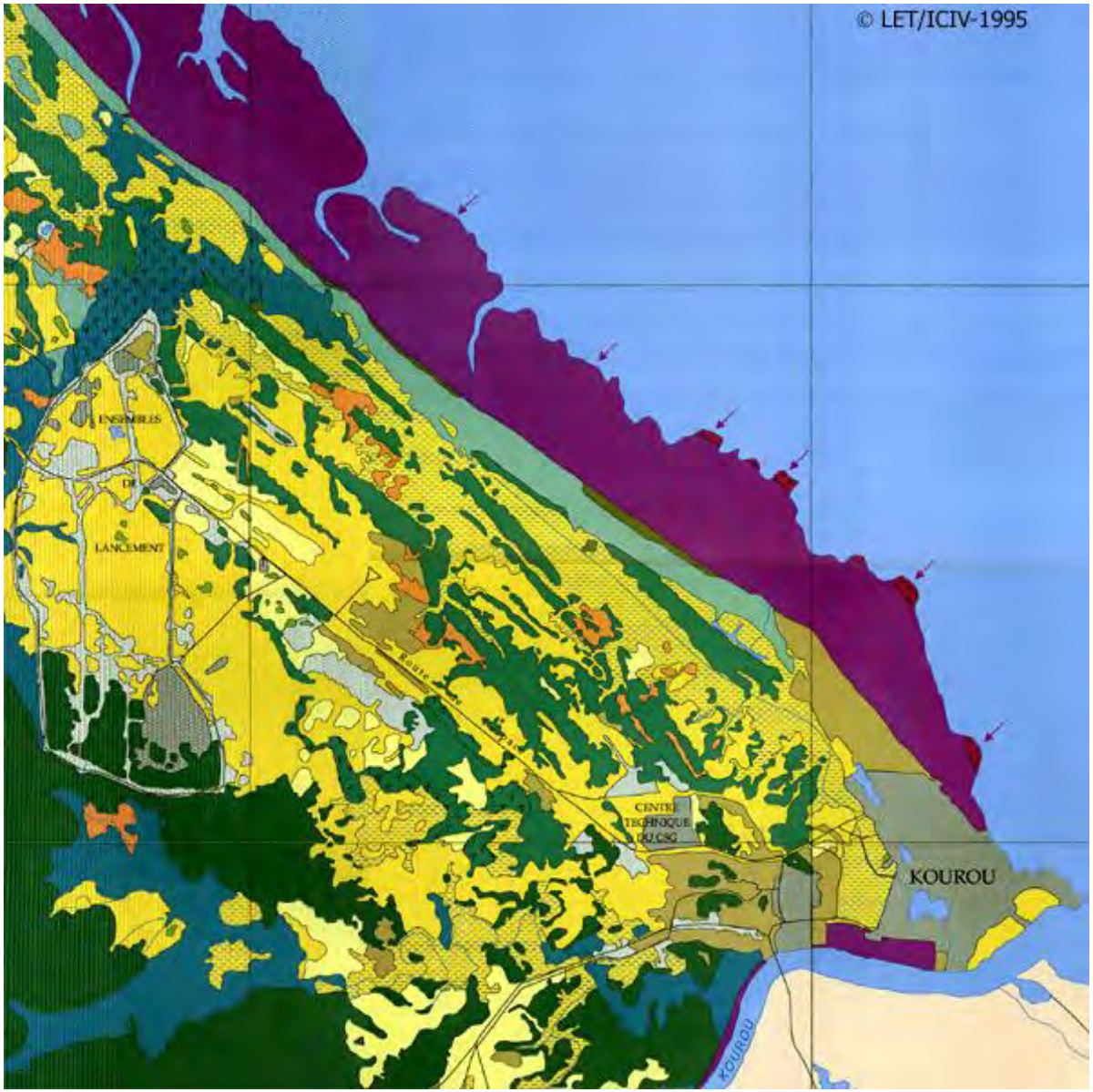

Radar response sensitivity

Temporal evolution monitoring
All weather: no seasonnal constraint

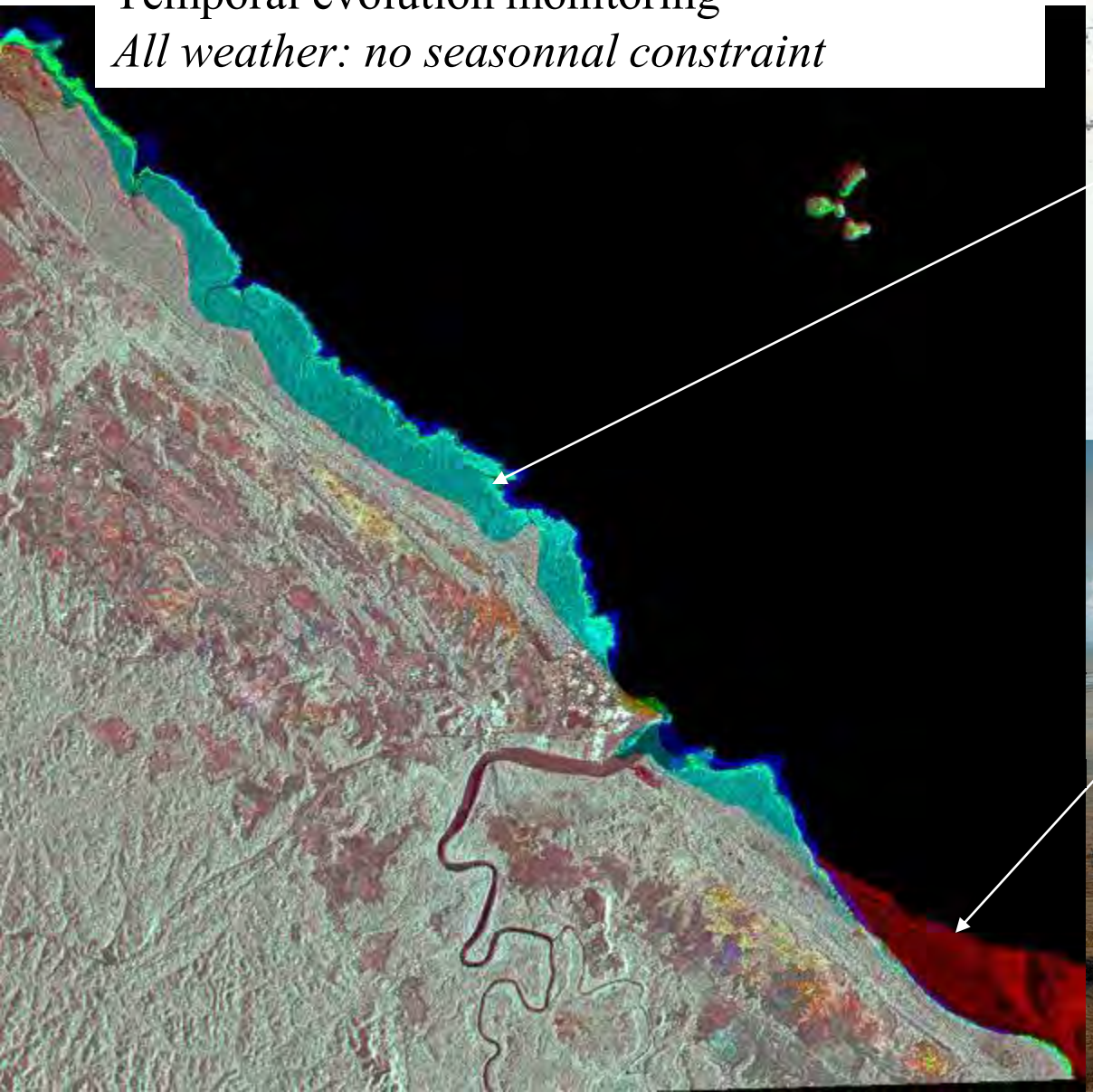

Érosion

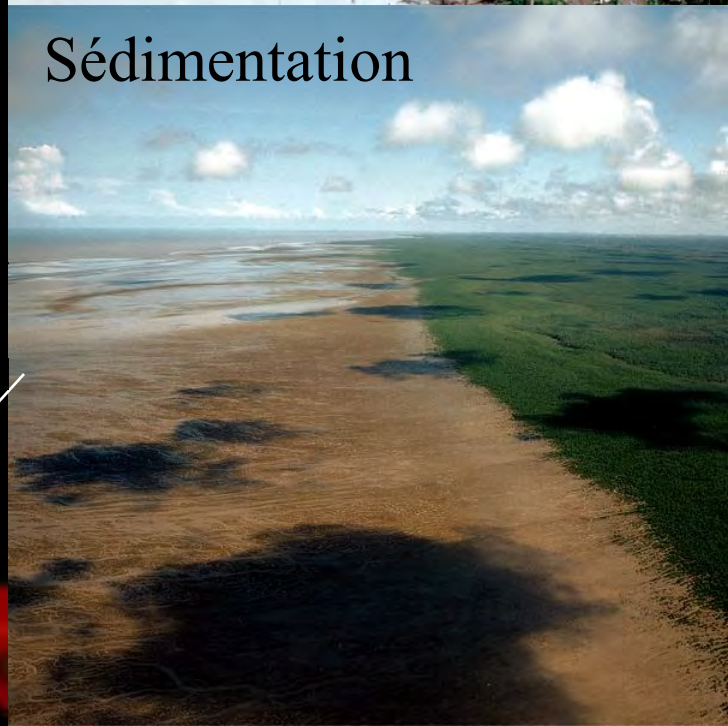

Sédimentation

Radar response sensitivity

2000: Update of the marine map

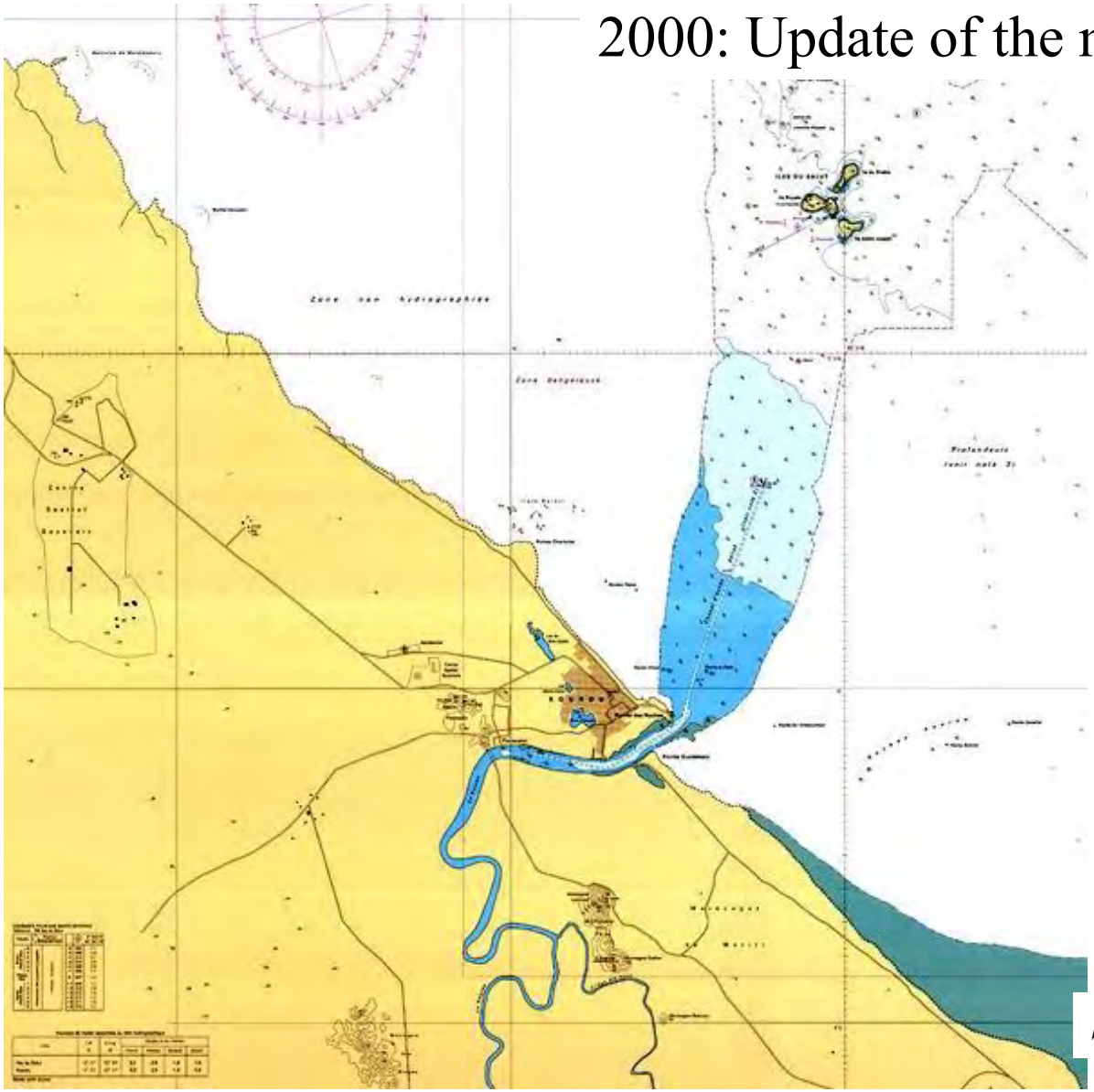

Source: SHOM/ Univ-MLV

Seasonal variations monitoring (Sahel)

ASAR (λ = 6 cm)

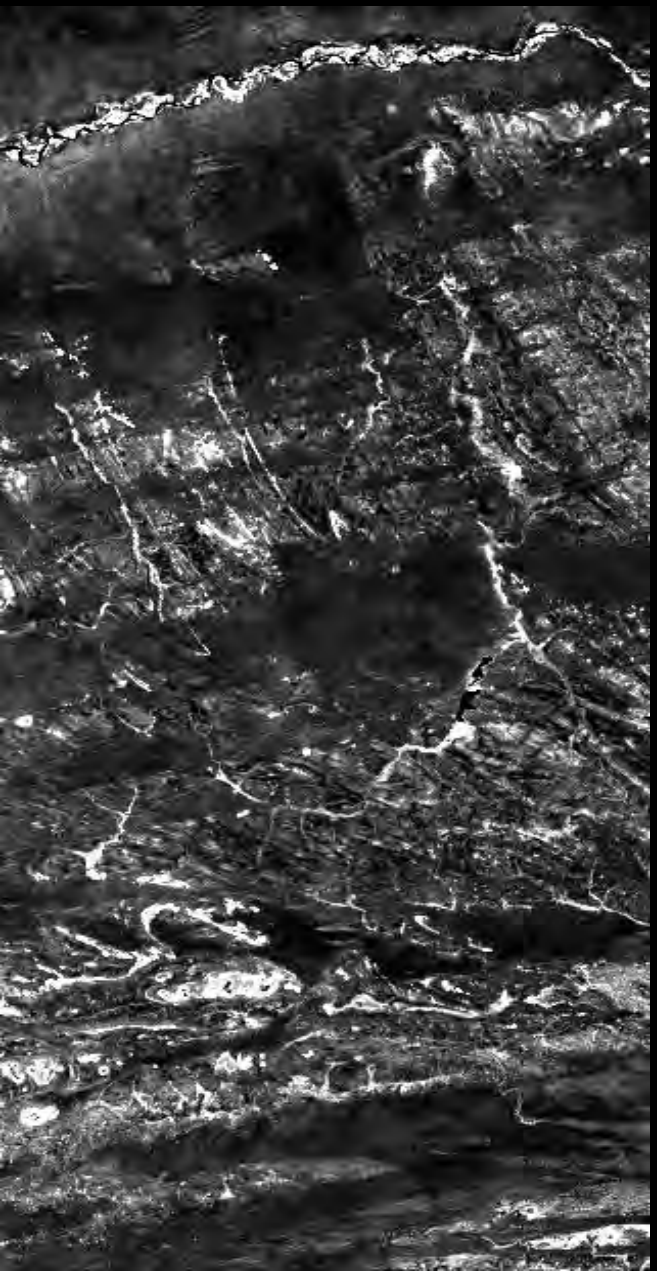

C Band (ASAR):
Sensitive to sandy and silty soils

***Bande L (PALSAR)**:*
Better discrimination
of geological structures

Remnant of alluvial system
and lacustrine depressions

PALSAR (λ = 24 cm)

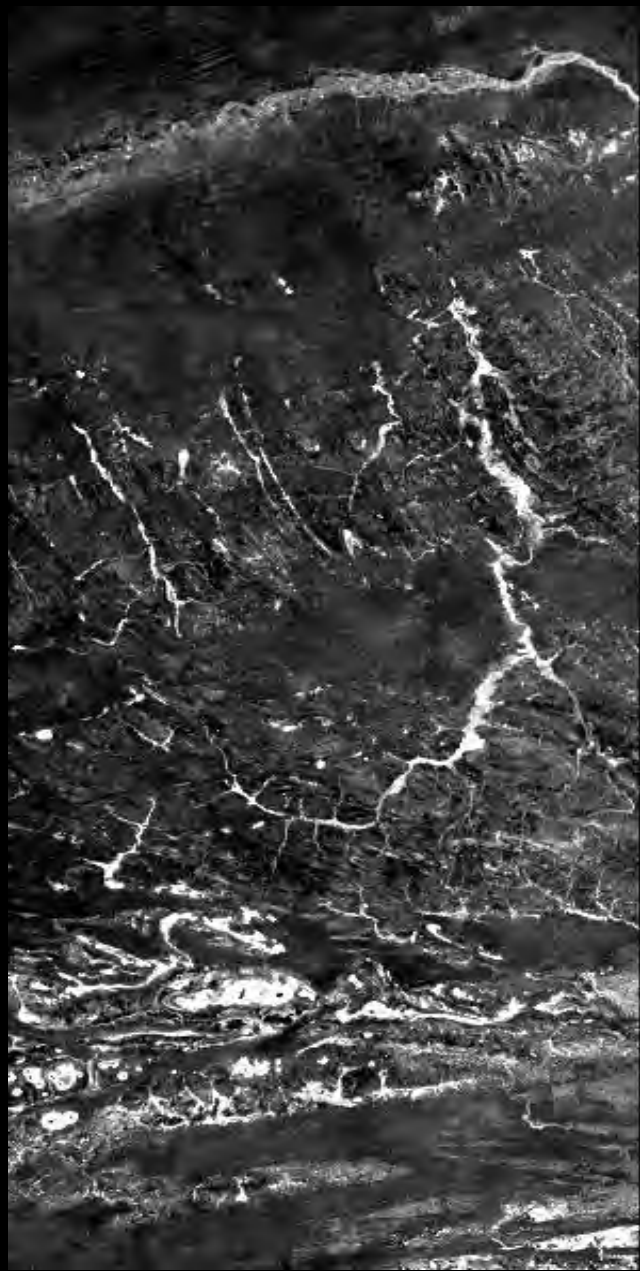

Change detection in a radar time series of 12 PALSAR images Jan. 2007 – apr. 2009

Color composite image

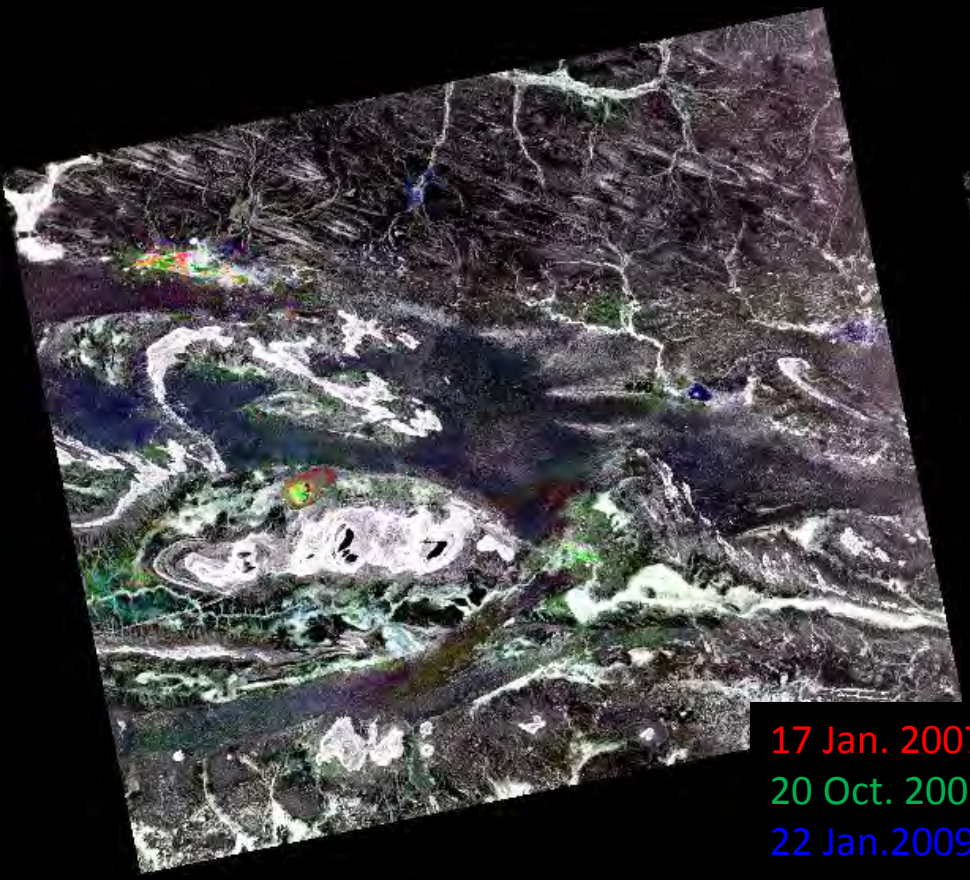

17 Jan. 2007
20 Oct. 2007
22 Jan.2009

PALSAR Fine Beam
HH polarization

Changes image(HSV)

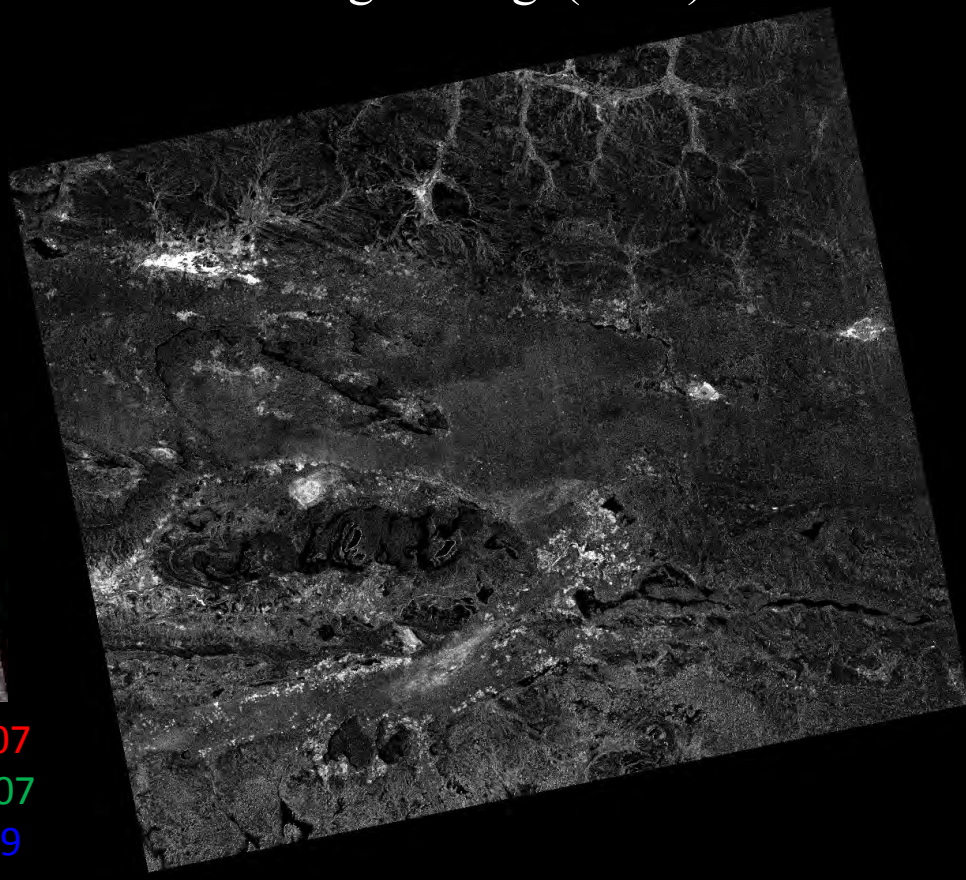

Jan. 2007 – Apr. 2009

Temporal changes detected (12 PALSAR acquisitions)

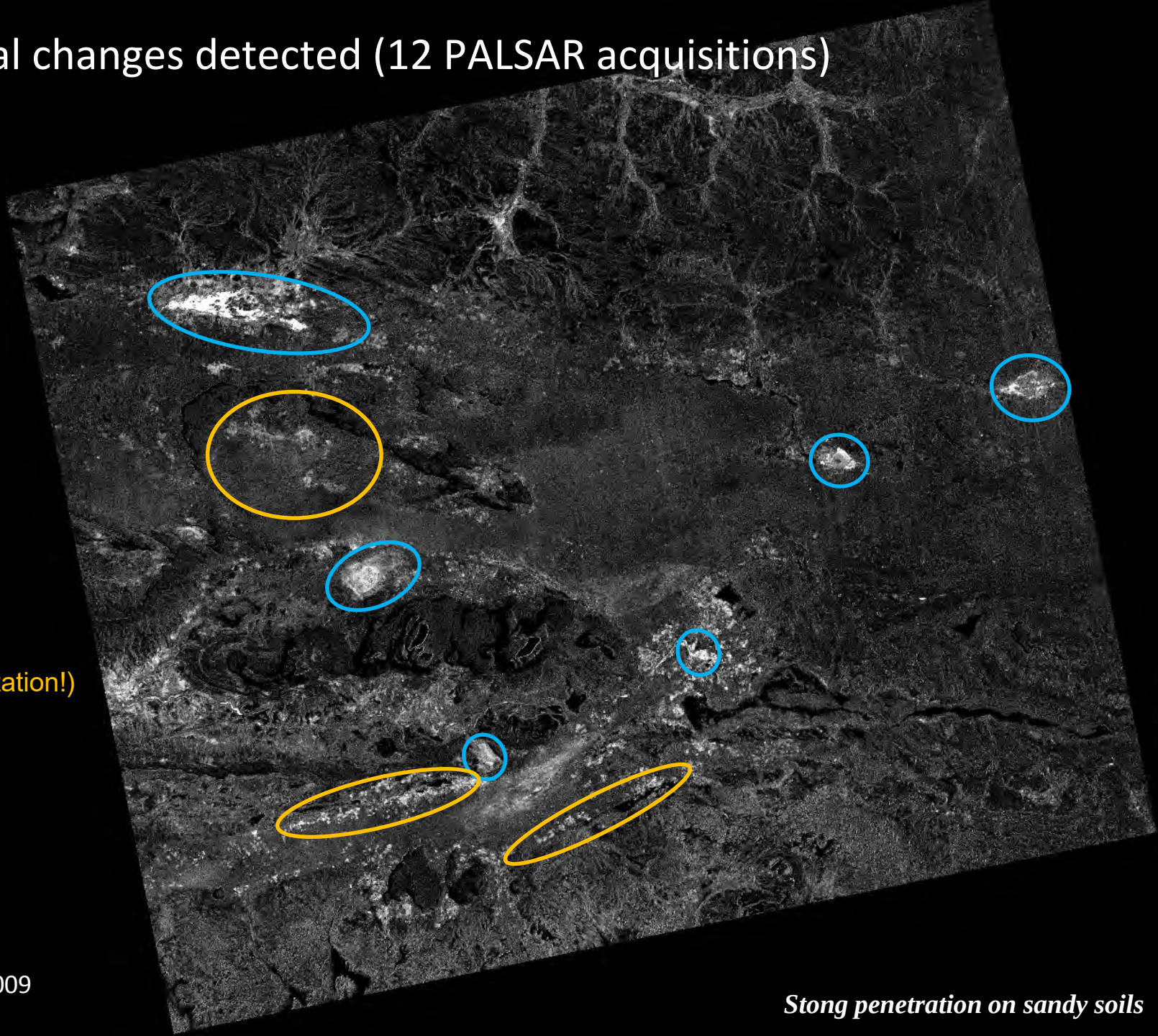

ponds

Millet fields
(depend on orientation!)

PALSAR
HH polarisation
Jan. 2007 – Mar. 2009

Stong penetration on sandy soils

Changes detection: C band / L band comparaison

PALSAR (λ = 24 cm)

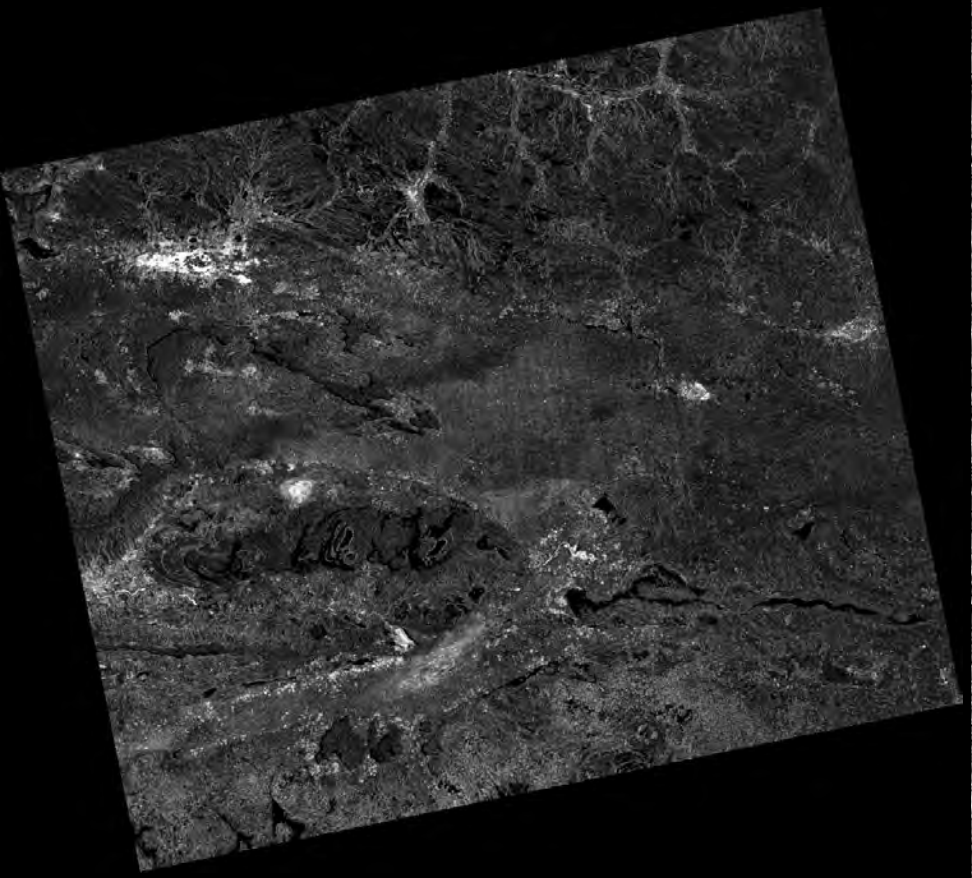

ASAR (λ = 6 cm)

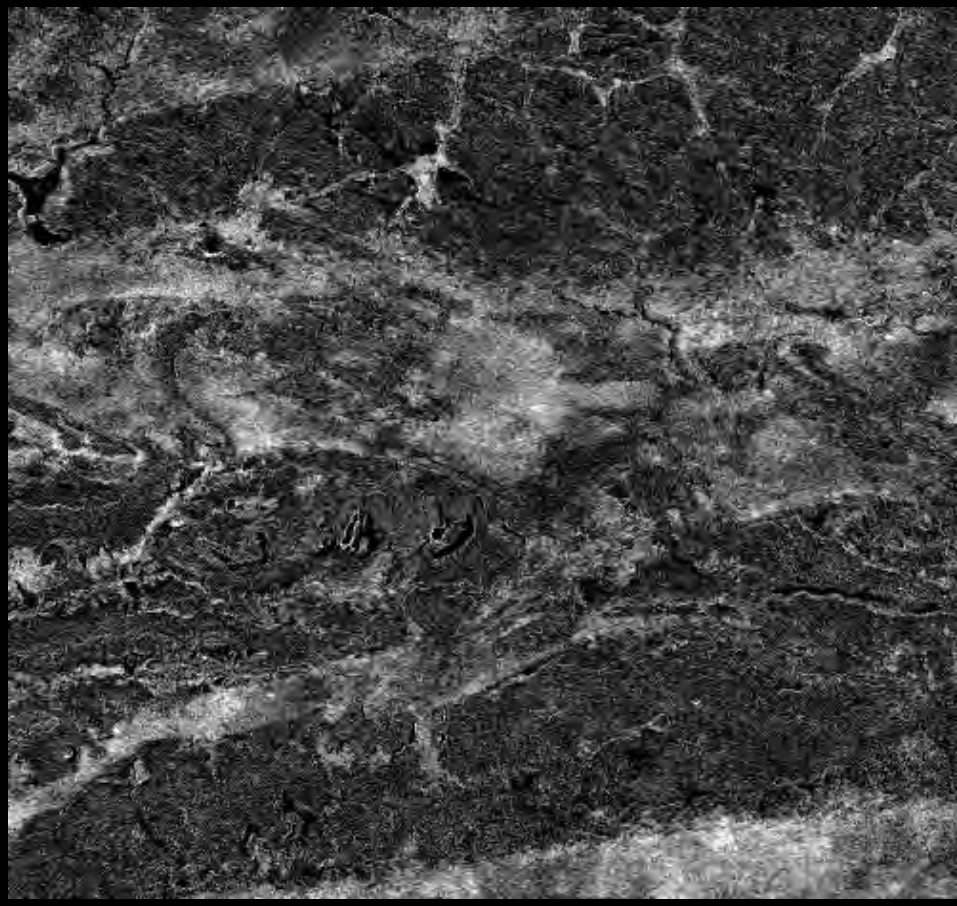

Changes detection: C band / L band comparaison

PALSAR (λ = 24 cm)

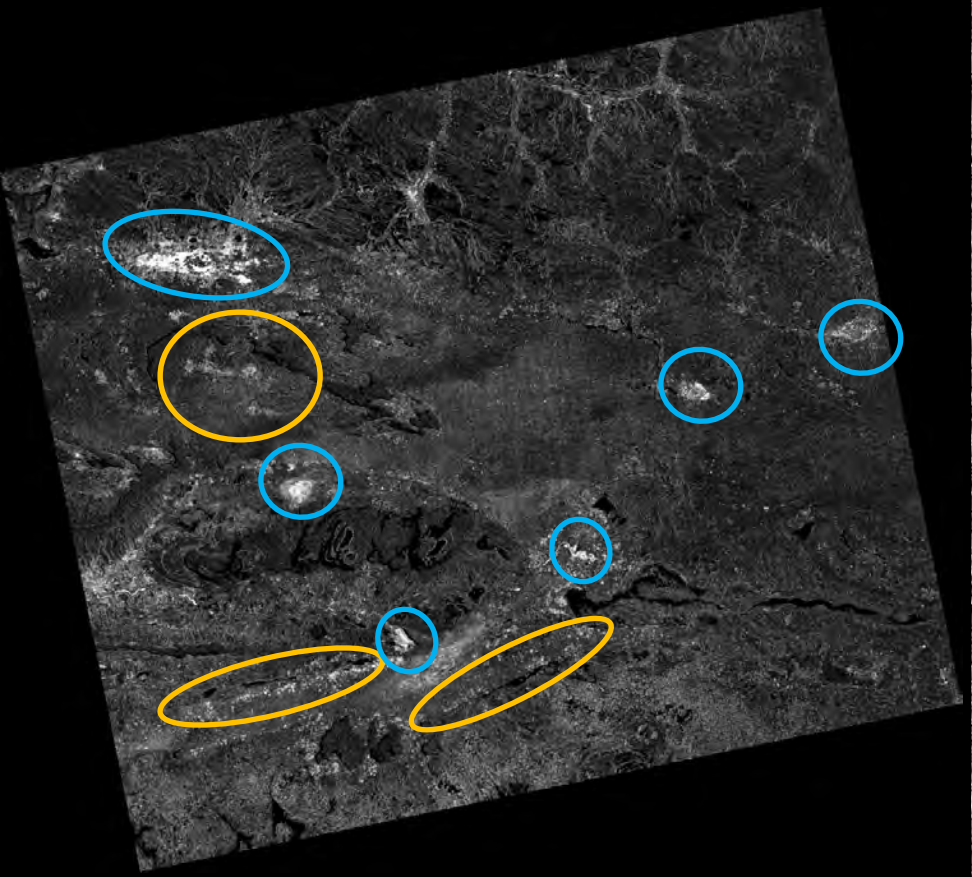

Strong penetration on sandy soils
ponds
Millet fields

ASAR (λ = 6 cm)

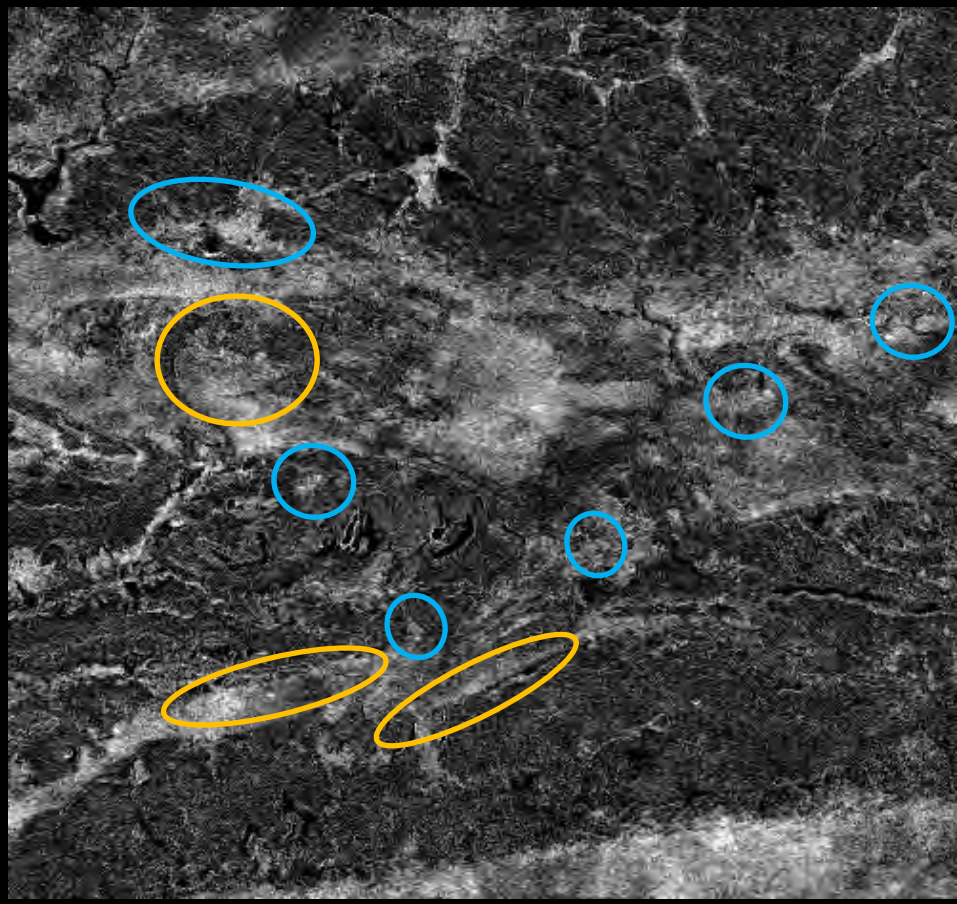

Weak penetration on sandy soils
surface states changes
sandy soils, ponds

TROPICAL RAIN FORESTS MONITORING

Tropical Forests monitoring

Role of biomass in the Carbon Global Cycle?

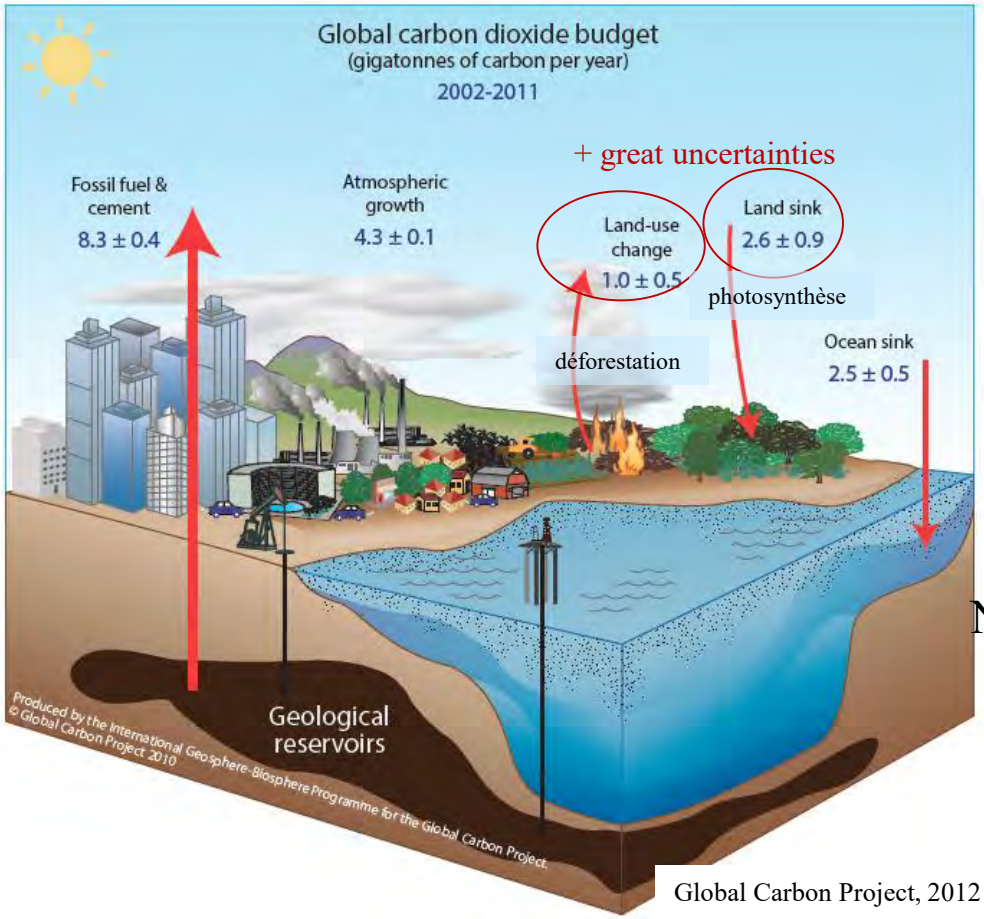

Global Carbon Project, 2012

C Stock C = 50% Biomass
Forests: 70-90% aerial biuomass

CO2 flux with land surfaces :
30% flux anthropiques
great uncertainty

Need for forest biomass estimation improvment:
- Spatial distribution
- Stocks
- dynamics

IPCC , UNFCCC

REDD+:
Financial incentive for sustainable forests ==> tropical countries

Mermoz *et al,.* 2016

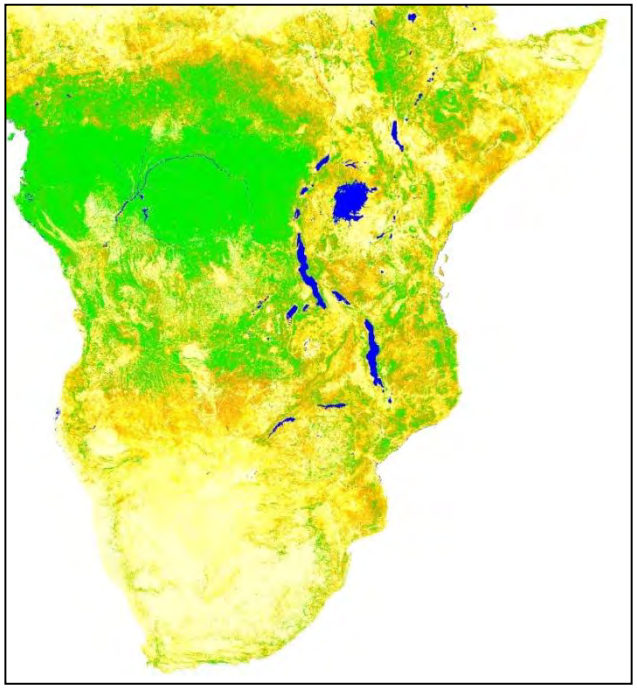

Saatchi *et al.,* 2011

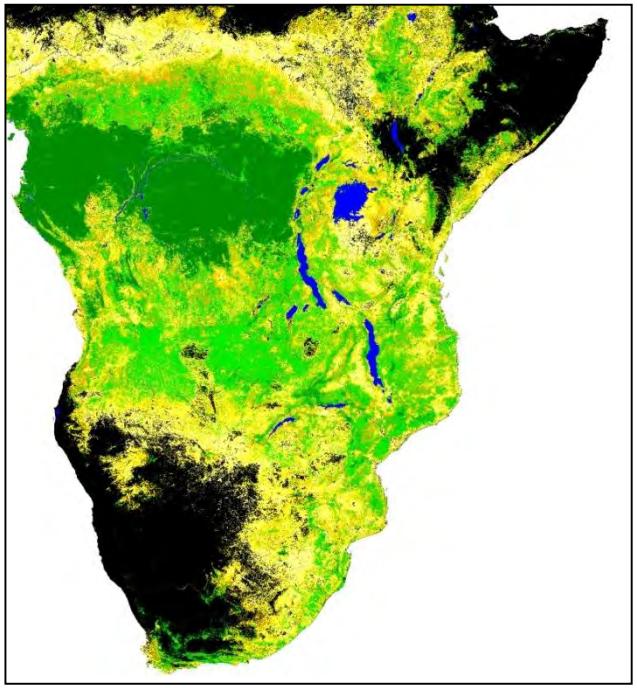

Baccini *et al.,* 2012

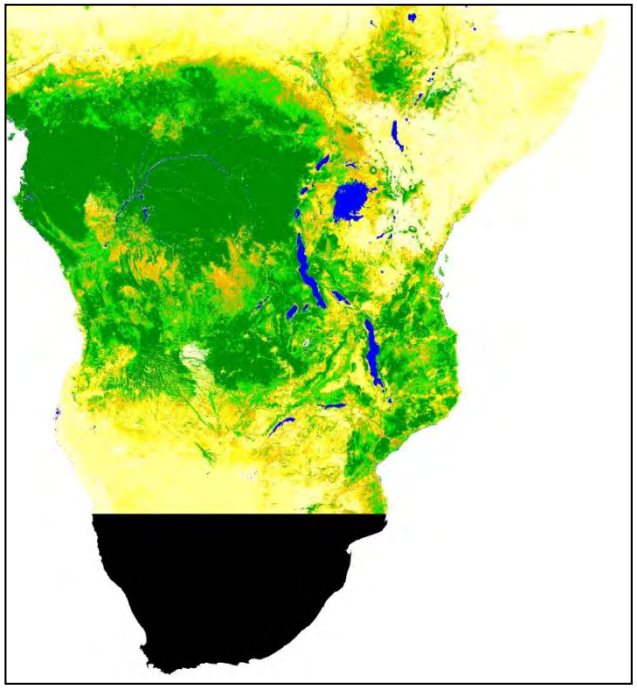

	0-10 Mg ha^{-1}
	10-20 Mg ha^{-1}
	20-30 Mg ha^{-1}
	30-40 Mg ha^{-1}
	40-50 Mg ha^{-1}

	50-60 Mg ha^{-1}
	60-100 Mg ha^{-1}
	> 100 Mg ha^{-1}
	water
	no data

CESBIO

Produit ‘Biomasse forestière’ Afrique

Map from CESBIO

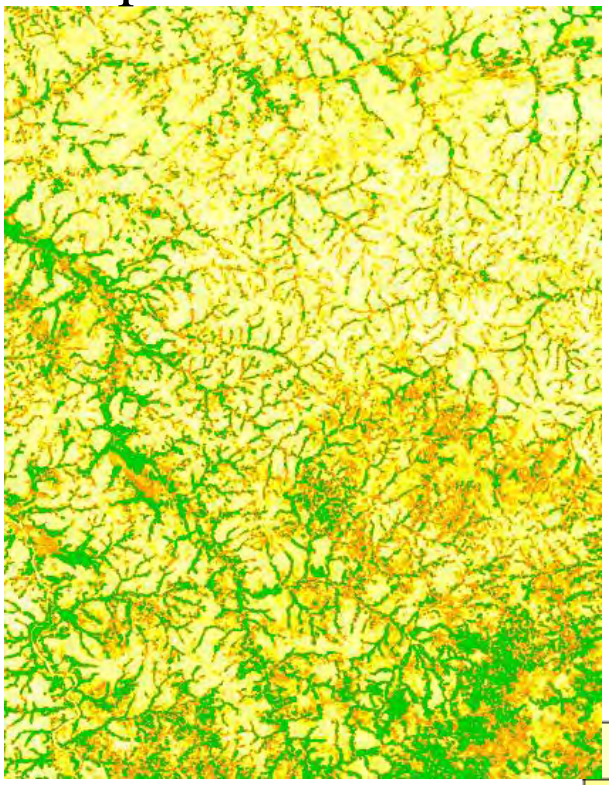

Saatchi et al., 2011

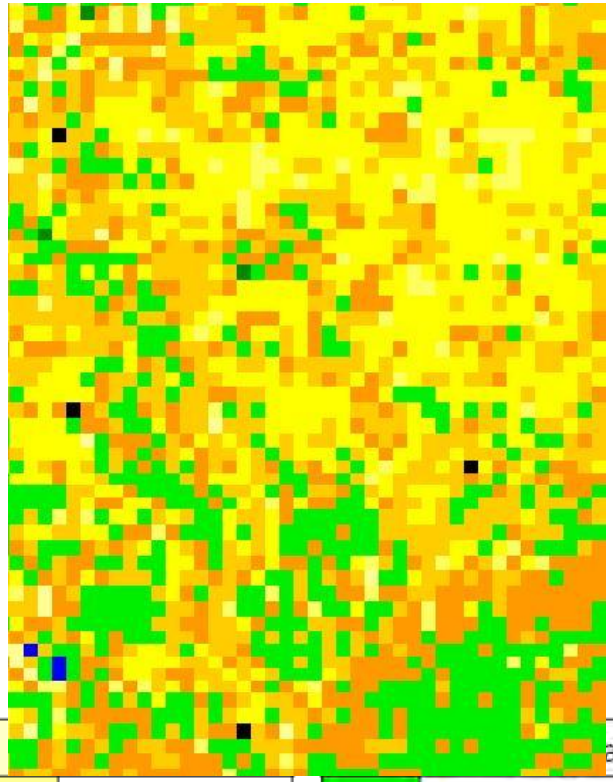

Baccini et al., 2012

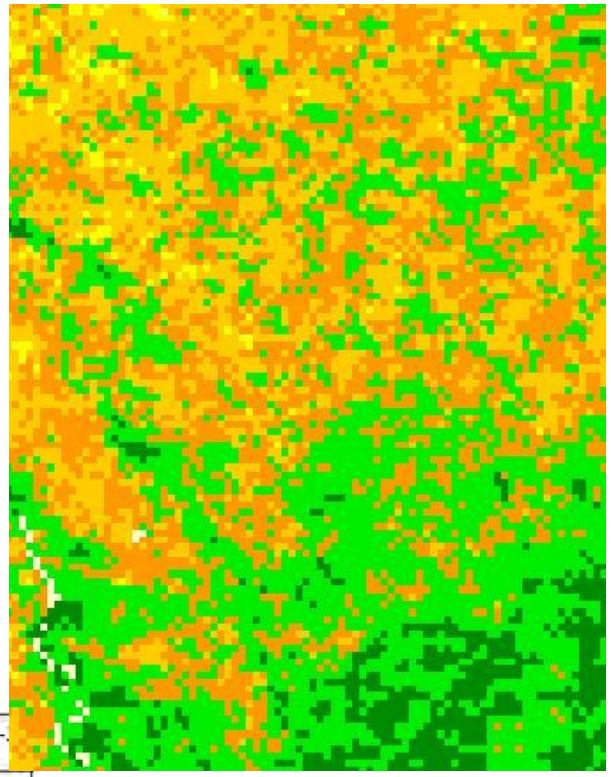

10-20 Mg ha^{-1}	60-100 Mg ha^{-1}
20-30 Mg ha^{-1}	> 100 Mg ha^{-1}
30-40 Mg ha^{-1}	water
40-50 Mg ha^{-1}	no data

Subset from:
Latitude: 10°S to 5°S
Longitude: 20°E to 25°E

Produit 'Biomasse forestière' Cameroun

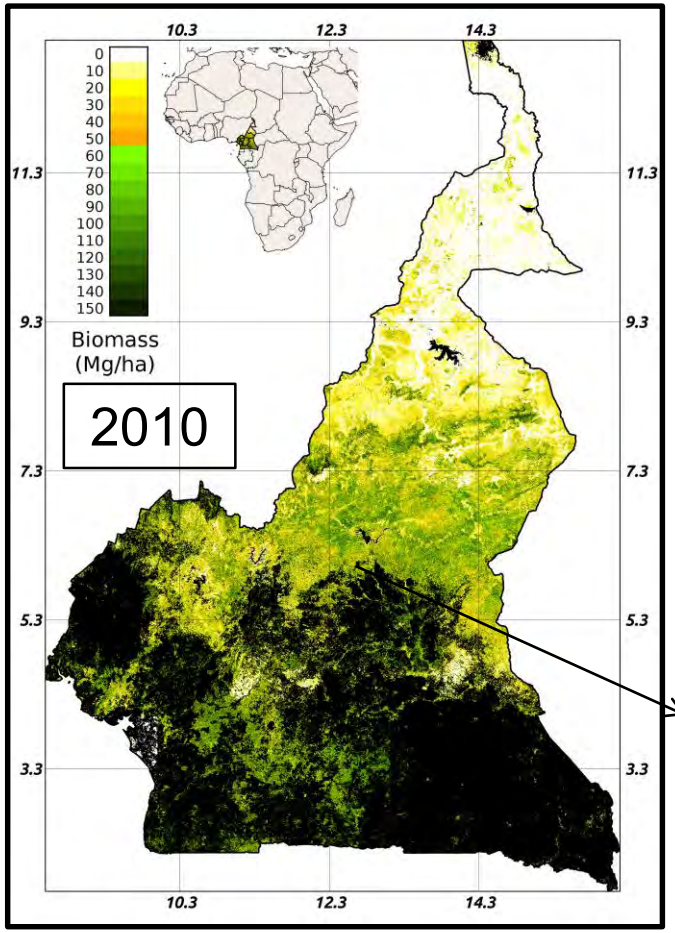

	Surface area (ha)	Mean AGB (Mg.ha^{-1})	AGB (Tg)	Carbon (TgC)
Mosaic forest-croplands	1,811,150	89.5	162.9	81.4
Mosaic forest-savanna	5,187,900	75.6	394.2	197.1
Deciduous woodland	10,352,400	53.3	553.6	276.8
Deciduous shrubland – sparse trees	1,949,000	30.7	59.8	29.9
Others	6,622,340	12.6	83.4	41.7
TOTAL	25,922,790	48.2	1253	**626.9**

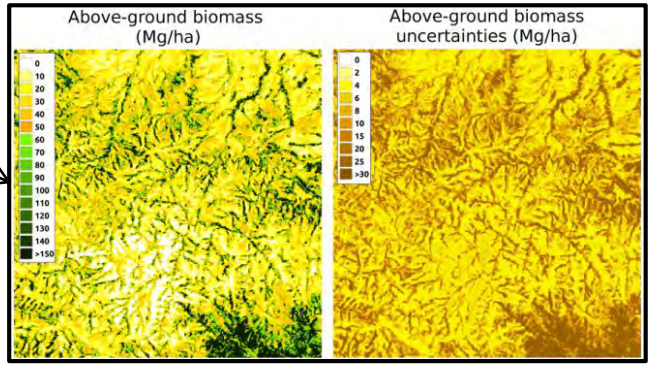

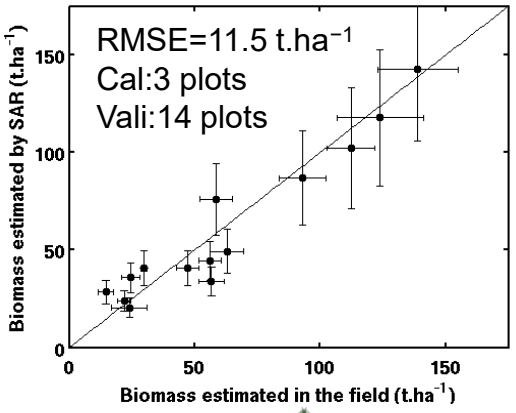

Total aboveground carbon stock:
- This study: 626.9 TgC
- Nasi et al. (2009): 710 TgC

Produit ‘Biomasse forestière’ Cameroun

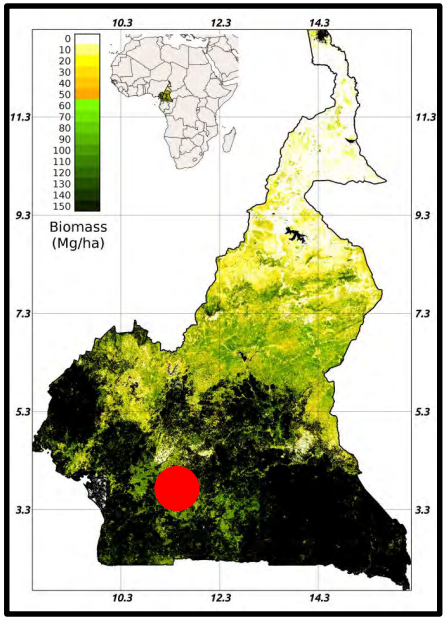

IIASA AMAP

University of Leicester

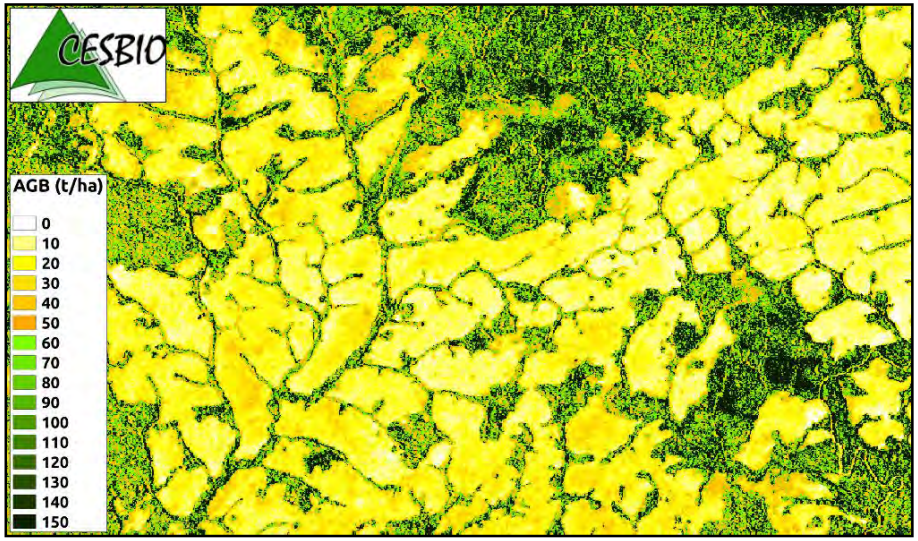

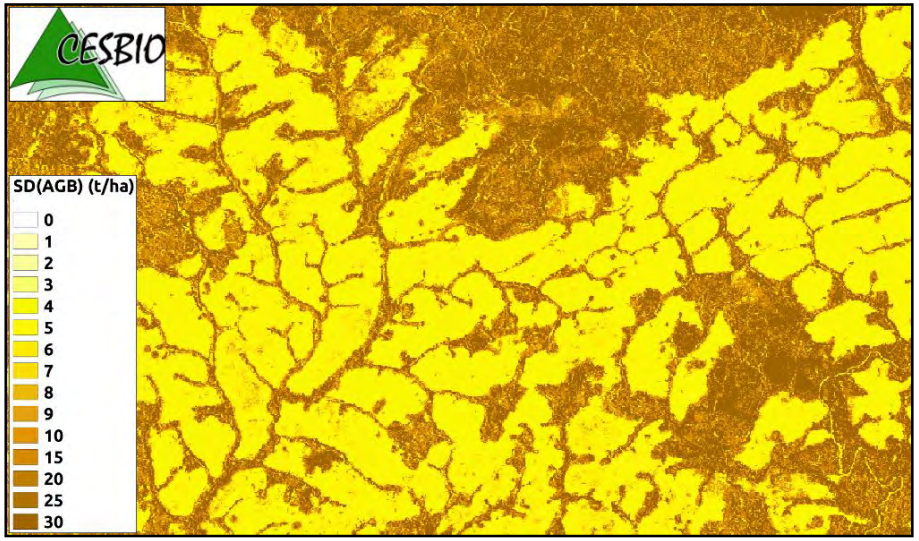

Tropical Forests monitoring

7th ESA Earth Explorer mission: BIOMASS (~ 2022)

Large wavelength for biomass cartography

1. Canopy penetration for every biomes
2. Interacts with woody elements of vegetation
3. Forest height estimation ability

→ P band band P *(λ = 70 cm) largest available wavelength from space*

P Band Radar
(λ = 70 cm)

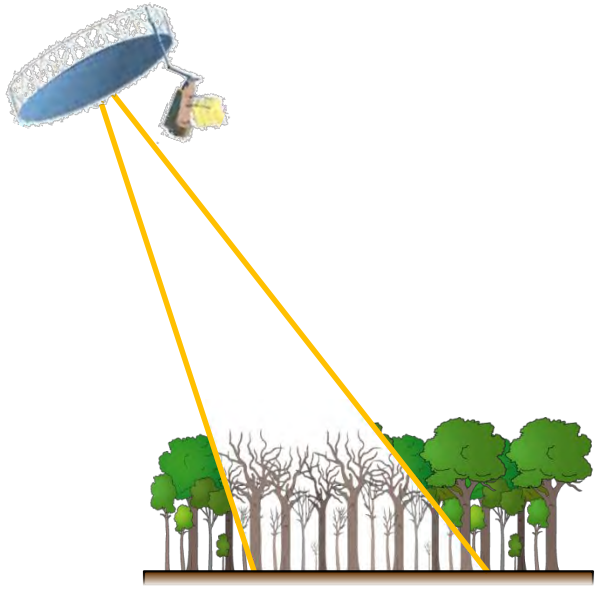

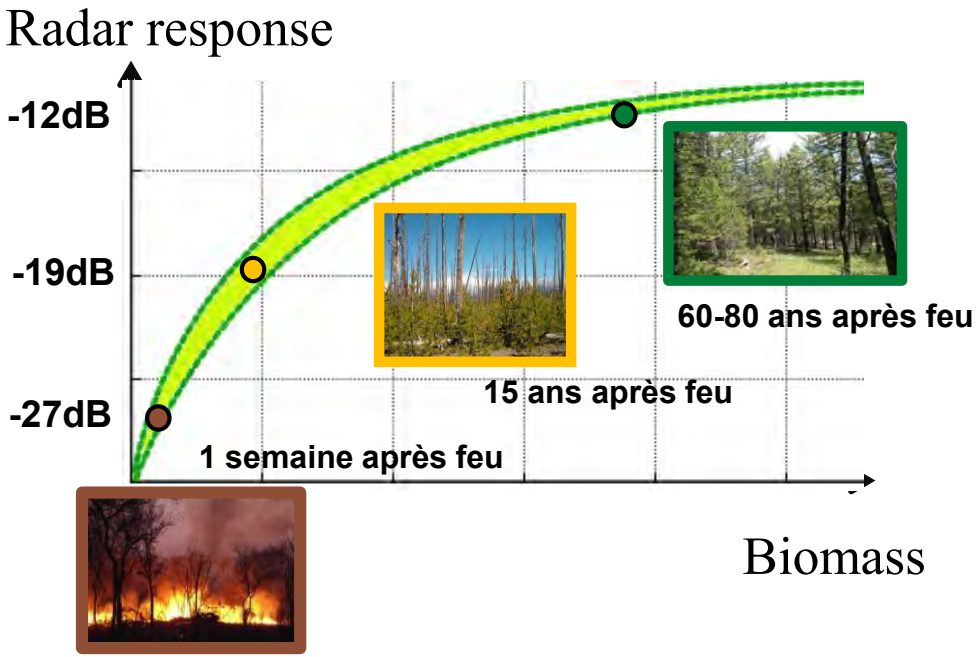

Tropical froest monitoring

7th ESA Earth Explorer mission: BIOMASS (~ 2022)

A key mission for a better understanding of Global Carbon Cycle

Aerial biomass (t / ha)

- Resolution: 200 m
- 1 map / 6 mois (4-year period)
- Global cover of forested areas
- Precision 20%, or 10 t ha^{-1} for biomass < 50 t ha^{-1}

Canopy height (m)

- Resolution: 200 m
- 1 map / 6 months (4-year period)
- Global cover of forested areas
- Precision 20 – 30%

Deforested areas (ha)

- Resolution: 50m
- 1 map / 6 months (4-year period)
- Global cover of forested areas
- Classification precision: 90%

Biomass Mission

PolSAR
(SAR Polarimetry)

PolInSAR
(Polarimetric SAR Interferometry)

TomoSAR
(SAR Tomography)

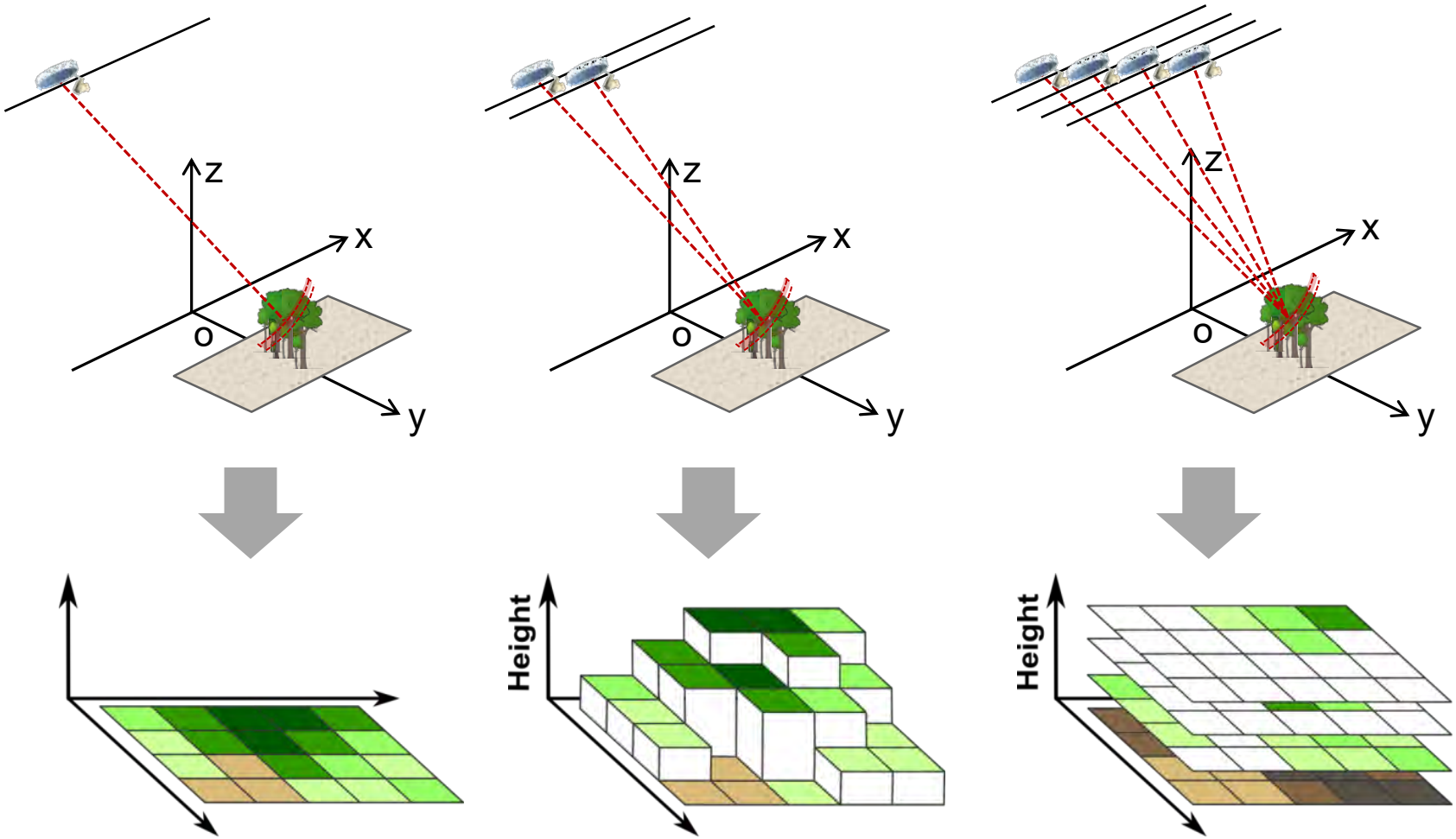

Radar response sensitivity

RADAR COHERENCE:

2 radar acquisitions

Temporal geometrical stability ($\leq \lambda$)
of the scatterers within each resolution cell

Complex coherence

$$\rho = \frac{\langle z_i z'^{*}_i \rangle}{\sqrt{\langle |z_i|^2 \rangle \langle |z'_i|^2 \rangle}}$$

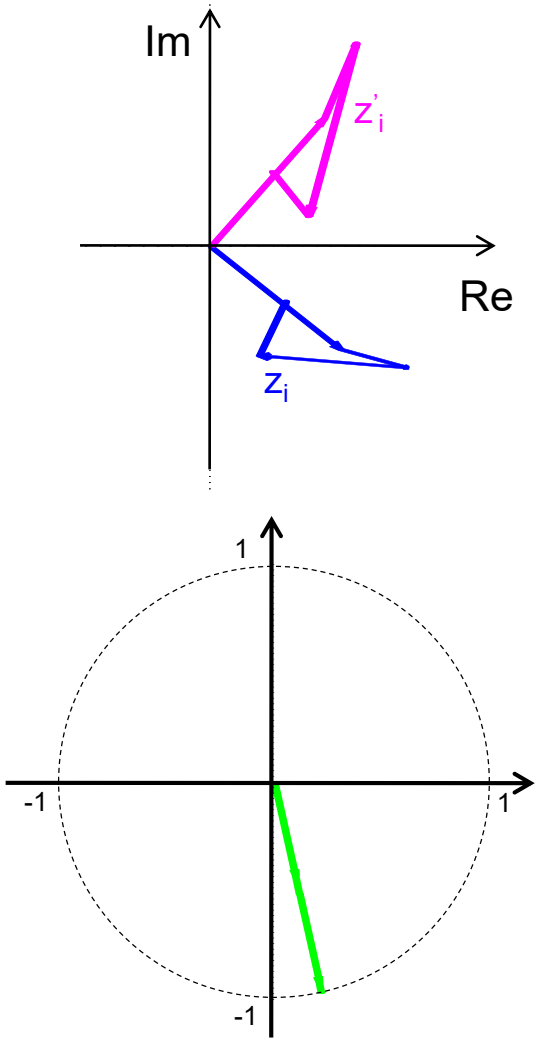

$|\rho| = 1$

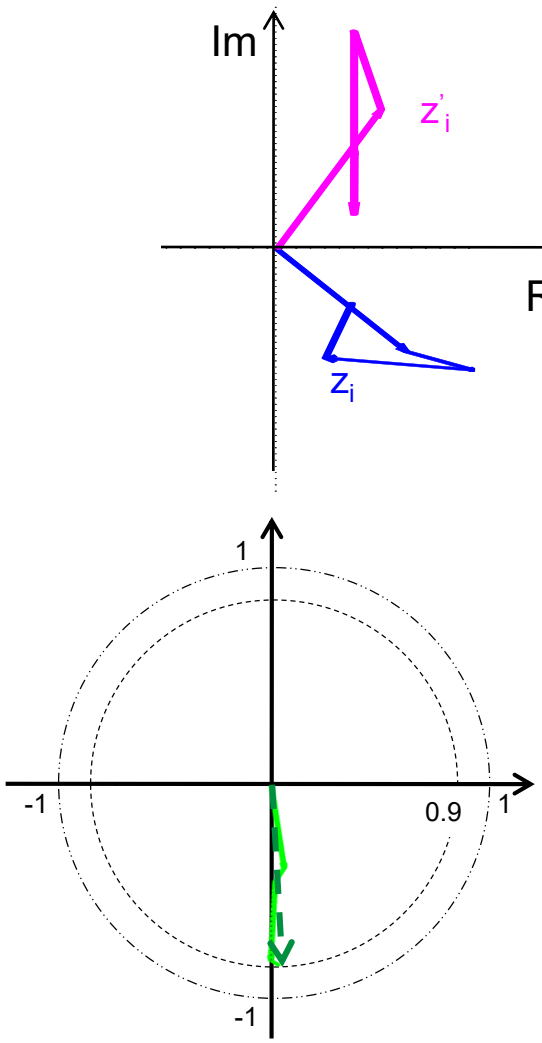

$|\rho| = 0.9$

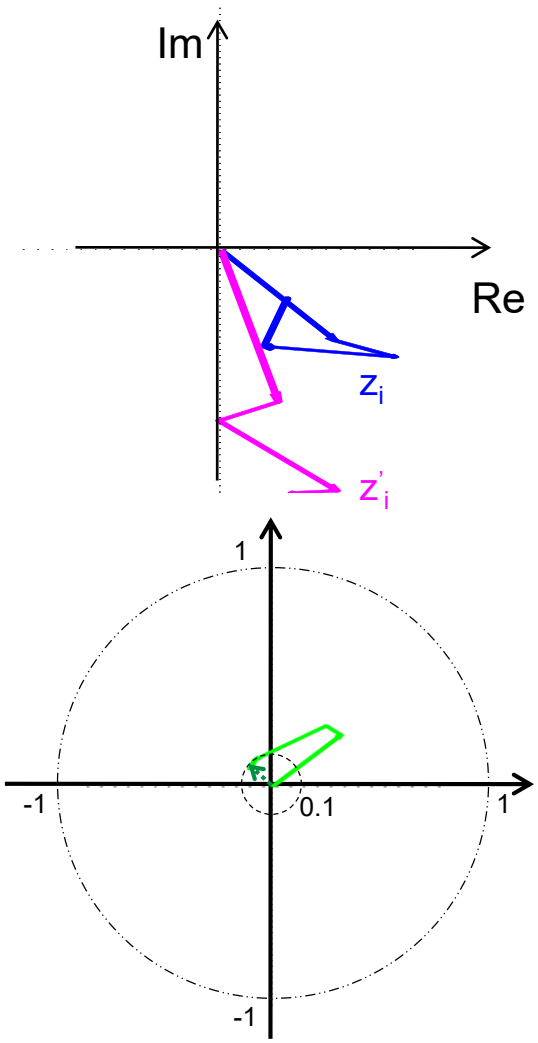

$|\rho| = 0.1$

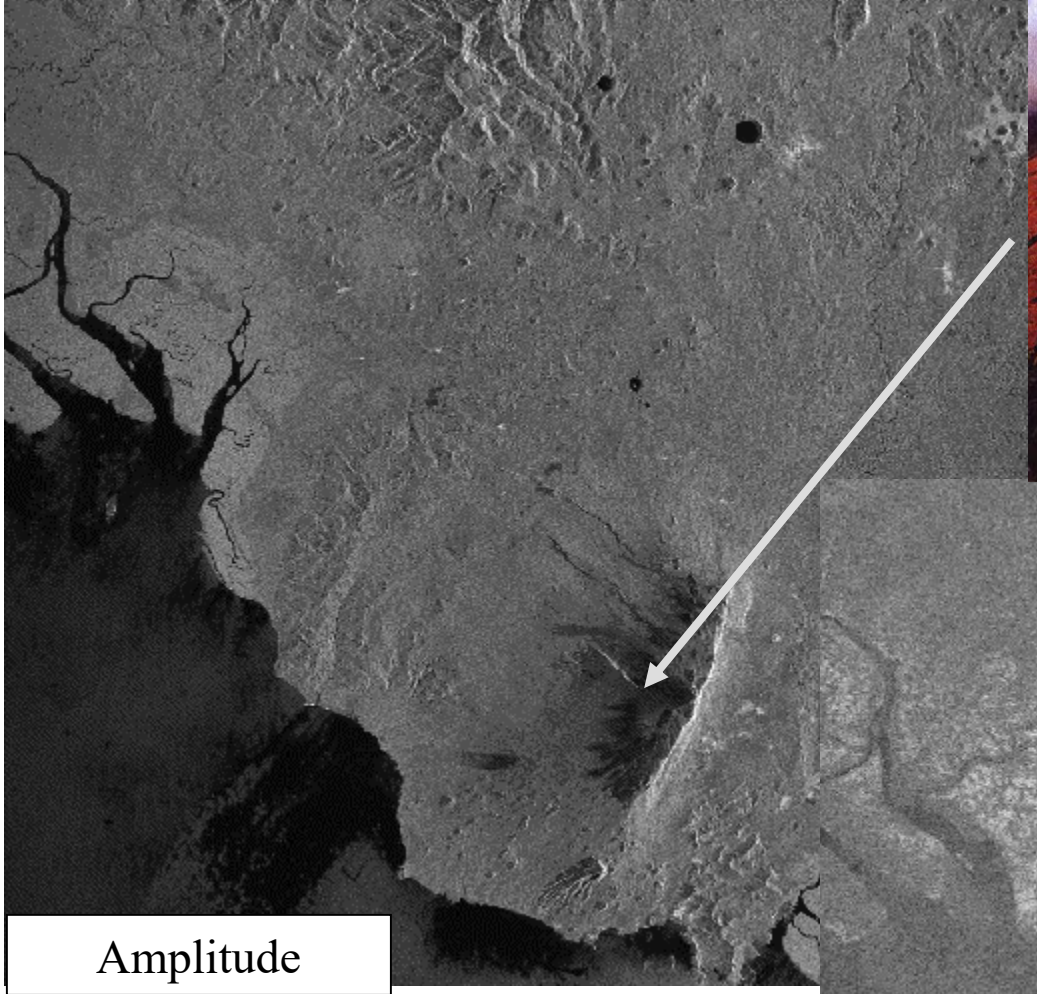

Amplitude

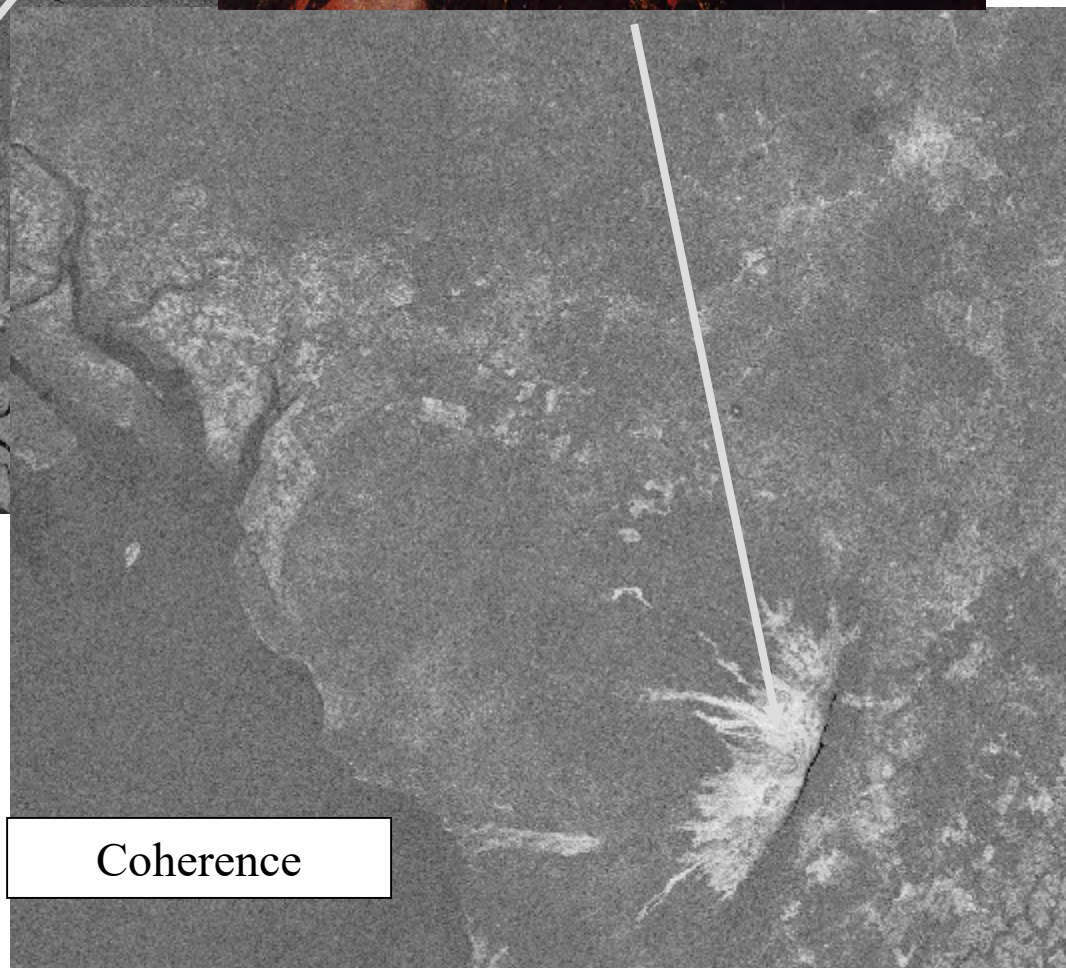

Coherence

Mount Cameroun, ERS

Radar response sensitivity

Mangroves

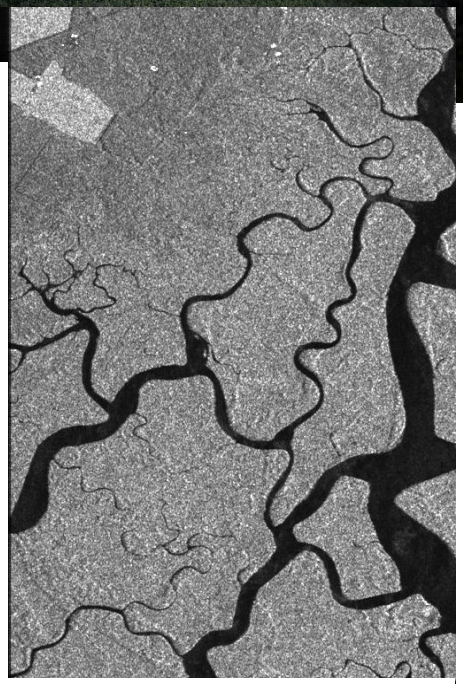

Amplitude ERS

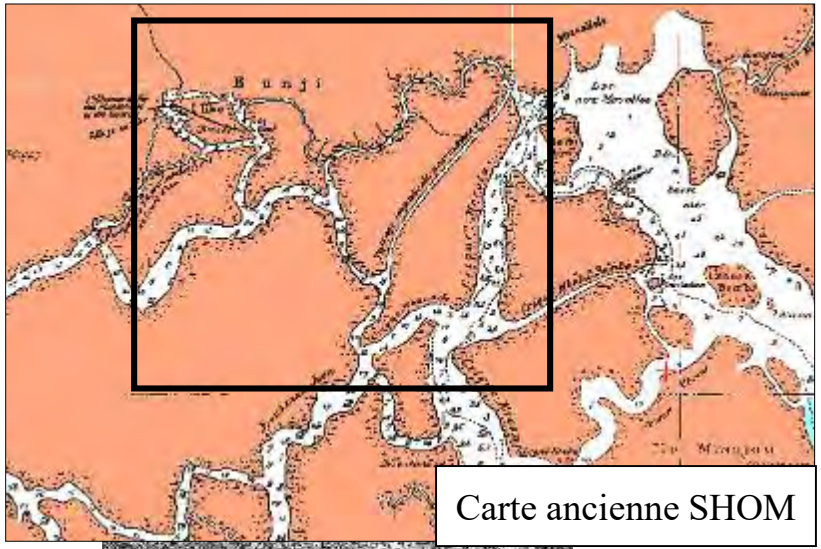

Carte ancienne SHOM

Coherence ERS

Amplitude ERS

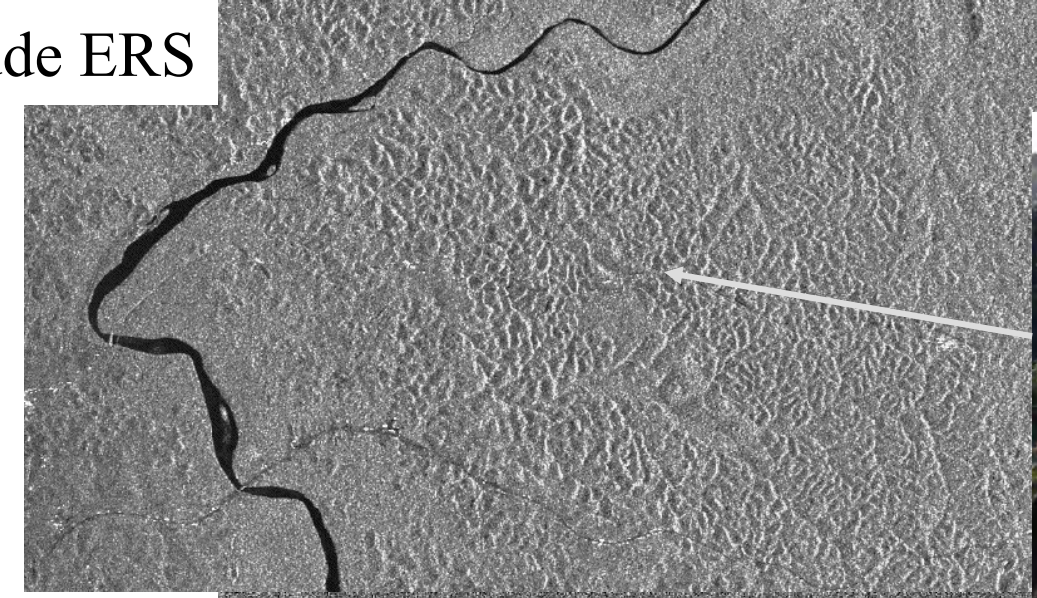

Coherence

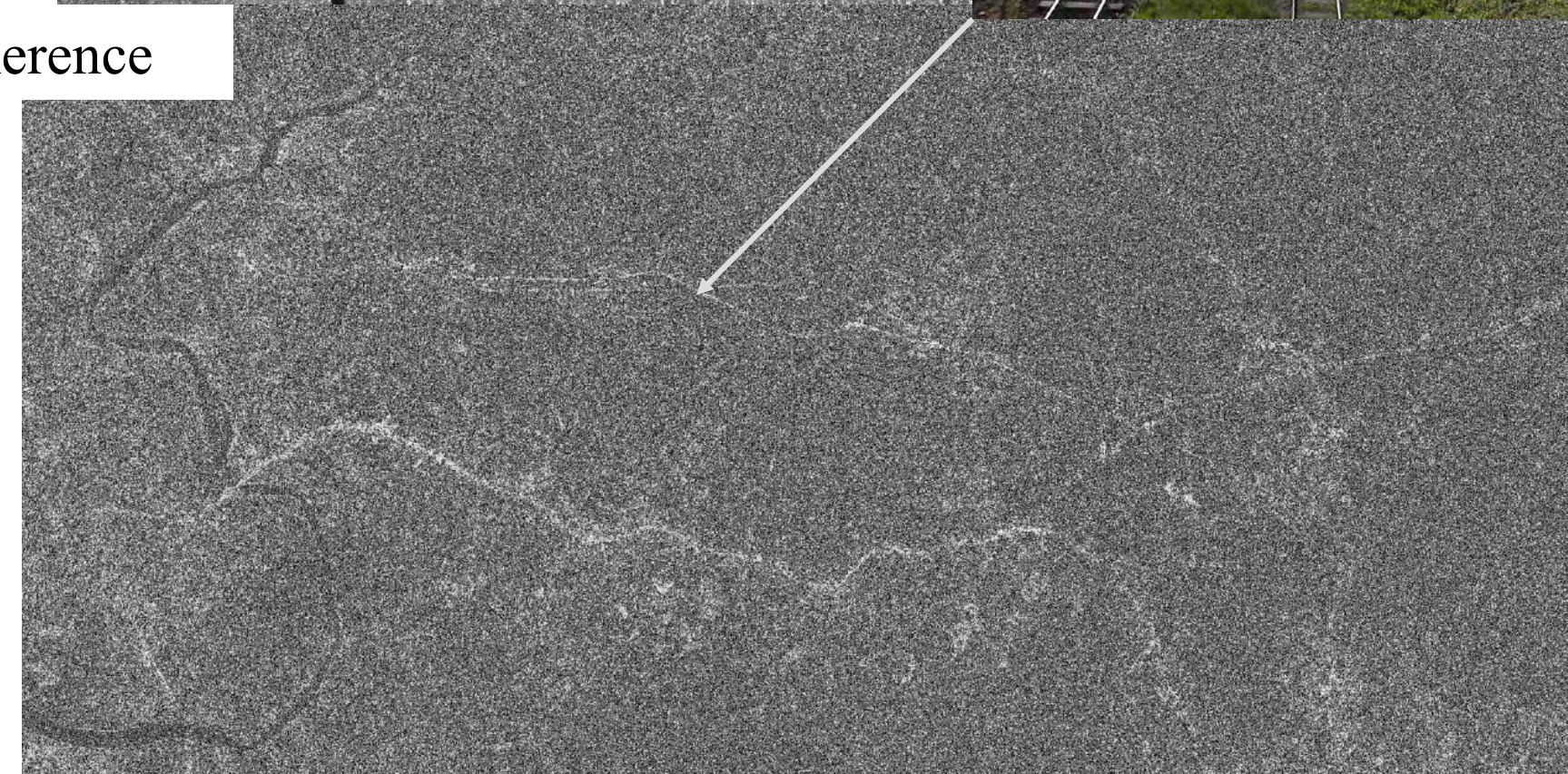

ASCAT/ASAR temporal signature over the **Chott el Jerid**

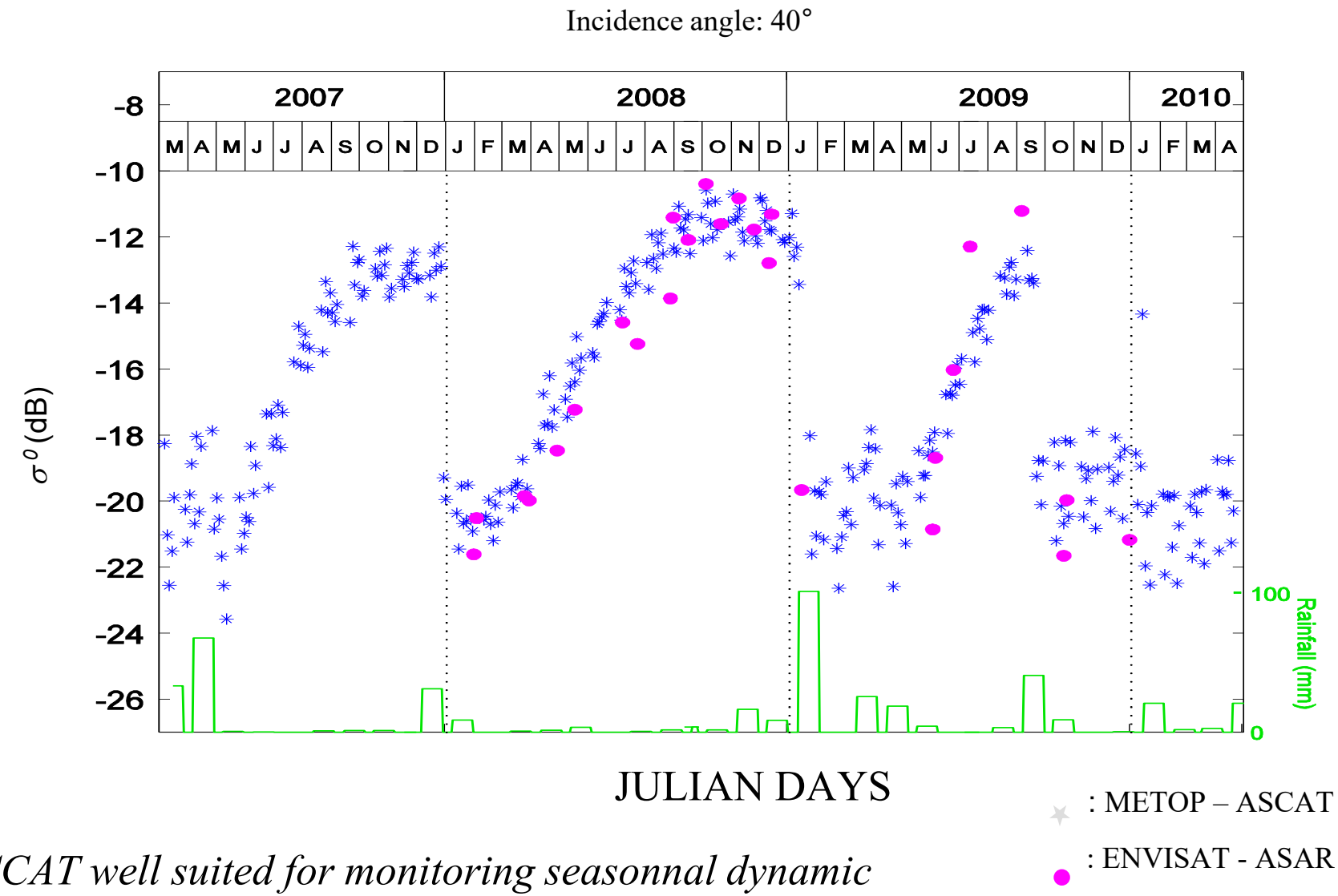

ASCAT well suited for monitoring seasonnal dynamic

Radar remote sensing for land surfaces monitoring

Side looking radar sensors

Scatterometers

☞ *Radar eflectivity estimation (σ°)*

- *low spatial resolution*: ~ *10 – 50 km*
- *high frequency of acquisitions (~ day)*

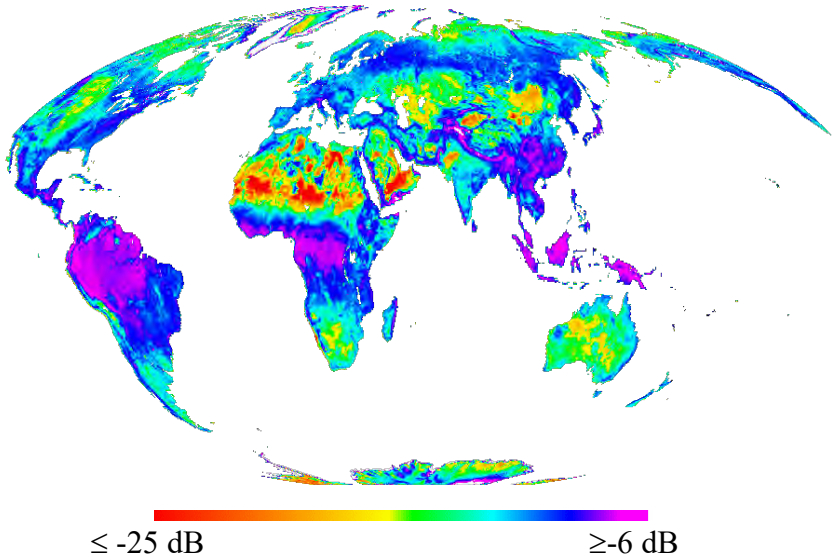

Scatt. ERS – May 1992

SAR

☞ *Surface imaging*

- *high spatial resolution*: ~ *10 m*
- *low frequency of acquisition (~ month)*

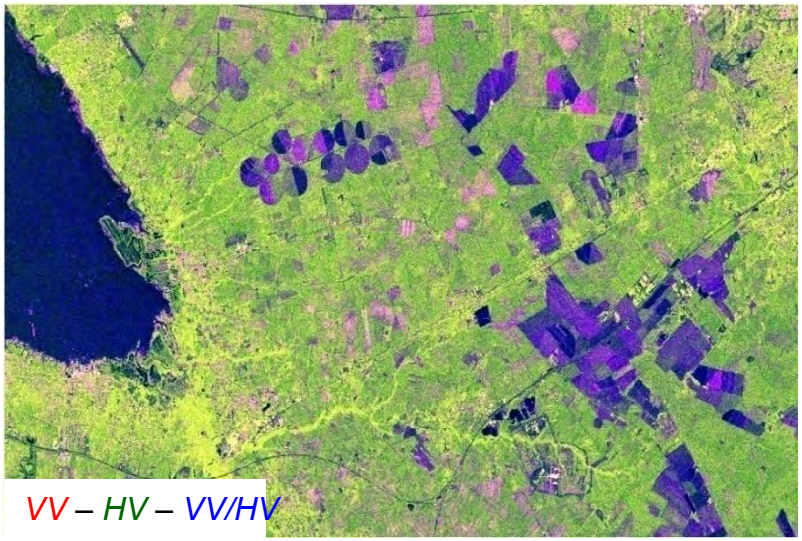

Sentinel-1
Les landes – March 2015

Radar remote sensing for land surfaces monitoring

Side looking radar sensors

Scatterometers

☞ *Radar eflectivity estimation (σ°)*

- *low spatial resolution*: ~ 10 – 50 km
- *high frequency of acquisitions (~ day)*

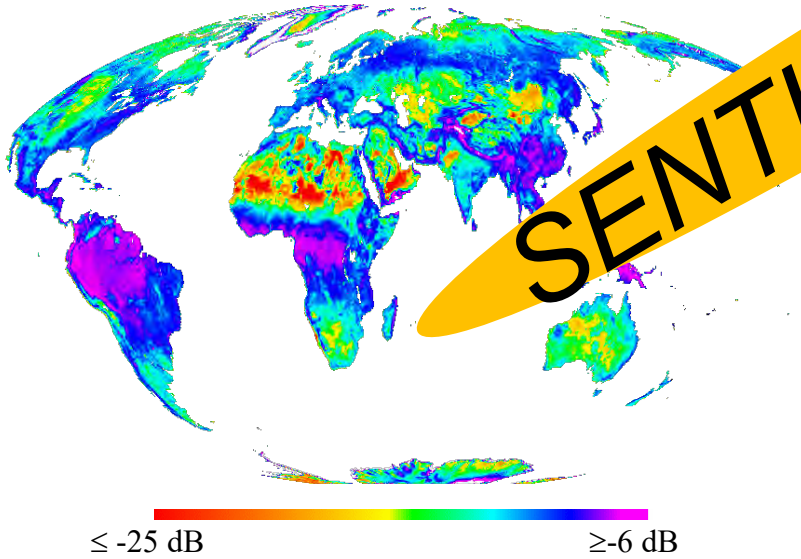

Scatt. ERS – May 1992

SAR

☞ *Surface imaging*

- *high spati… …tion: ~ 10 m*
- *l… …cy of acquisition (~ month)*

SENTINEL-1 MISSION

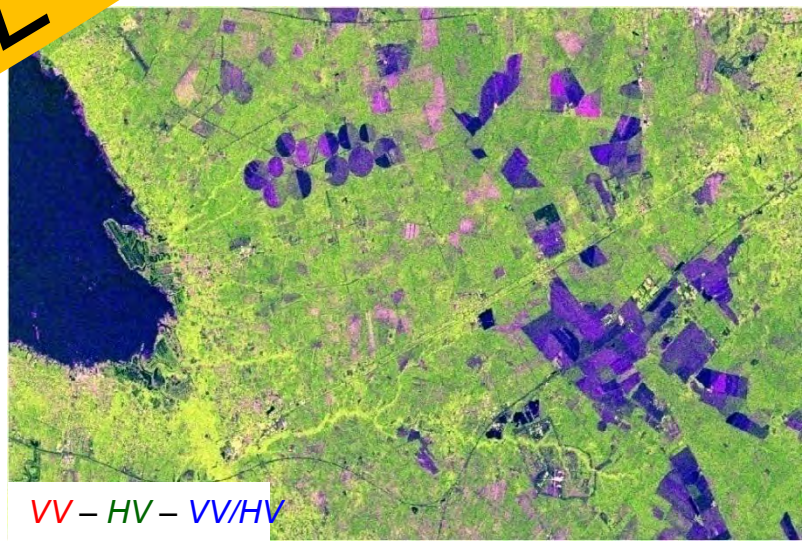

Sentinel-1
Les landes – March 2015

The Sentinel-1 misions

Sentinel-1A: launched the 3rd April 2014
== > SAR data from March 2015 Revisit time: 12 days

Sentinel-1B: launched the 22th April 2016 Revisit time: 12 days
== > SAR data from September2016

} *6 days!!*

- C band
- Spatial resolution: 20 m
- Swath width: 250 km
- Two polarizations over land surfaces: VV and VH

SAR ⟷ **SENTINEL-1** ⟷ **Scatterometers**

Acquisitions period: ***12 days*** (S1-A) – ***6 days***(S1- A+B)

Planned mode over land surfaces: ***Interferometric Wide (IW)***

BIG DATA

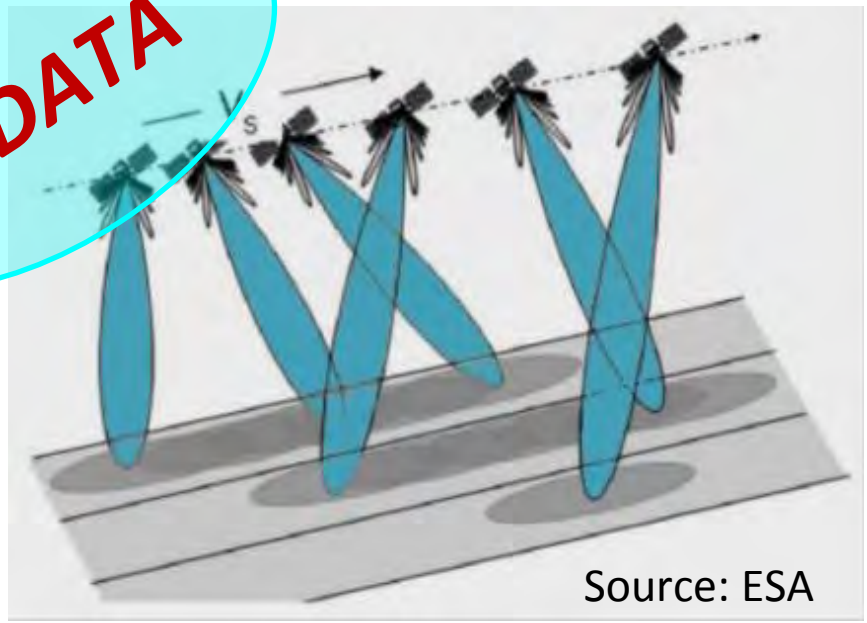

2 Polarisations: ***VV –VH***

Swath: 250 km (3 sub-swaths)

GRD Products :

- Spatial resolution: **20 m**
- Pixel: 10 m

SLC Products

- Spatial resolution: 3 x 20 m;
- Pixel: 2 x 14 m (rge x az.)

Temporal monitoring of seasonal variations of land surfaces

Radar Backscattering Coefficient σ^0

Interferometric Coherence $|\rho|$

Sentinel: Apport des séries temporelles

Formations végétales
Parc de la Pendjari, Bénin

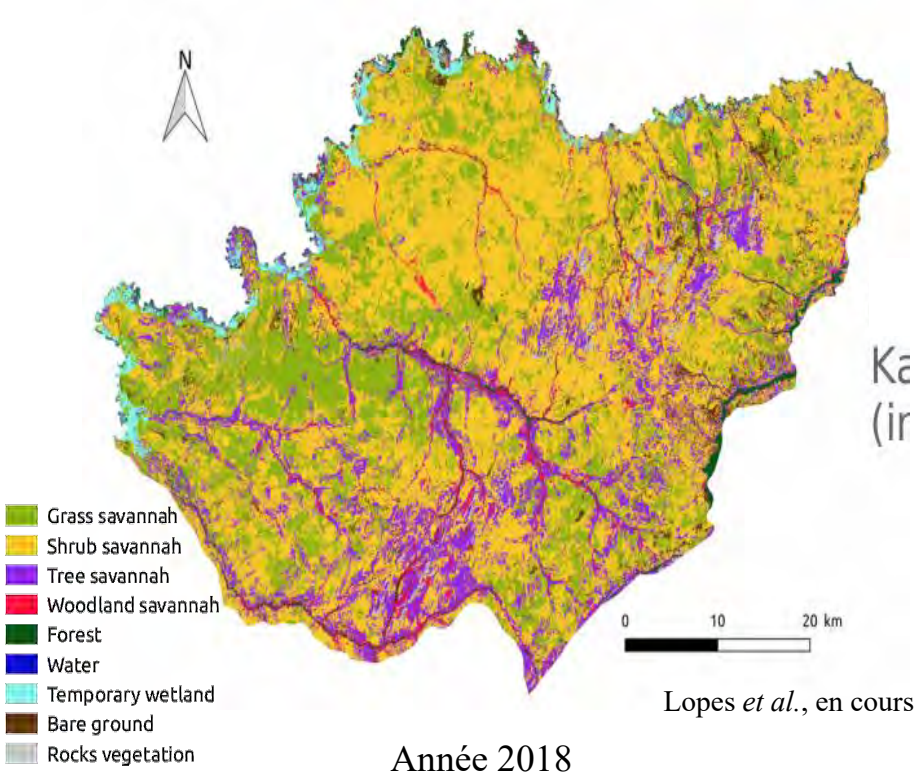

Lopes *et al.*, en cours

Année 2018
Données Sentinel-1 et -2

Données Sentinel *(Big Data)*

- Fouille de donnees
- Intelligence artificielle
- Deep learning

Complémentarité optique / radar

Acquisitions over the Paris region

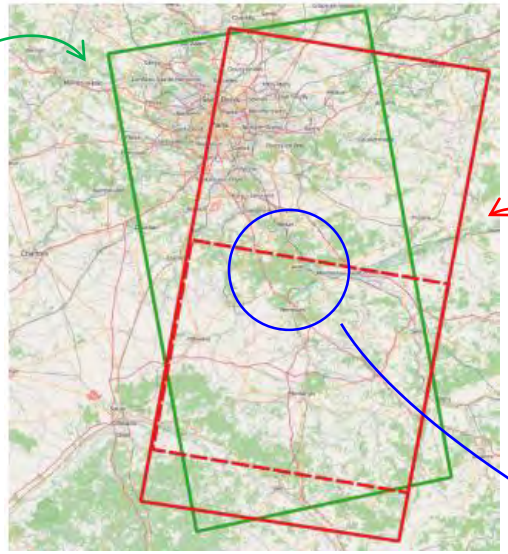

Fontainebleau Forest

Oaks, pines and beeches stands

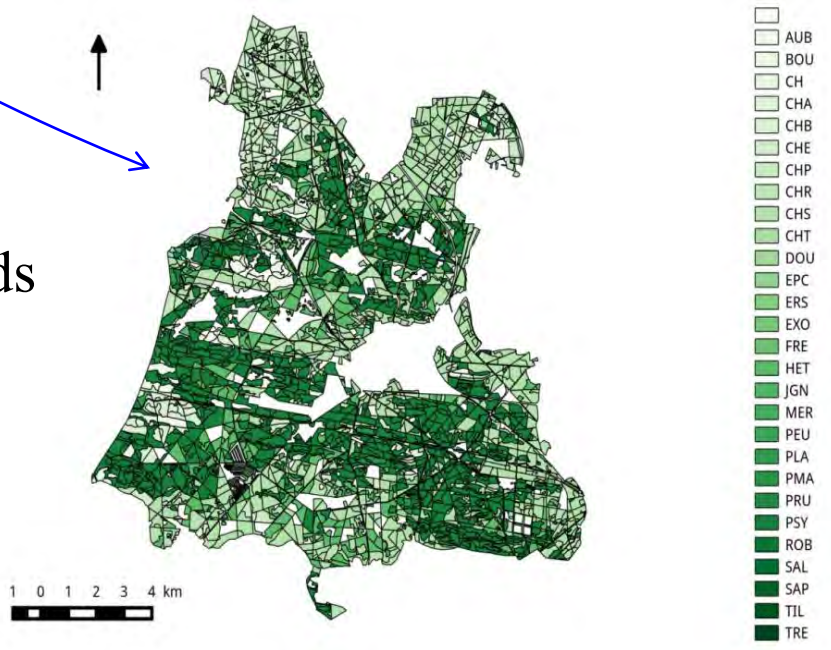

Collab. ESE / Paris Sud

18th March 2015 IW Acquisition

Radar reflectivity (σ^0) image

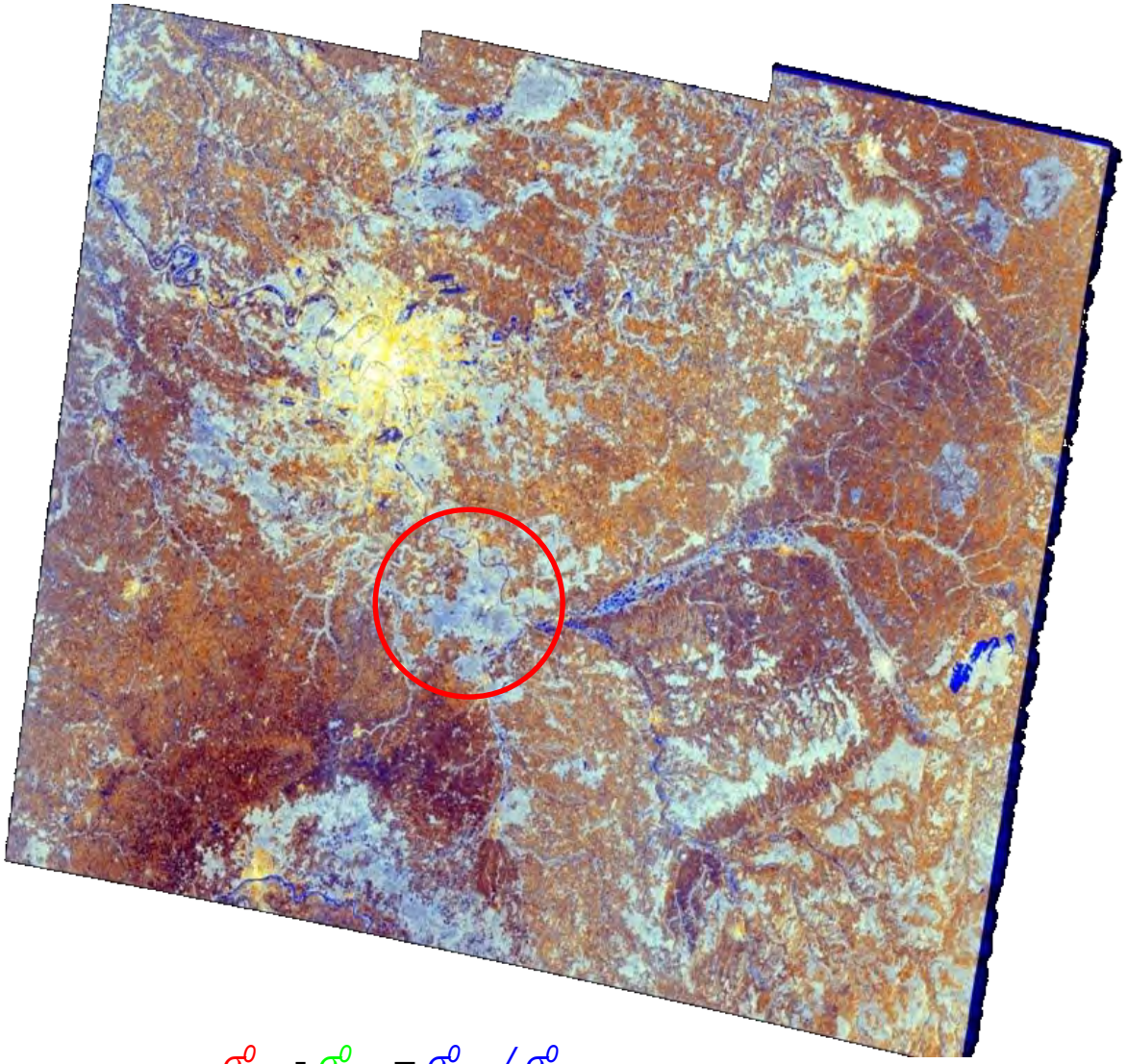

σ^0_{VV} - σ^0_{VH} – σ^0_{VH} / σ^0_{VV}

18 – 30 March coherence image

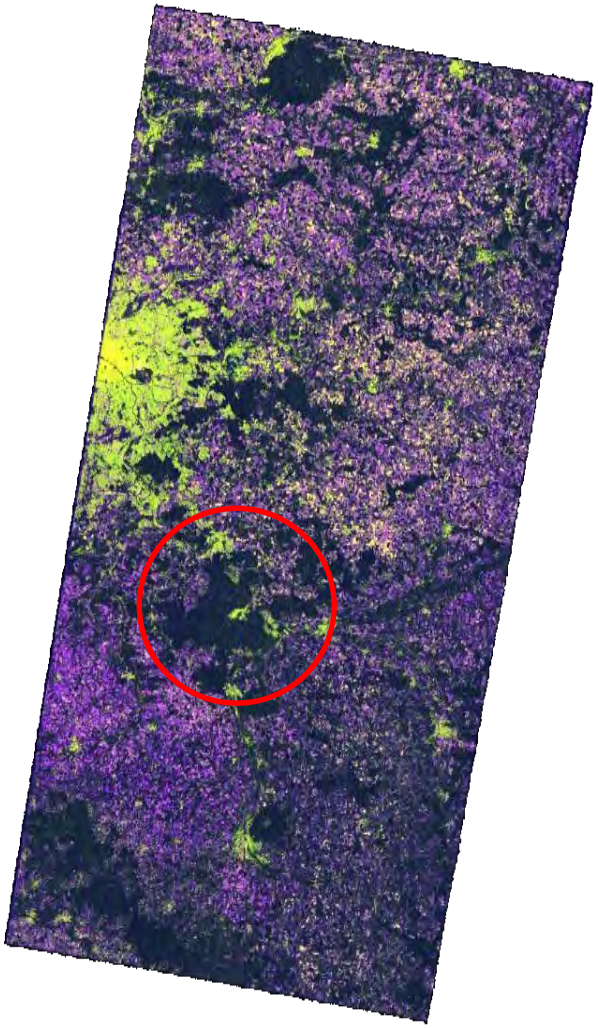

$|\rho_{VV}|$ - $|\rho_{VH}|$ – $|\rho_{VV}|$ / $|\rho_{VH}|$

σ^0 Color composite image

5 May - 2 Sept. - 19 Dec. 2015

Polarisation ***VV***

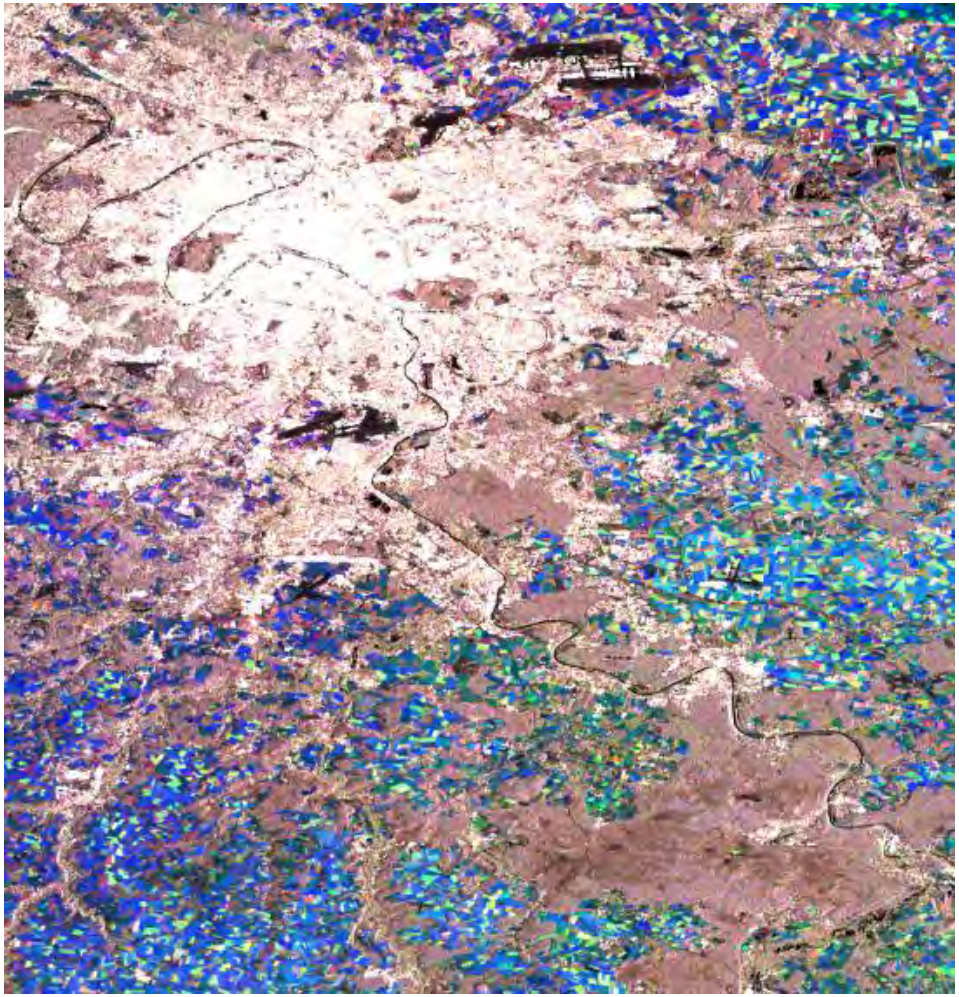

Polarisation ***VH***

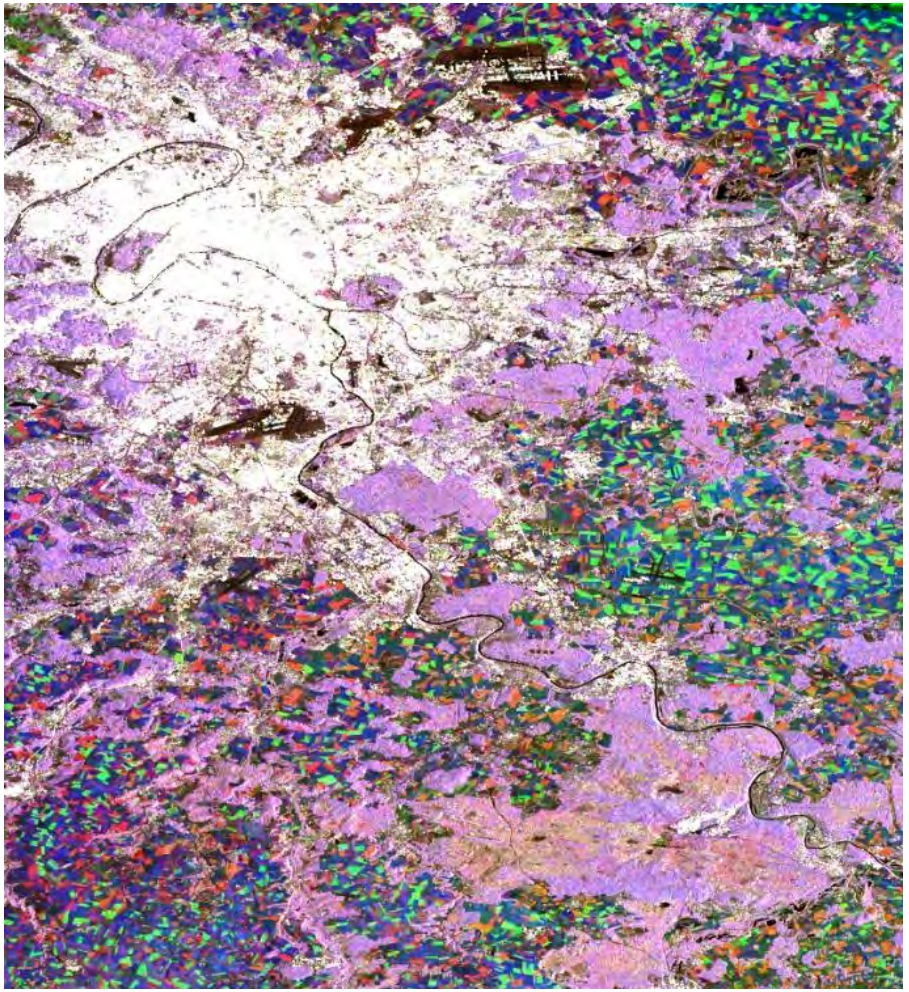

☞ *High spatio-temporal variability over crop fields*

Oaks stand

Radar Backscat. Coeff. σ^0

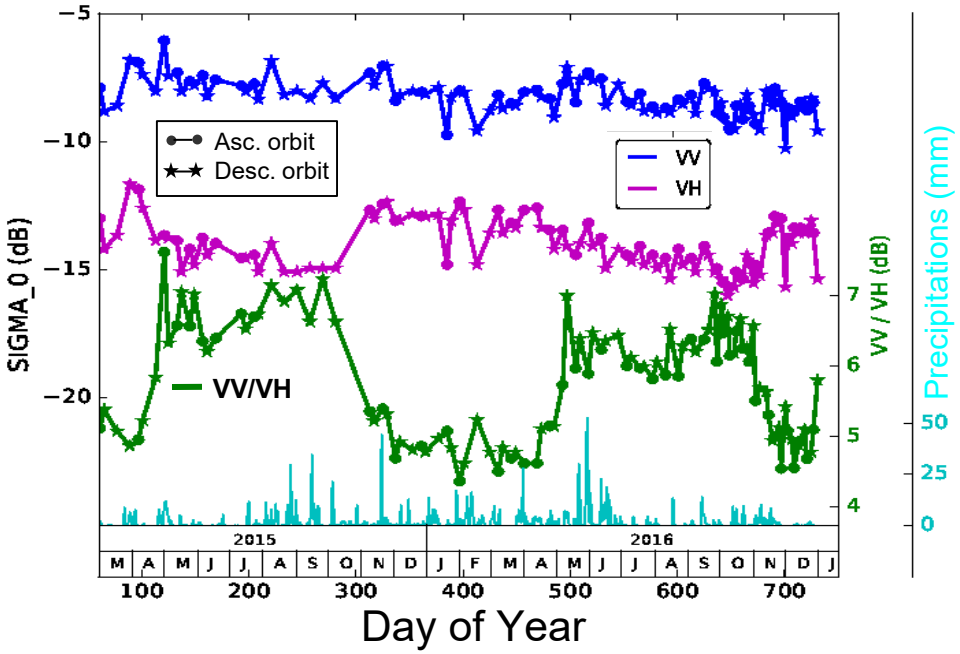

Coherence $|\rho|$

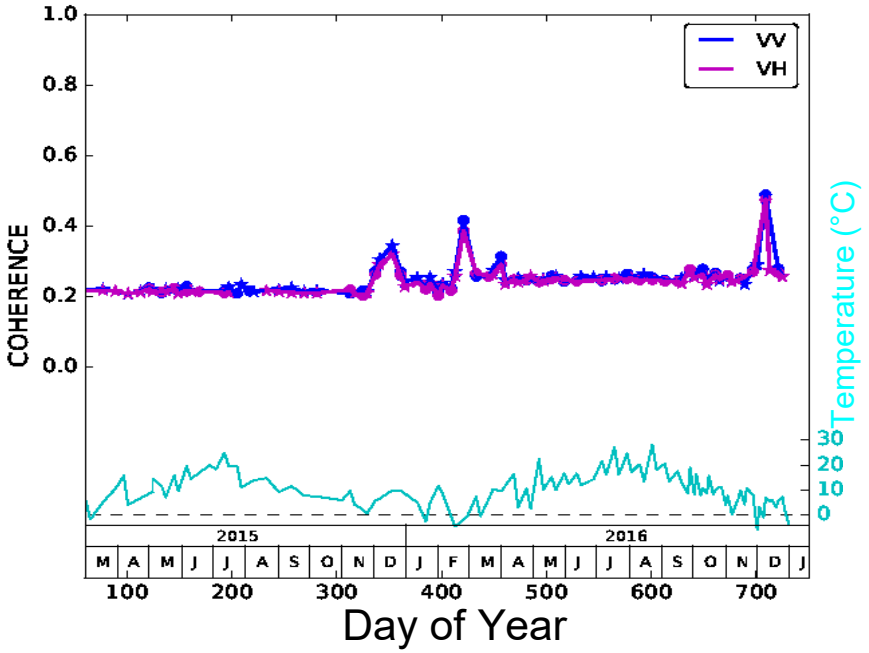

- No seasonal cyle s^0_{VV}
- Seasonal cycles s^0_{VH} ==> σ^0_{VV} / σ^0_{VH}

(yearly amplitude 3 dB)

- signal low and constant (Mar. - Nov.)
- $|\rho_{VV}|$ et $|\rho_{VH}|$ Identical
- higher values for low temperatures

Oaks stand

Radar Backscat. Coeff. s^0

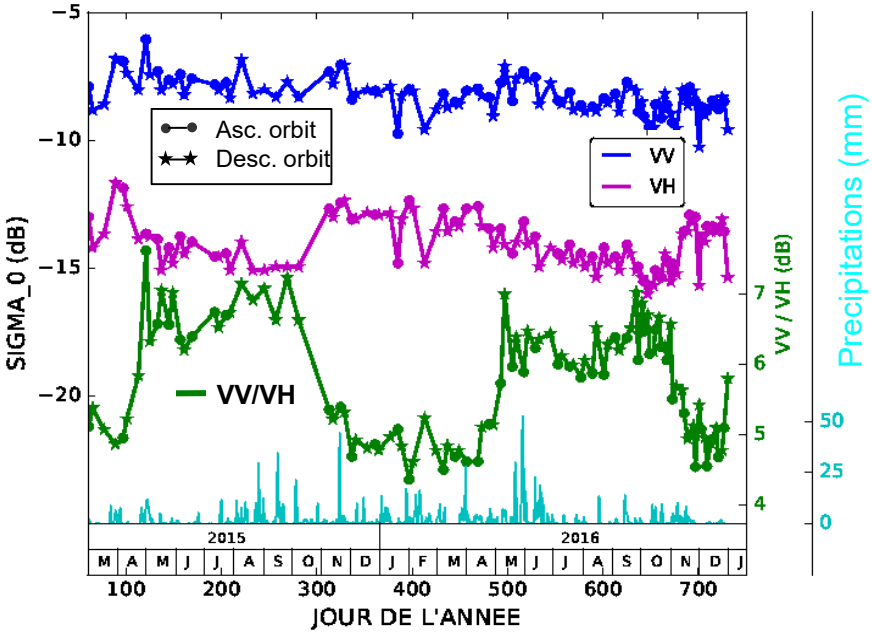

ERS *(VV) temporal signature*

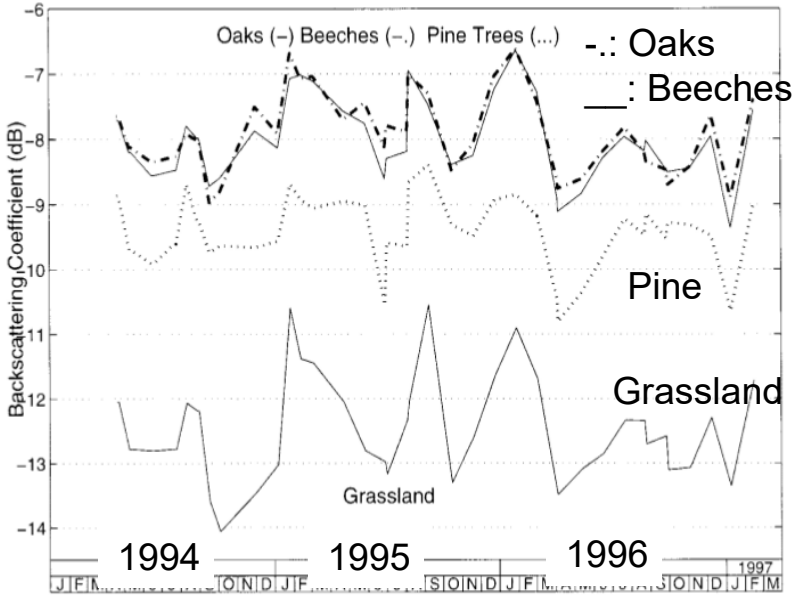

Proisy et al., 1999

- ☞ no seasonal cycle in VV pol.
- ☞ Seasonal cycle σ^0_{VH} ==> σ^0_{VV} / σ^0_{VH}

Oaks stand

Radar Backscat. Coeff. σ^0

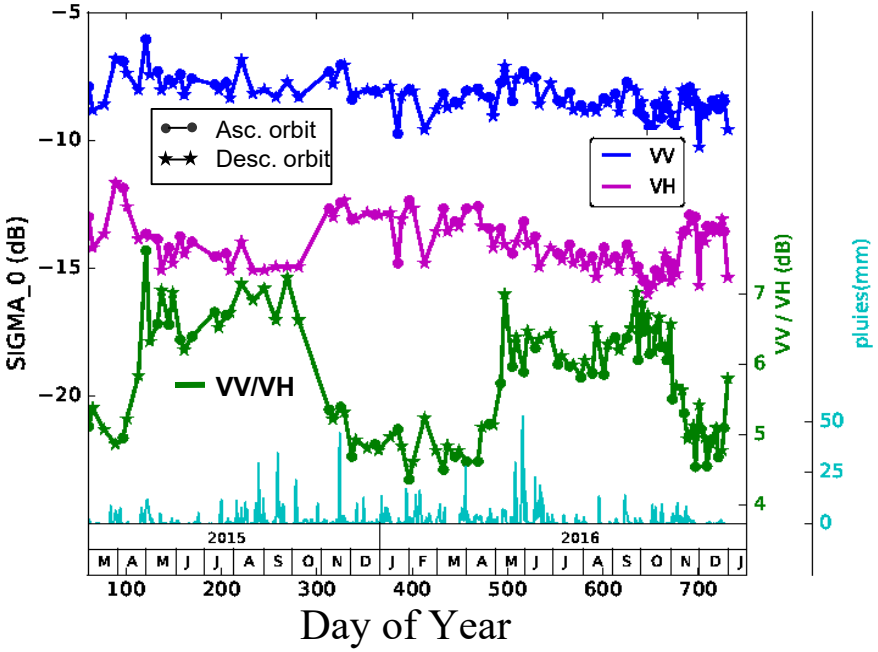

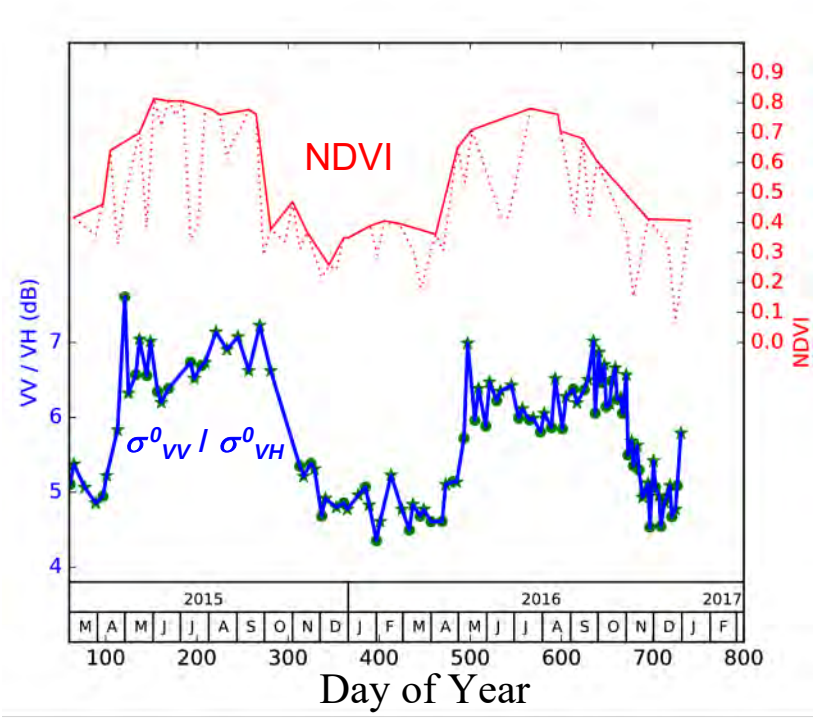

σ^0_{VV} / σ^0_{VH} and NDVI in phase

☞ C band sensitive to foliar activity

Crops monitoring – Lamasquère region

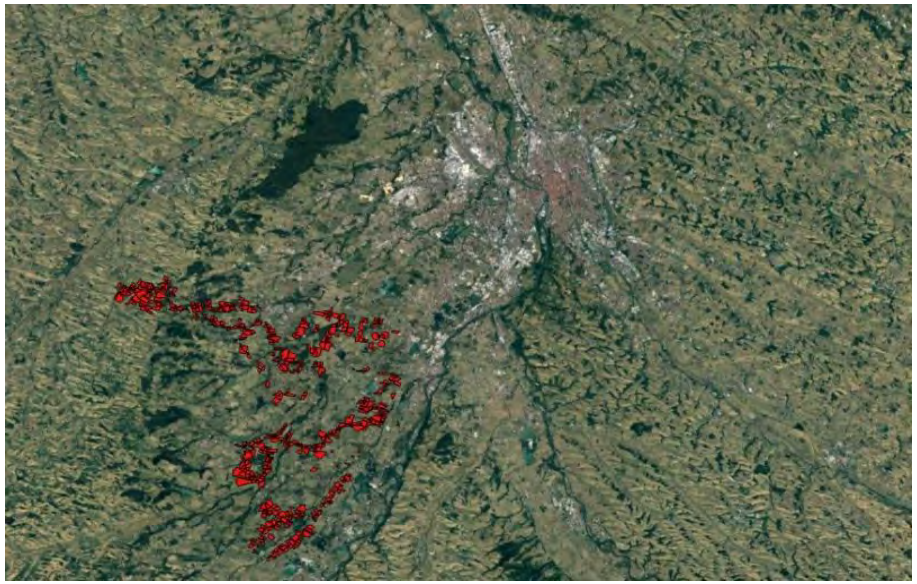

in situ survey (CESBIO)

Winter crops: wheat, barley, rapeseed

Summer crops: soybean, sorghum, maïze, sunflower

Agricultural area (Lamasquère region)

Multi-temporal color-composite images

Radar Backscatterin Coeff.

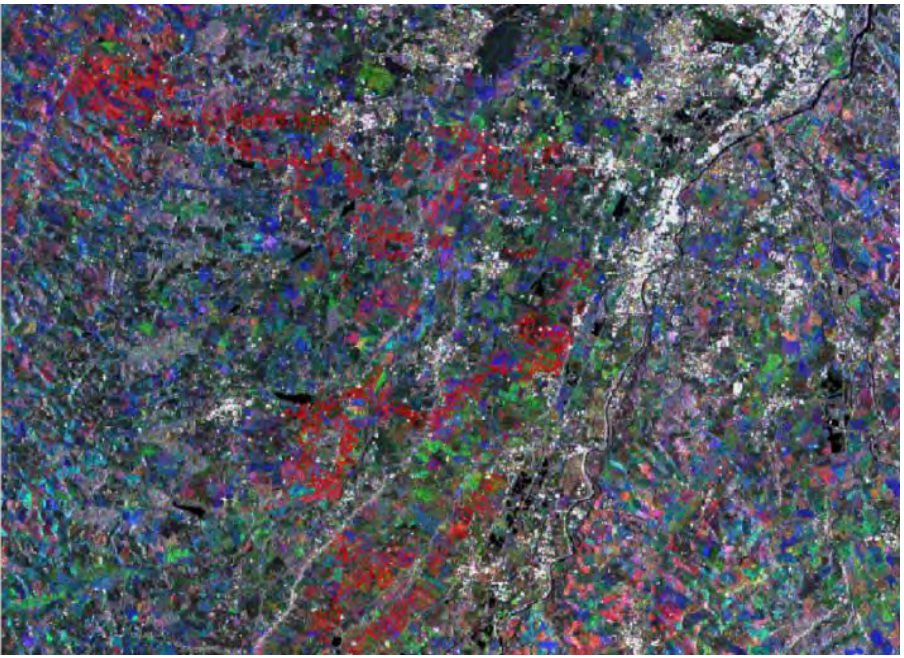

10 June- 14 Sept. – 7 Dec.

Cohérence

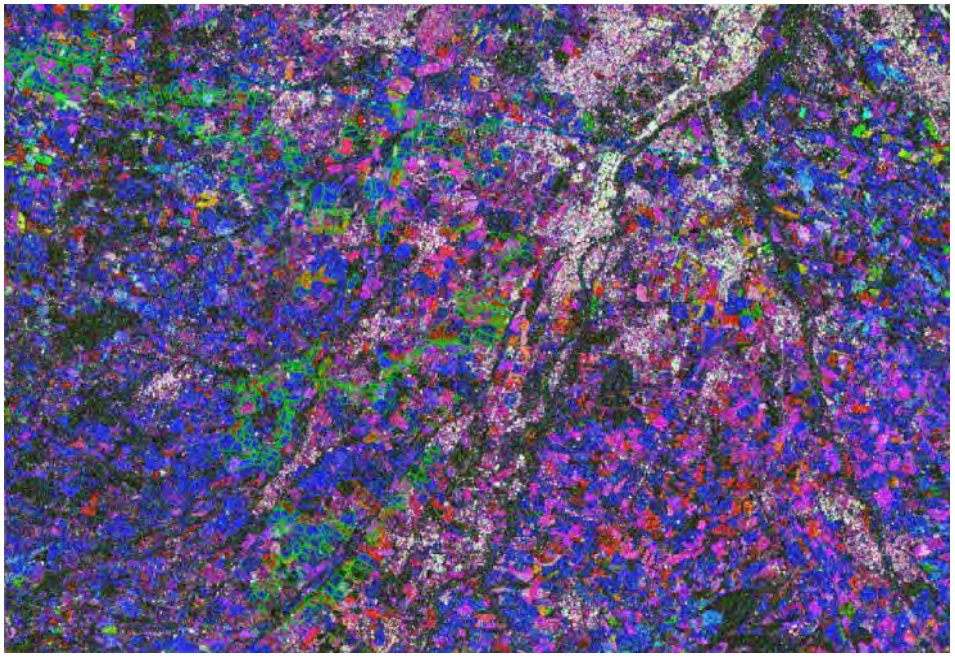

4-16 Jul .- 9-16 Aug. – 7-19 Dec.

CROP FIELDS: Temporal profile σ^0

WHEAT

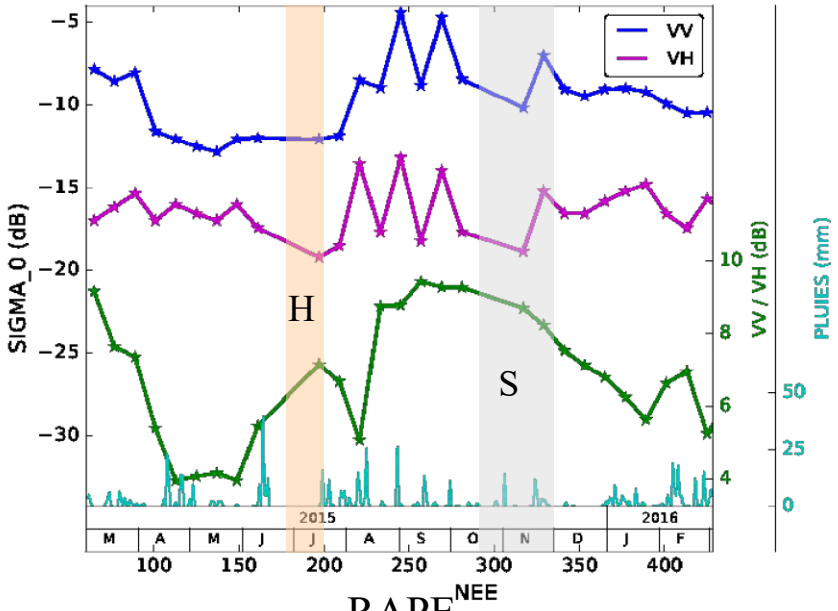

CORN – SOYA - SORGHUM

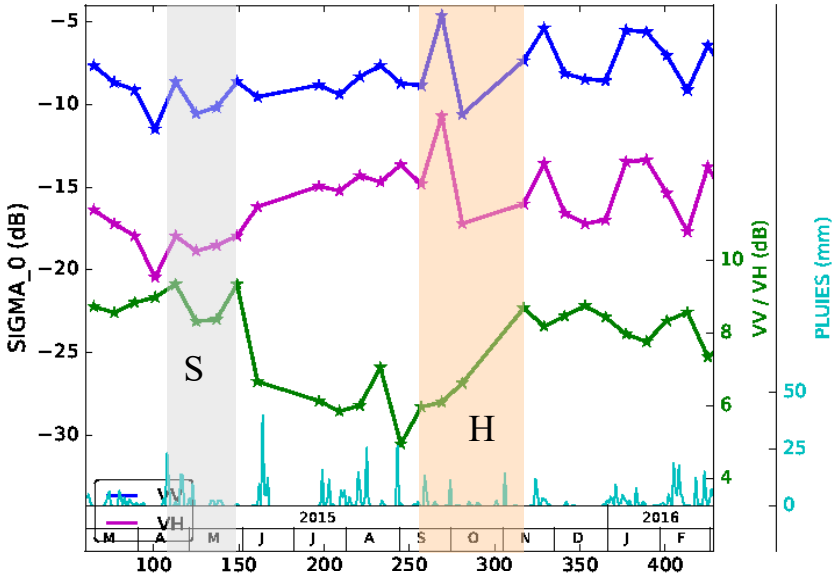

RAPE

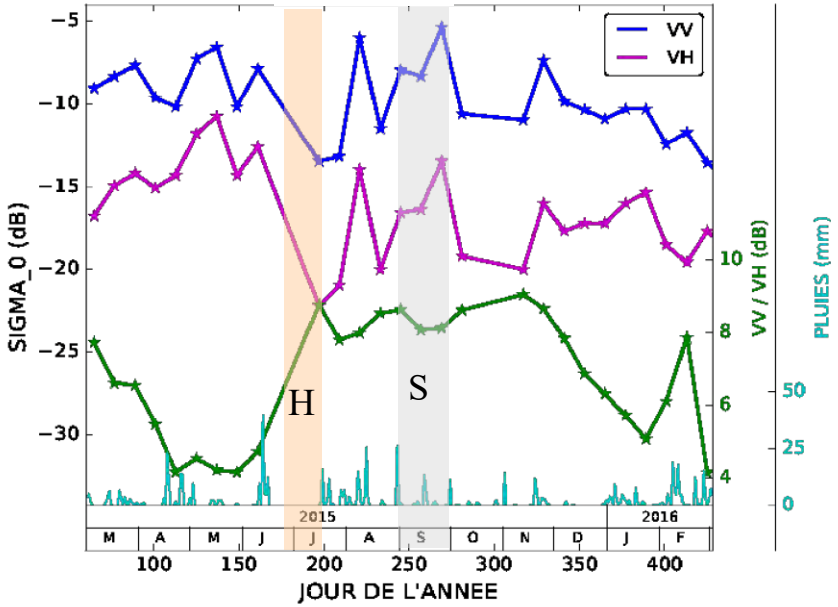

NEE

SUNFLOWER

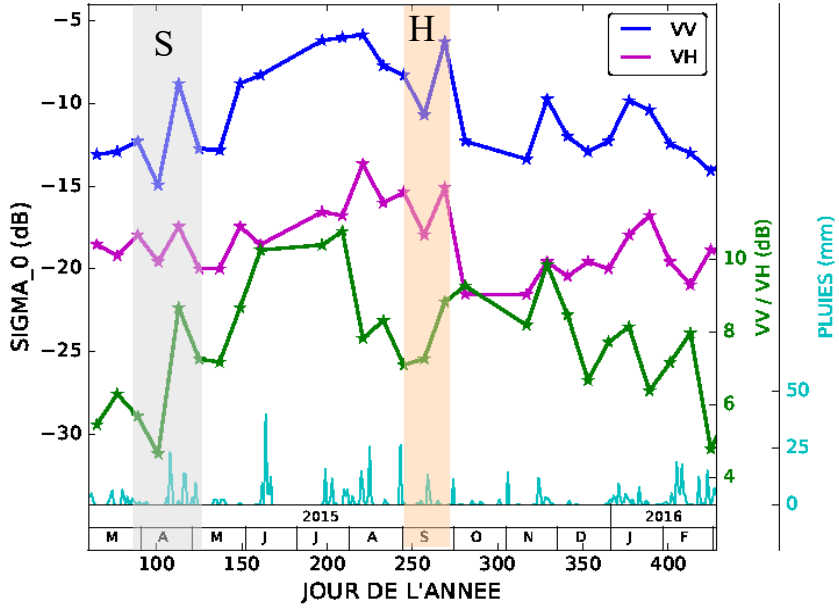

CROP FIELDS: Temporal profiles coherence

BLE - ORGE

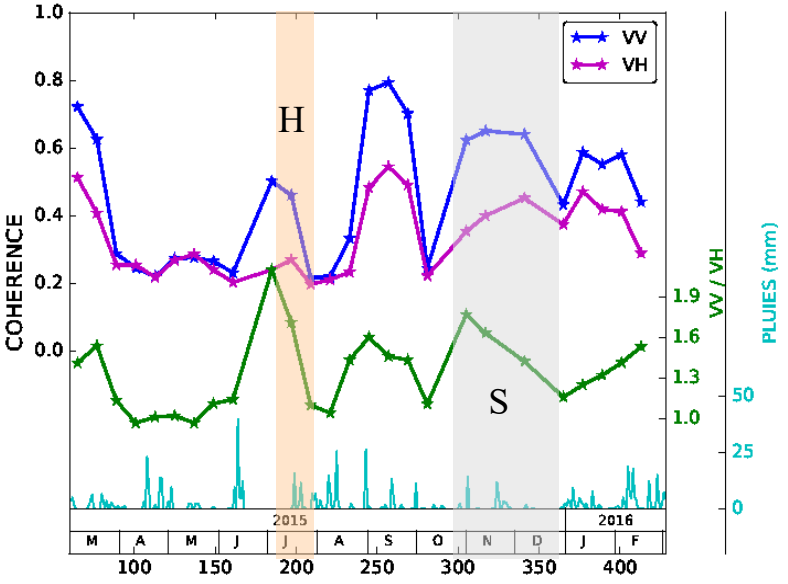

MAIS – SOJA - SORGHO

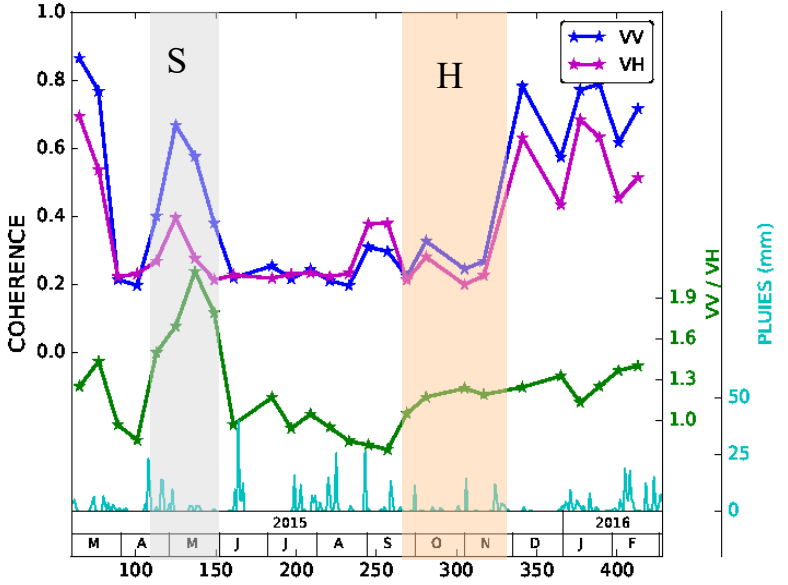

COLZA

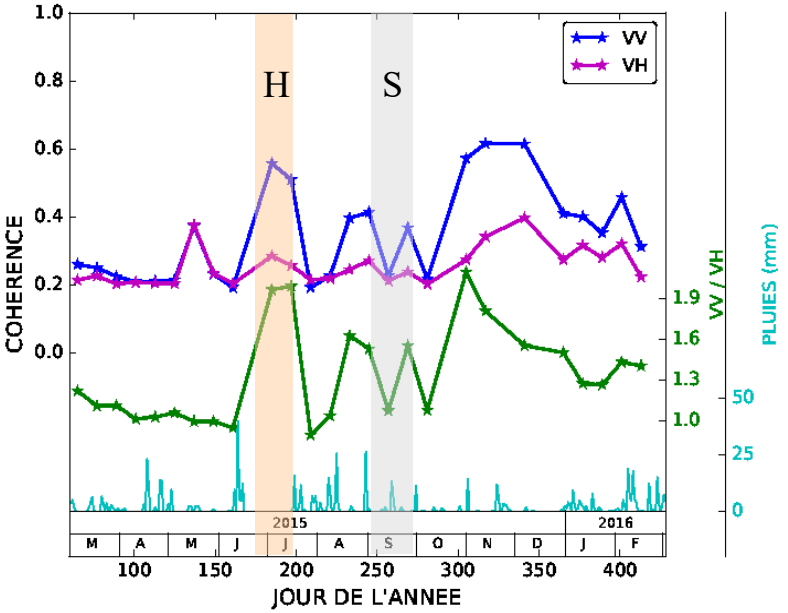

TOURNESOL

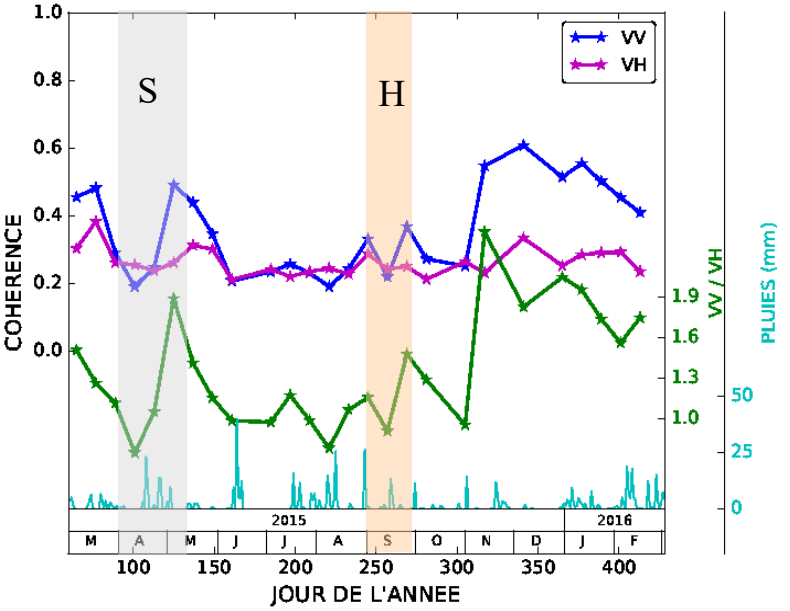


THAT'S ALL FOLK!!

OUTLINE

I. Radar imaging - Spatial resolution

II. Polarization

III. Radar response sensitivity

IV. Relief effects

V. Speckle and filtering

Electromagnetic coherent wave

Coherent wave: ***temporal*** behaviour

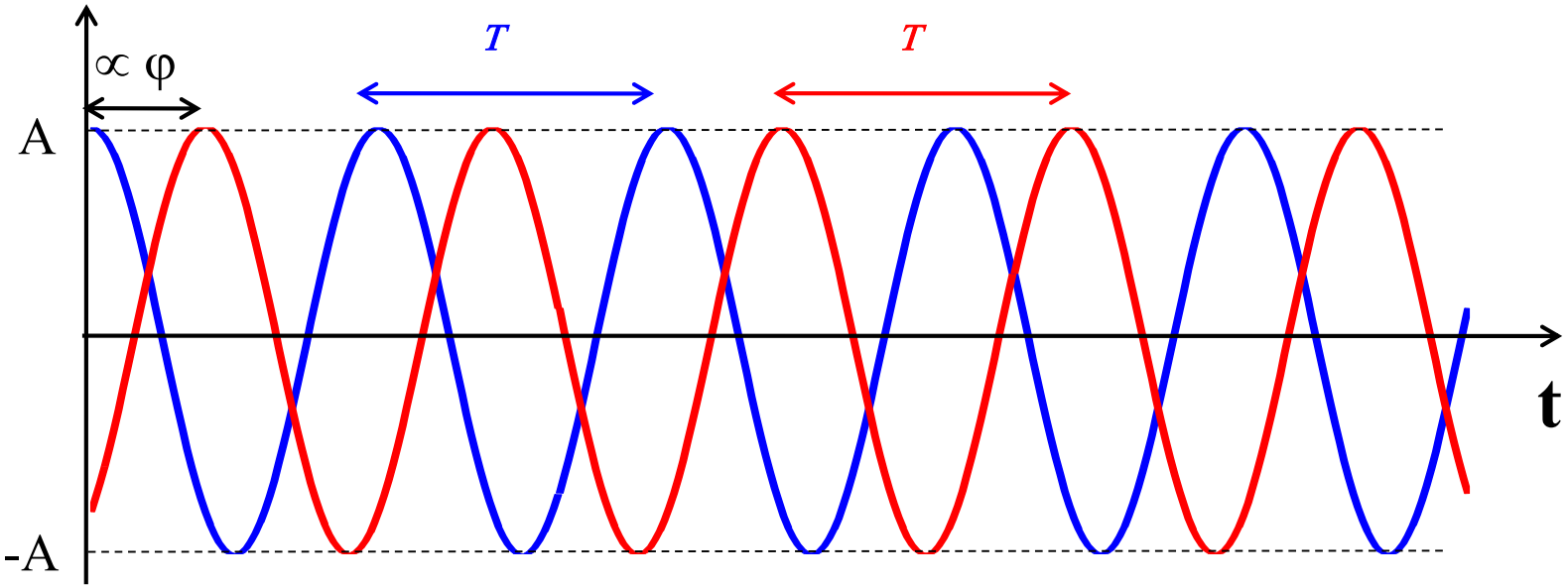

$$y(t) = A\cos\left(\frac{2\pi}{T}t\right)$$

$$y(t) = A\cos\left(\frac{2\pi}{T}t - \varphi\right)$$

$$T = \frac{1}{f_0}$$

A: amplitude

T: time period

φ: phase shift

Electromagnetic coherent wave

Coherent wave: ***spatial*** behaviour

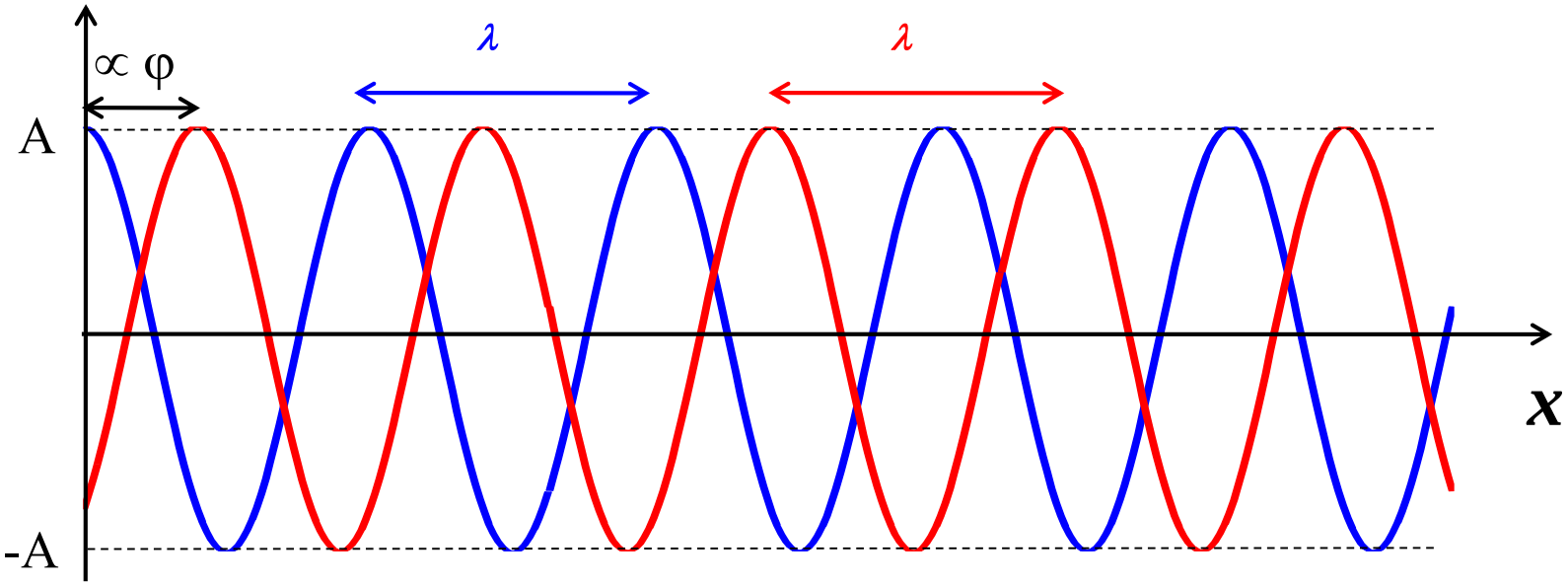

$$y(x) = A\cos\left(\frac{2\pi}{T}x\right)$$

$$y(x) = A\cos\left(\frac{2\pi}{T}x - \varphi\right)$$

$$\lambda = c\,T = \frac{c}{f_0}$$

A: amplitude
λ: spatial period = wavelength
φ: phase shift
c: light celerity = 3.10^8 m/s

Electromagnetic coherent wave

Coherent wave: ***spatial*** and ***temporal*** behaviour

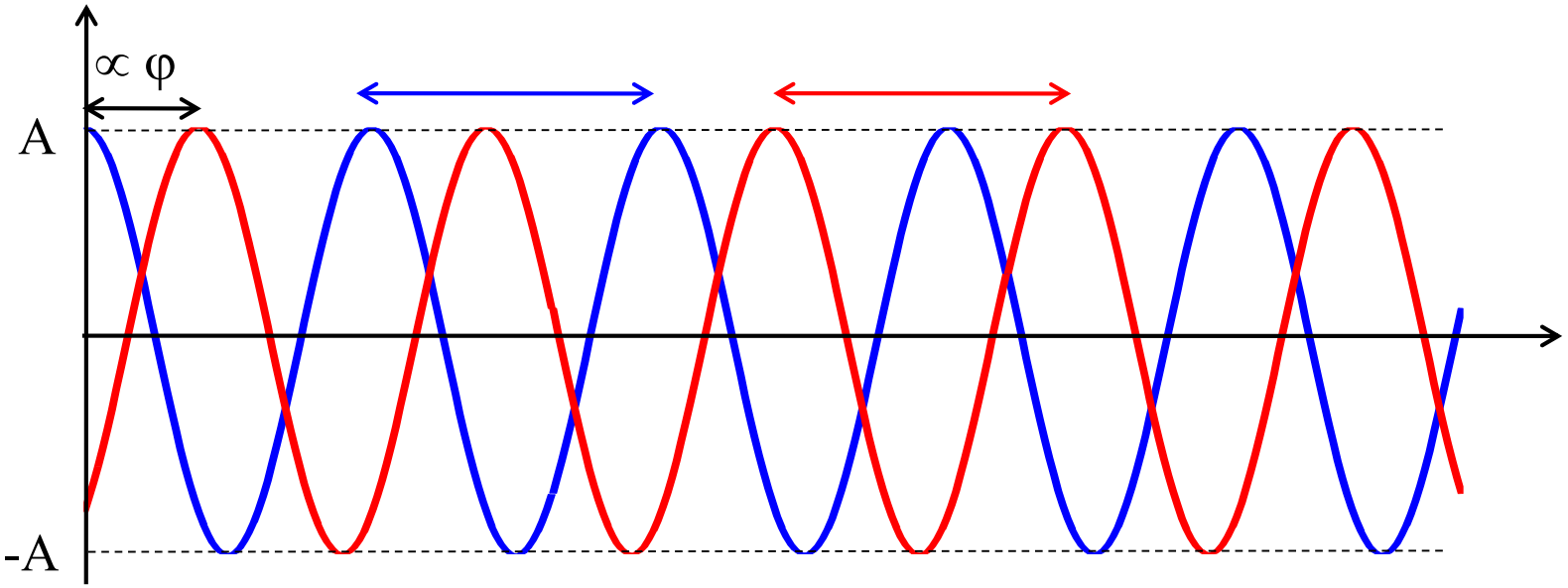

$$\psi(x,t) = A\cos\left(2\pi f_0 t - \frac{4\pi}{\lambda}x + \varphi\right)$$

RARE EXCEPTIONS!

Rainy events on X Band

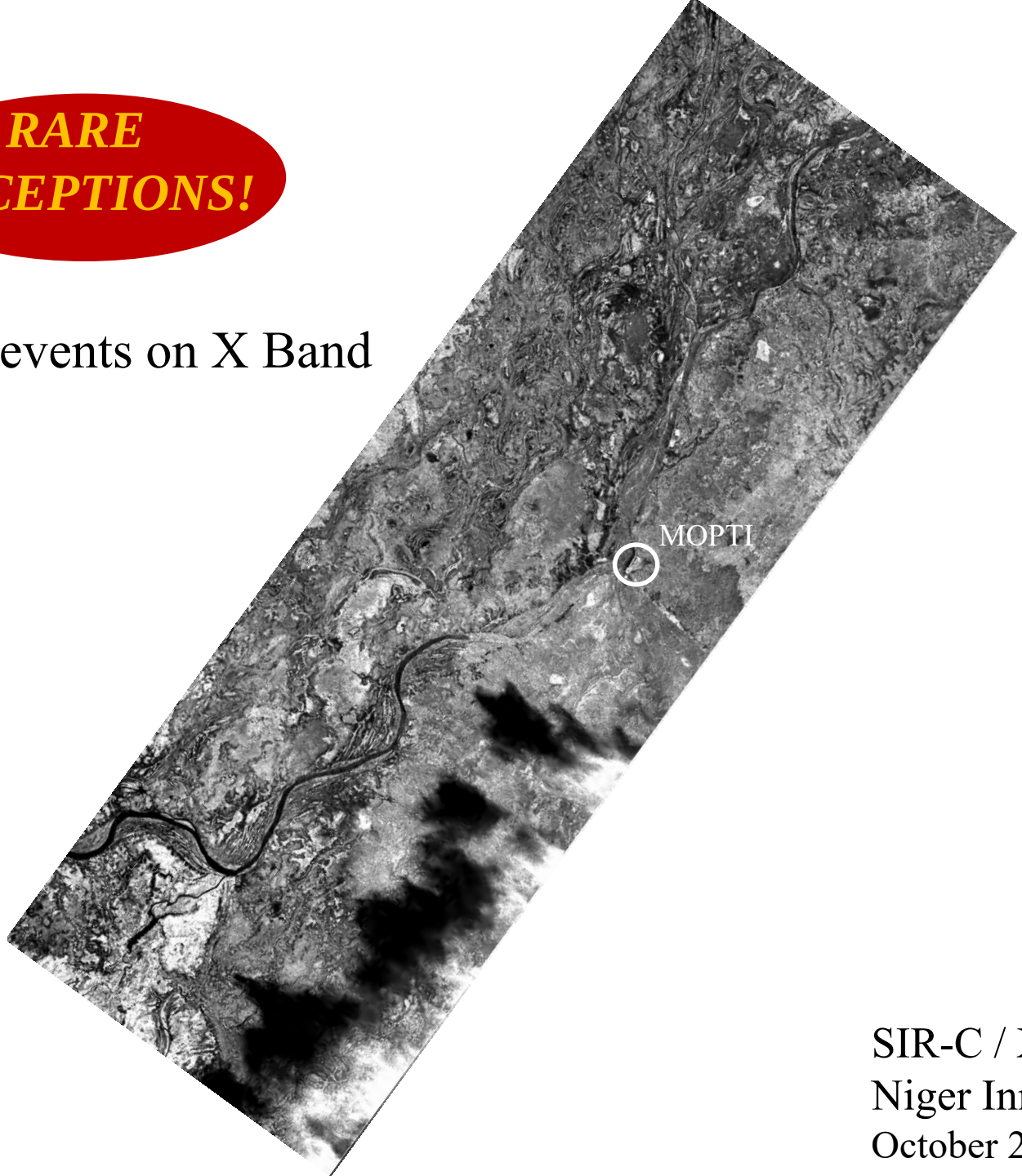

SIR-C / X-SAR
Niger Inner Delta, Mali
October 2, 1994

Rainy events on X Band

RARE EXCEPTIONS!

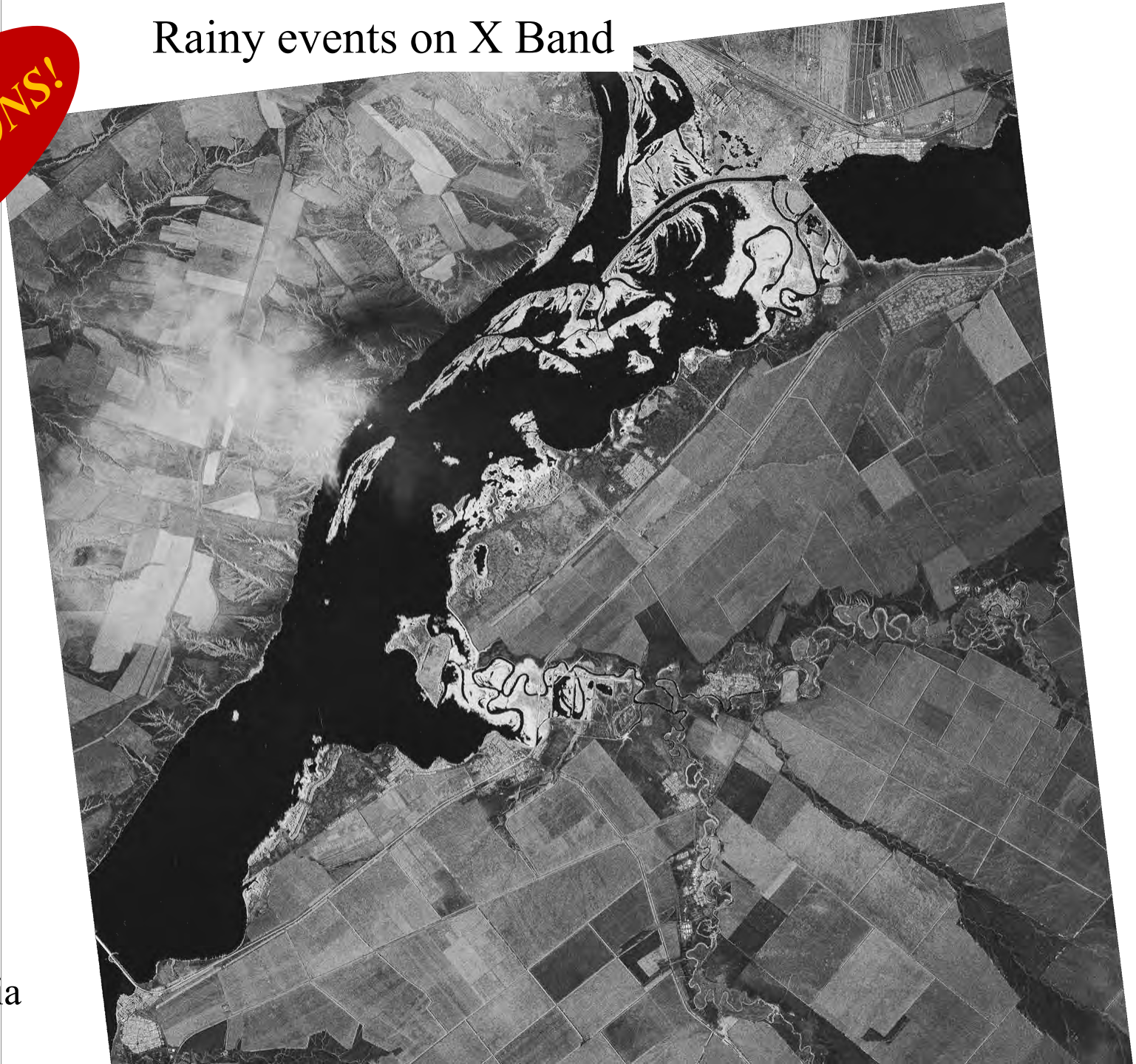

TerraSAR-X

Don River, Russia
June 19, 2007

Ionospheric effects on L Band

RARE EXCEPTIONS!

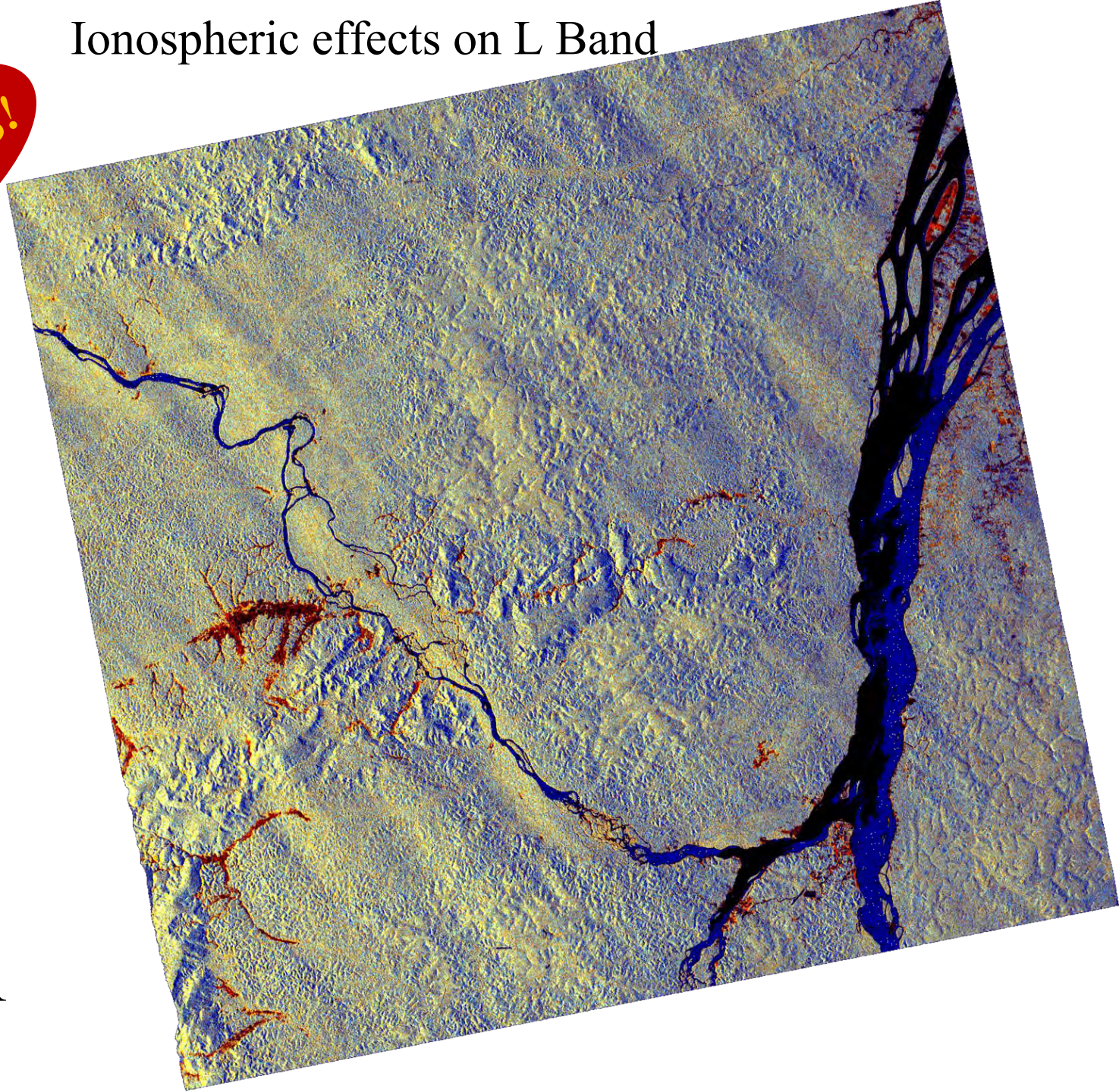

ALOS-PALSAR

AMAPA, Brazil

Frequency - wavelength

Radar: all weather acquisition

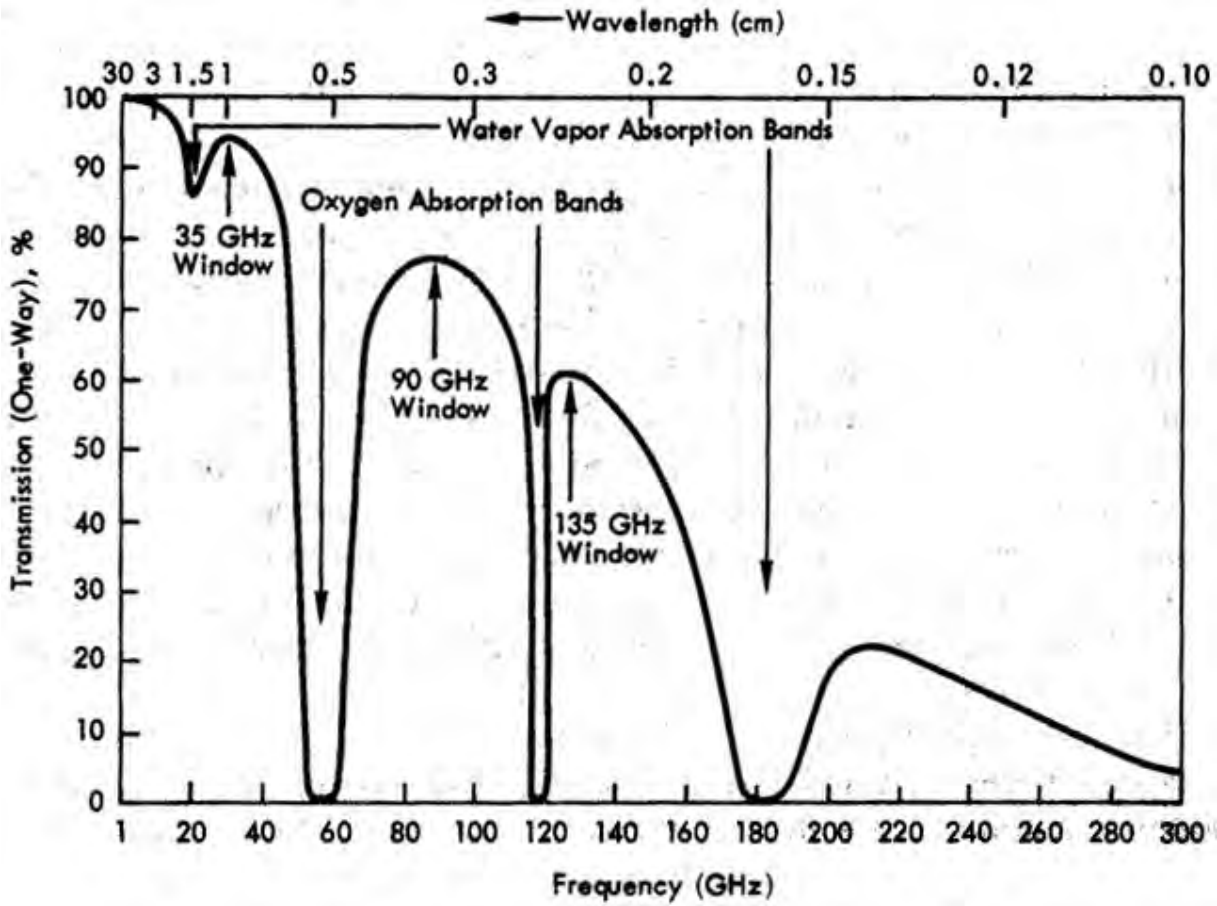

Source: Ullaby *et al.*

Radar spaceborne sensors

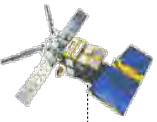

ERS1
RSO
Diffusiomètre
Bande C

RADARSAT2
RSO
Bande C

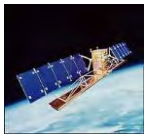

TerraSAR X
RSO
Bande X

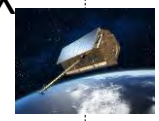

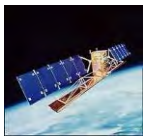

RADARSAT
RSO
Bande C

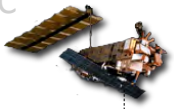

ENVISAT
RSO
Bande C

ALOS
RSO
Bande L

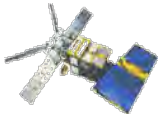

ERS2
RSO
Diffusiomètre
Bande C

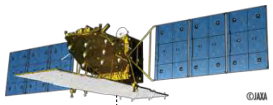

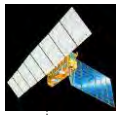

JERS
RSO
Bande L

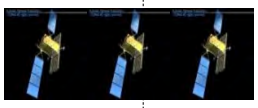

COSMO-SkyMed
RSO
Bande X

ALOS 2
RSO
Bande L

Quikscat
Diffusiomètre
Bande Ku

METOP
Diffusiomètre
Bande C

Tandem X
RSO
Bande X

1991 1992 1995 1999 2002 2006 2007 2010 2014 2016

Radar Fundamentals

RADAR:
RAdio **D**etection **A**nd **R**anging

Active mode
with **coherent wave**

Echoes are **ranged** according to
Antenna – target distance

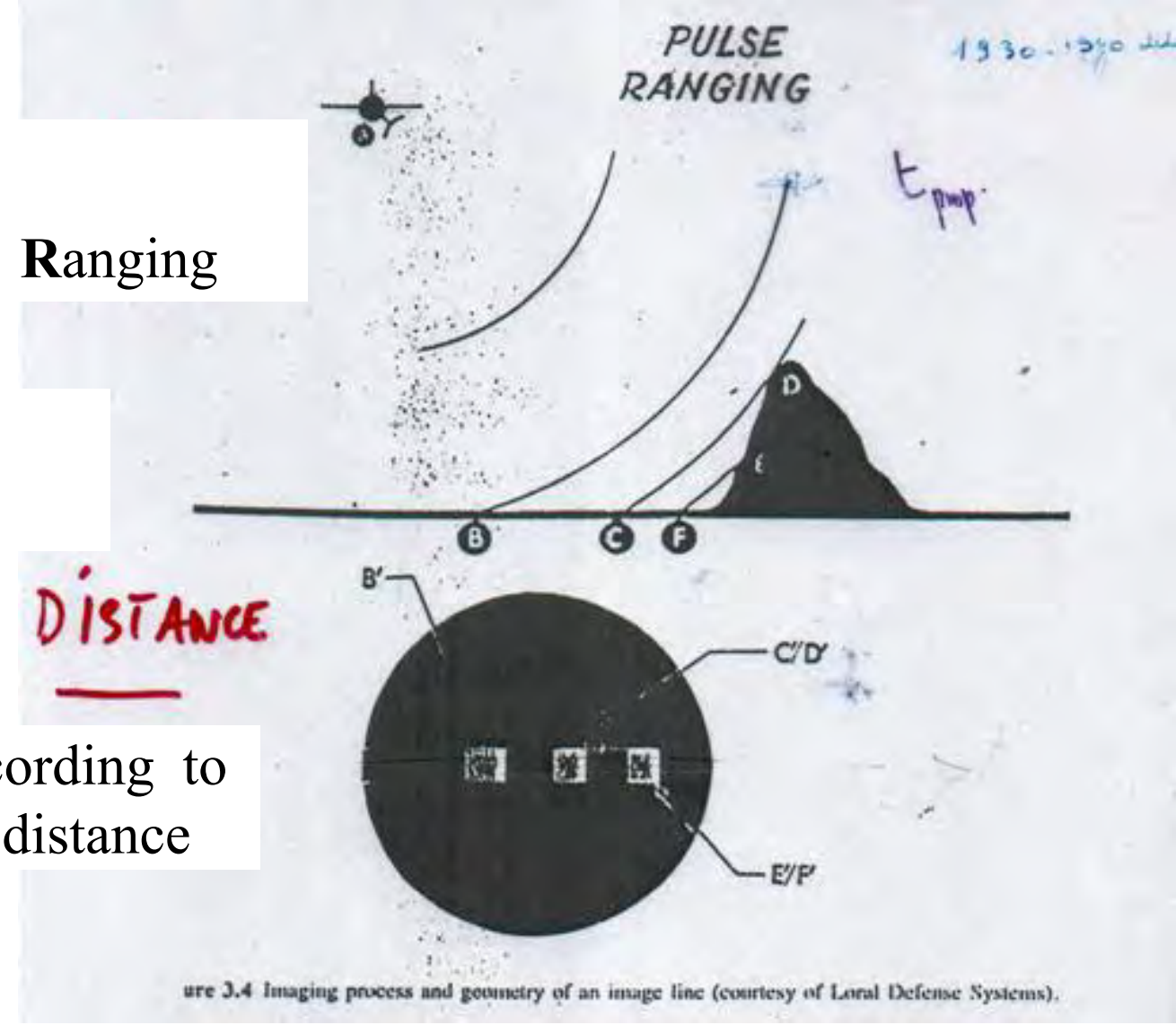

ure 3.4 Imaging process and geometry of an image line (courtesy of Loral Defense Systems).

Polarization

1995

1997

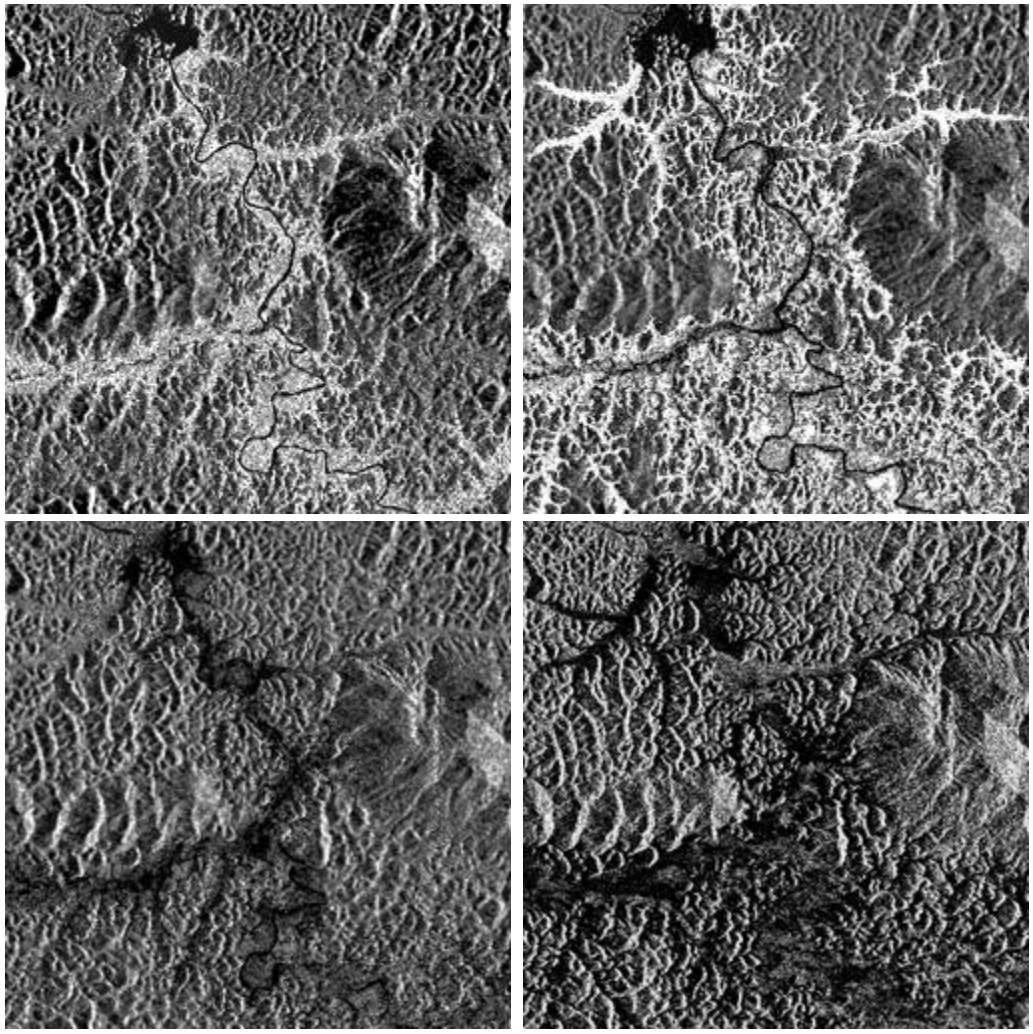

JERS

ERS

Petit Saut Dam

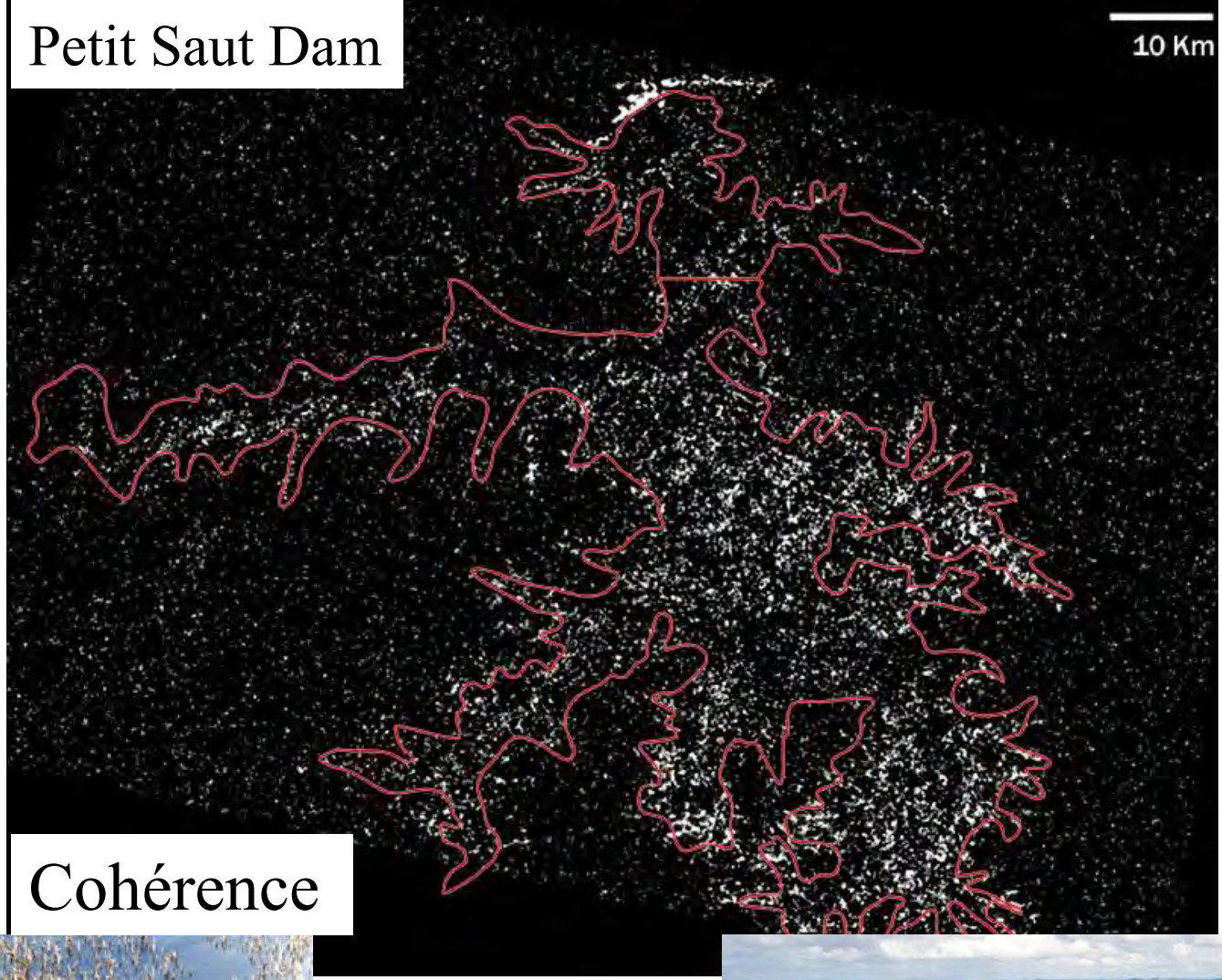

Cohérence